DOCTORAATSPROEFSCHRIFT

2004

Faculteit Geneeskunde

Characterization of primary cultured rabbit MTAL cells and effects of metabolic inhibition on intracellular pH

Proefschrift voorgelegd tot het behalen van de graad van
Doctor in de Medische Wetenschappen
te verdedigen door

Frank JANS

Promotor : Prof. dr. P. Steels (L.U.C.)
Co-promotor : Prof. dr. M. Ameloot (L.U.C.)
Prof. dr. P. Wouters (K.U.Leuven)

LIMBURGS UNIVERSITAIR CENTRUM
PARTNER IN DE UNIVERSITEIT LIMBURG

2004

Faculteit Geneeskunde

Characterization of primary cultured rabbit MTAL cells and effects of metabolic inhibition on intracellular pH

Proefschrift voorgelegd tot het behalen van de graad van
Doctor in de Medische Wetenschappen
te verdedigen door

Frank JANS

Promotor : Prof. dr. P. Steels (L.U.C.)
Co-promotor : Prof. dr. M. Ameloot (L.U.C.)
Prof. dr. P. Wouters (K.U.Leuven)

LIMBURGS UNIVERSITAIR CENTRUM
PARTNER IN DE UNIVERSITEIT LIMBURG

According to the guidelines of the Limburgs Universitair Centrum, a copy of this publication has been filed in the Royal Library Albert I, Brussels,as publication D/2004/2451/15

Members of the jury

Prof. dr. E. Van Kerkhove, L.U.C., chairman

Prof. dr. R. Beauwens, U.L.B.

Prof. dr. M. Schetz, U.Z. en K.U.Leuven

Prof. dr. E. Schlatter, Westfälische Wilhelms-Universität, Münster

Prof. dr. N. Lameire, U.Z. en Universiteit Gent

Prof. dr. W. Van Driessche, K.U.Leuven

Prof. dr. L. Verresen, Z.O.L. en L.U.C.

Prof. dr. M. Ameloot, L.U.C., co-promotor

Prof. dr. P. Wouters, U.Z. en K.U.Leuven, co-promotor

Prof. dr. P. Steels, L.U.C., promotor

Table of Contents

List of abbreviations

A6	: cell line derived from the kidney of *Xenopis Laevis*
Ab	: antibody
ABC	: avidin/biotin/peroxidase complex
ADP	: adenosine diphosphate
AEC	: aminoethylcarbazole
AMP	: adenosine monophosphate
ARF	: acute renal failure
ATN	: acute tubular necrosis
ATP	: adenosine triphosphate
AVP	: arginin-vasopressin
BAPTA	: 1,2-bis(2-aminophenoxy)ethane-N,N,N',N'-tetraacetic
BCECF-AM	: 2',7'-bis(carboxyethyl)-5(6)-carboxyfluorescein acetoxymethyl
BBM	: brush border membrane
BSA	: bovine serum albumin
C	: cortex
$[Ca^{2+}]_I$	: intracellular calcium concentration
cAMP	: 3'5'-cyclic adenosine monophosphate
CCD	: charge coupled device *or* cortical collecting duct
CHA	: N^6-cyclohexyladenosine
CTAL	: cortical thick ascending limb
DMEM	: Dulbecco's modified Eagle's medium
DMEM/F12	: DME/Ham's F12 medium
DMSO	: dimethylsulfoxide
DOG	: 2-deoxyglucose
□pH_i	: difference in intracellular pH
DT	: distal tubule
DTT	: dithiothreitol
EDTA	: ethylenediaminetetraacetic acid
EGF	: epidermal growth factor
EGTA	: ethylene glycol-bis(ß-aminoethyl ether)-tetraacetic acid
EIPA	: ethyl-isopropyl-amiloride
ETC	: electron transport chain
EtHD-1	: ethidium-homodimer-1
FACS	: fluorescence-activated cell sorting
FCS	: fetal calf serum

FFA	: free fatty acids
G-6-P	: glucose-6-phosphate
GDP	: guanosine diphosphate
GFR	: glomerular filtration rate
GTP	: guanosine triphosphate
HB-BSS	: HEPES buffered balanced salt solution
HEPES	: N-2-hydroxyethylpiperazine-N'-2-ethanesufonic acid
IBMX	: isobutylmethylxanthine
ICAM-1	: intercellular adhesion molecule 1
IL-4	: interleukin 4
IM	: inner medulla
IRI	: ischemia reperfusion injury
IS	: inner stripe
I_{sc}	: short circuit current
ISOM	: inner stripe of the outer medulla
JE	: immediate early gene induced by platelet-derived growth factor
LLC-PK	: cell line derived from proximal cells from canine kidney
MDCK	: Madin-Darby canine kidney cells
MEM	: mimimum essential medium
MI	:metabolic inhibtion
MPT	: mitochondrial pore transition
MTAL	: medullary thick ascending limb
NAD(P)	: nicotinamide adenine dinucleotide (phosphate)
NECA	: 5'-(*N*-ethylcarboxamido)adenosine
NGS	: normal goat serum
NHE	: Na^+/H^+ exchanger
NKCC2	: $Na^+/K^+/2Cl^-$ cotransport process
$NMDG^+$	: N-methyl-D-Glucamine
NMR	: nuclear magnetic resonance
OK	: cell line derived from *Opossum* kidney
OMCD	: outer medullary collecting ducts
OS	: outer stripe
PBS	: phosphate buffered saline
PCr	: phosphocreatine
PCT	: proximal convoluted tubule
PEPCK	: phosphoenolpyruvate carboxykinase
PFK	: phosphofructokinase
PGE_2	: prostaglandin E_2
P_i	: inorganic phosphate

PLA_2	: phospholipase A_2
PT	: proximal tubule
PTFE	: polytetrafluoroethylene
RAO	: renal artery occlusion
ROMK	: renal outer medullary potassium channel
ROS	: reactive oxygen species
R_{te}	: transepithelial resistance
RT-PCR	: reverse transcript polymerase chain reaction
S1	: early and middle portions of the PCT
S2	: late convoluted and cortical straight portion of the PT
S3	: outer medullary portion of the PT
SBTI	: soybean trypsin inhibitor
SEM	: standard error of the mean
TAL	: thick ascending limb
TALH-SVE	: immortalized cell line derived from rabbit MTAL
TBS	: TRIS buffered saline
TCA	: tricarboxylic acid cycle
TEA	: tetraethylammonium
THP	: Tamm-Horsfall protein
TRIS	: tris(hydroxymethyl)aminomethane base
TRPV5	: recently cloned Ca^{2+} channel
V_{te}	: transepithelial potential difference.

Chapter 1
General introduction

The work presented in this thesis belongs to the research on the cellular pathophysiology of renal ischemia. In combination with whole organ studies, studies on animals and clinical studies, the ultimate goal of this type of research is a better understanding of the pathophysiology of human ischemic Acute Renal Failure (ARF), in the clinic often referred to as "Acute Tubular Necrosis (ATN)".

1.1 Acute Renal Failure: Definition, incidence and mortality

Acute Renal Failure is a syndrome characterized by rapid (hours to weeks) decline in glomerular filtration rate (GFR) and retention of nitrogenous waste products such as blood urea nitrogen and creatinine. ARF is caused by ischemic (50%) or nephrotoxic (35%) injury to the kidney. However, in 50% of the cases of hospital-acquired ARF, the cause is multifactorial (Lameire & Vanholder, 2001). ARF complicates approximately 5% of hospital admissions and up to 30% of admissions to intensive care units (Brady et al., 2000). When ARF occurs in the setting of multi-organ failure, especially in patients with severe hypotension or respiratory failure, the mortality rate often exceeds 50%. The most common causes of death are sepsis, cardiovascular dysfunction, and pulmonary complications (Stoelting & Dierdorf, 2002). Despite major advances in dialysis therapy and critical care, the mortality rate among patients with severe ARF requiring dialysis has not decreased greatly over the last 50 years. This observation can be explained by the fact that, in comparison with patients that were treated for ARF 50 years ago, ARF patients today are often elderly and have multiple co-existing diseases (Stoelting & Dierdorf, 2002; Lameire & Vanholder, 2001). However, the high mortality rate in ARF is not explained by the underlying conditions alone. Renal failure appears to increase the risk of developing severe nonrenal complications that lead to death and should not be regarded as a treatable complication of serious illness (Levy et al., 1996). Therefore, a better understanding of the pathophysiology of ARF may lead to new treatment strategies and improved patient survival. At this moment, the awareness in the clinical setting of the added risk factors (volume depletion, pre-existing renal failure, heart failure, vasoconstrictor hormones or drugs, elevated body temperature) when there is a potential for renal hypoperfusion, probably could do more to reduce morbidity and mortality than any therapy currently available for established ARF (Conger, 2001).

As stated in the title of this thesis, the presented research will focus on the changes of the intracellular pH during simulated ischemia (metabolic inhibition) in a new model of distal (post-proximal) tubular cells (primary cultures of MTAL cells). In order to clarify why this specific subject and model was chosen for our research,

the general introduction to this thesis will start with an overview of the "whole organ" pathophysiology of ARF and end with a discussion on the role of intracellular pH during cell ischemia.

First, since changes in tubular cell function are not the only factor contributing to the decrease in GFR, which is the hallmark of ischemic ARF, a brief overview of all the elements that lead to a decrease in GFR are summarized in paragraph 1.2.1. In this way, the pathophysiology of tubular cells can be situated in a broader picture of the pathophysiology of the ischemic kidney as a whole.

Second, in paragraph 1.2.2, several lines of evidence are presented that highlight the crucial role of one particular nephron segment, namely the MTAL, in ischemic ARF. The reason for discussing this in the general introduction, is that, until now, the vast majoriy of studies on renal cell ischemia have been performed on proximal tubular cells.

Third, the current concepts on the cellular pathophysiology of renal ischemia, with emphasis on what has been published on the changes of intracellular pH, are presented in paragraph 1.3.

Finally, in paragraph 1.4, the possible advantages and disadvantages of using primary cultured cells as a model system for (distal) renal cell ischemia are discussed.

1.2 Pathophysiology of ARF at the whole organ level: causes of reduced GFR and the crucial role of the MTAL

1.2.1 Causes of reduced GFR in ischemic ARF

The reduced GFR, that is the hallmark of ischemic ARF, results not only from ischemic injury to tubular cells, but also from hemodynamic changes, decreased glomerular capillary permeability and infiltration of leukocytes (Fig. 1.1).

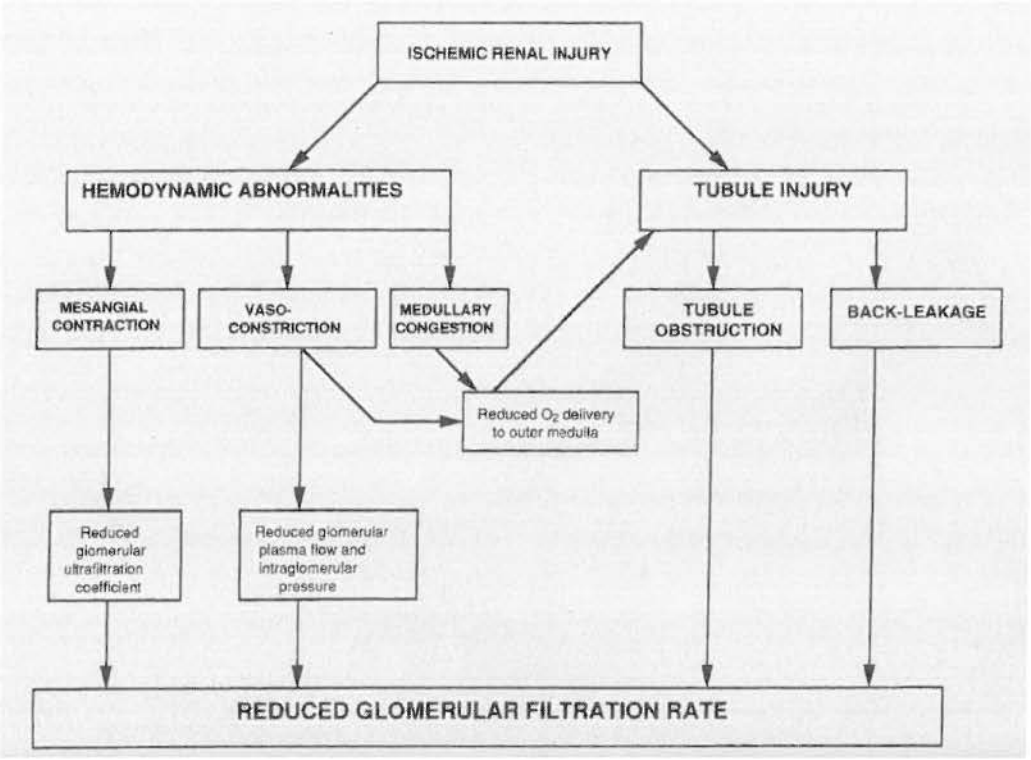

Figure 1.1 *The pathophysiology of ischemic renal failure. The profound reduction in GFR associated with renal ischemia is due to a combination of intrarenal hemodynamic alterations and renal tubule epithelial injury leading to back-leakage of glomerular ultrafiltrate and tubule obstruction (adapted from Brady et al., 2000, p 1212).*

1.2.1.1 Reduction in total renal blood flow

A reduction in total renal blood flow to 50% of normal has been consistently reported following renal ischemia in experimental models and humans. Persistent and severe regional disturbances in renal blood flow, affecting predominantly the outer medulla, contribute to the maintenance phase of ARF (Sheridan & Bonventre, 2000). This observation has been conceptualized as the "no-reflow" hypothesis (Leaf, 1973). Yamamoto et al. (Yamamoto et al., 2002). have recently examined this phenomenon with intravital videomicroscopy. In ischemic rat kidneys, they observed a similar pattern for glomerular microcirculation and peritubular capillary flow: initial recovery of blood flow is followed by its temporal cessation, despite the fact that renal artery occlusion (RAO) is no longer present. Although glomerular circulation recovers by 60 minutes, peritubular capillaries show a significant delay in the recovery of blood flow. These findings suggest that the peritubular capillaries are more vulnerable to acute ischemia or that the rate of their functional recovery is hampered by the effects exerted by the ischemic epithelial cells. It must be noted that in this study only the cortical microvasculature was examined. Despite intensive investigation, the mechanisms responsible for the "no reflow" phenomenon are not fully understood. Both endothelial cell dysfunction and obstruction of the microvascular lumen by red and white blood cells are thought to be involved.

Sublethal endothelial injury may be responsible for intrarenal vasoconstriction by causing an imbalance in the production of endothelin and endothelium-derived NO (Brady et al., 2000). Recently, it has been demonstrated that "transplantation" of endothelial cells or their surrogates expressing functional endothelial nitric oxide synthase in the renal microvasculature resulted in a dramatic functional protection of ischemic kidneys (Brodsky et al., 2002).

Vascular congestion with red and white blood cells, particularly in the outer medulla following ischemia, has been widely reported in both animals and humans (Mason et al., 1987). The cause is probably multifactorial. *First*, in the rat RAO-model, very early after ischemia-reperfusion injury, increased expression of ICAM-1 (intercellular adhesion molecule-1) in the inner stripe of the outer medulla (ISOM) goes along with monocyte and T-cell accumulation. This may result in the adhesion of leukocytes to the vasa recta resulting in their plugging by red and white blood cells (Degreef et al., 2003). The importance of leukocyte adhesion is underscored by the observation that prevention of intravascular activation and adhesion of neutrophils, monocytes and T-cells by anti-adhesion approaches (anti-ICAM-1 antibodies, anti-B7-1 antibodies) results in functional and morphological protection of ischemic kidneys (Degreef et al., 2001; Degreef et al., 2003). *Second*, the

congestion is probably accentuated by egress of plasma water, because of either high pressure or increased capillary permeability, thus increasing blood viscosity (Rabb & Star, 2001). *Finally*, endothelial cell swelling may contribute to the narrowing of the vascular lumen (Flores et al., 1972).

Apart from endothelial cell dysfunction and obstruction of the microvascular lumen, a decrease in renal blood flow autoregulation may allow small decreases in blood pressure to provoke recurrent ischemic damage (Lameire & Vanholder, 2001).

1.2.1.2 Decreased glomerular capillary permeability

Decreased glomerular capillary permeability has been documented to play a role in the pathogenesis of ARF. The precise mechanism of this abnormality has not been well defined, although endothelial cell swelling, particularly after an ischemic insult has been implicated as an important contributor to this phenomenon (Nissenson, 1998). Also contraction of mesangial cells may play a role by reducing the surface area for filtration.

1.2.1.3 Ischemic injury to tubular cells

Ischemic injury to tubular cells plays a central role in the reduction of GFR in ischemic ARF. There is general agreement that tubules are obstructed by detached tubule epithelial cells and debris following renal arterial occlusion and reperfusion (Brady et al., 2000). The subcellular events leading to detachment will be discussed in detail in the following section. Injured epithelial cells are detached from the basement membrane and released into the tubular lumen, where they mix with intraluminal proteins and result in cast formation. These casts obstruct tubules, lead to increased intratubular pressure, and may result in sufficient back-pressure to offset transglomerular hydrostatic pressure. If this occurs, glomerular filtration ceases. If intratubular pressure continues to rise, tubular disruption occurs, with resultant back-leak of tubular contents into the interstitium (Nissenson, 1998). The importance of back-leak of filtrate in the reduction of GFR has been demonstrated in experimental models as well as in humans (Donohoe et al., 1978; Myers et al., 1979).

Ischemic injury to tubular cells also impairs vectorial sodium transport and thereby decreases tubular sodium reabsorption, leading to increased fractional sodium excretion in established human ARF (Lameire & Vanholder, 2001). This enhanced delivery of solute to the macula densa may in turn contribute to the

reduction in total renal bloodflow (see 1.2.1.1) by activation of the tubuloglomerular feedback (Bonventre& Weinberg, 2003).

It is the combination of the above-mentioned abnormalities that forms the basis for the acute decrease in GFR in ischemic ARF. For example, some nephrons may be primarily obstructed, with the potential for normal function if the obstruction is eliminated, while other nephrons may have negligible glomerular blood flow independent of any tubular obstruction (Conger, 2001).

1.2.2 A crucial role for the MTAL segment in ischemic ARF

Although the vast majority of studies on ischemic ARF have focused on the proximal tubular cells, more specifically the straight portion of the proximal tubule, several lines of evidence suggest an important role for the MTAL segment in the pathophysiology of ischemic ARF.

1.2.2.1 Anatomy of the kidney

The kidneys have a remarkably high blood flow per unit of tissue weight and a relatively low oxygen extraction fraction. Intuitively, it would be assumed that these features would make the kidneys relatively resistant to ischemic injury. However, it is well established that the kidney is one of the organs most susceptible to ischemia that is related to changes in systemic hemodynamics. This apparent paradox is explained, at least in part, by the special functional anatomy of the kidney circulation. Renal blood flow, a quarter of the cardiac output, is directed mostly to the cortex to optimize glomerular filtration and the absorption of solute. By contrast, blood flow to the renal medulla is low, to preserve osmotic gradients and enhance urinary concentration. Within the medulla, tubules and vasa recta are disposed in a hairpin pattern to maximize the concentration of urine by countercurrent exchange. Oxygen diffuses from arterial to venous vasa recta, which leaves the outer medulla deficient in oxygen. In this region, the MTAL is responsible for the generation of an osmotic gradient by active absorption of sodium, a process that requires a large amount of oxygen. The medullary partial pressure of oxygen is in the range of 10 to 20 mmHg (Brezis & Rosen, 1995). Therefore, most investigators agree that the tubular segments situated within the outer medulla of the kidney are likely to suffer from the most severe injury after an ischemic insult due to the persistent reduction in blood flow to this region of the kidney (Fig. 1.2).

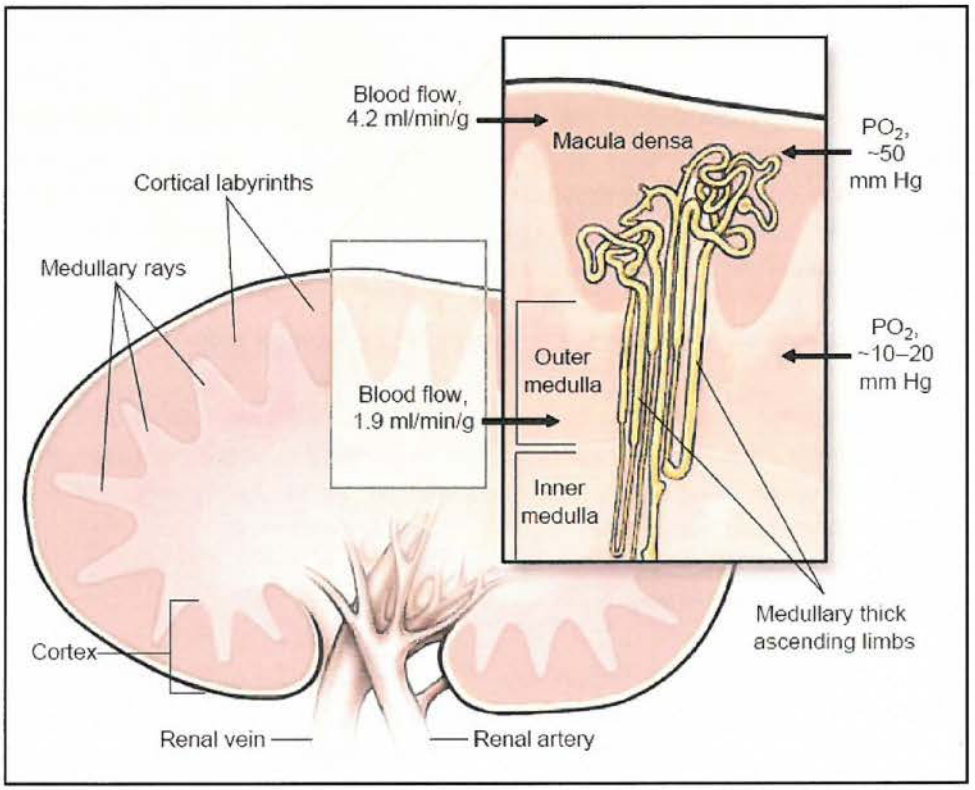

Figure 1.2 *The kidney cortex is generally well oxygenated, except for the medullary-ray areas devoid of glomeruli, which are supplied by venous blood ascending from the medulla. Medullary hypoxia results both from countercurrent exchange of oxygen with the vasa recta and from the consumption of oxygen by the medullary thick ascending limbs. Renal medullary hypoxia is an obligatory part of the process of urinary concentration (adapted from Brezis & Rosen, 1995, p 648).*

1.2.2.2 Injury to the MTAL in different model systems of renal ischemia

There has been an ongoing debate regarding the nephron segment (S3 or MTAL) most severely injured in ARF (Lieberthal & Nigam, 1998; Heyman et al., 2002; Rosen & Heyman, 2002). The controversy on which part of the nephron is most vulnerable to ischemia-reperfusion injury (IRI), arose from the use of different model systems. The most popular model, the renal artery occlusion (RAO) model, gives rise to extensive necrosis of the S3 segment. On the other hand, the studies with transplanted kidneys (cold ischemia-reperfusion injury) and the isolated erythrocyte-free perfused kidney can be classified as "distal nephron models", in that they are characterized by distal tubular and extensive MTAL damage (Rosen & Heyman, 2001).

The vulnerability of the MTAL segment in the isolated erythrocyte-free perfused kidney model results from the high metabolic requirements of this cell type in combination with the small amount of dissolved oxygen that can be delivered by the aqueous phase of the perfusate: it was demonstrated that in this specific model, pre-existing proximal tubular necrosis (and thereby diminished GFR) prevents "downstream" MTAL damage by diminishing the workload (and thus metabolic requirement) of the MTAL (Heyman et al., 2002). Similarly, the relative preservation of the MTAL segment in the rat RAO model may be attributed to the total cessation of GFR.

In 1980, Hanley used the isolated tubule microperfusion technique to investigate different nephron segments, freshly isolated from rabbit kidneys that had been subjected to 60 minutes of ischemia. Morphological alterations were noted in the proximal segments but not in the distal segments. Cortical proximal straight tubule fluid reabsorption was reduced by 88%, and the ability of the TAL to lower perfusate Cl^- concentration was reduced by 60% (Hanley, 1980).

1.2.2.3 Anatomo-pathological findings in humans

Renal biopsies of ARF patients suggest that despite the clinical term of Acute Tubular Necrosis, frank necrosis of tubular cells is relatively inconspicuous. The major abnormality is usually patchy and focal loss of individual or clusters of cells from tubular epithelium (Rosen & Heyman, 2001).

While changes in the proximal nephron may predominate in some animal models of tubular cell injury, clinical biopsies often show prominent injury in the distal nephron segments in the cortex and outer medulla. Injury to the MTAL and to the distal nephron is commonly seen, and it is not infrequent in clinical renal

biopsies to see injured distal tubules while proximal tubules remain relatively intact (Racusen, 2001).

These data strongly suggest that distal tubular cells are at least as important as proximal tubular cells in the pathophysiology of human ARF. It is therefore surprising to find only a limited number of studies that focus on distal tubular cells and at the same time it is one of the major reasons why in this work the MTAL cells will be investigated.

1.2.2.4 Differences in metabolism between proximal tubular cells and MTAL cells

Because glucose can be metabolized under both aerobic (to CO_2) and anaerobic (to lactate) conditions to produce ATP, many studies have examined whether nephron segments such as the proximal tubule and MTAL can maintain normal ATP contents and transport rates when mitochondrial oxidative phosphorylation is inhibited. This is a particularly important issue in terms of the difference in susceptibility of the different nephron segments to hypoxic or anoxic injury (Gullans & Hebert, 1996).

In the rabbit kidney, hexokinase activity (glycolytic activity) was found to be lowest in the proximal convoluted tubule and to increase along the following nephron segments, with highest activity in the connecting tubule. The gluconeogenetic enzyme phosphoenolpyruvate carboxykinase (PEPCK) was found exclusively in the proximal tubule (Vandewalle et al., 1981). In the isolated perfused rabbit TAL, Wittner et al. (Wittner et al., 1984) examined the role of different substrates in providing ATP for transepithelial NaCl reabsorption by measuring the short circuit current (I_{sc}): glucose, lactate, acetate and ß-hydroxybutyrate, but not glutamine and glutamate, represent efficient substrates for sustaining active ion transport. Addition of CN^- (1 mM) in the presence of glucose, reduced the I_{sc} by 60%. This indicates that in rabbit TAL, mitochondrial oxidative phosphorylation is dominant over anaerobic glycolysis in providing ATP for NaCl reabsorption. The same investigators observed that removal of substrates from both sides of the epithelium lead to a rapid and pronounced fall in I_{sc}. Therefore the TAL cells seem to be devoid of large energy reservoirs (such as glycogen) from which they could live on in the absence of external substrate. Na^+,K^+-ATPase activity is quite high in TAL, so that the turnover rate of the ATP pool is very fast (ATP half-life is about 4-5 s) (Morel & Doucet, 1992).

These data indicate that TAL cells, in contrast to proximal tubular cells, contain high activities of glycolytic enzymes which points to the role of glucose as a metabolic fuel in this nephron segment (Doucet & Morel, 1992). This difference in metabolism between proximal and distal tubular cells may explain a relative

resistance of the distal nephron to hypoxia and anoxia, since in the presence of glucose, ATP production can be at least partially sustained by anaerobic glycolysis. However, it is likely that during ischemia (cessation of blood flow which results not only in hypoxia, but also in the absence of substrates), anaerobic glycolysis will persist only for a very limited amount of time (seconds rather than minutes) since extracellular glucose will be very rapidly depleted. Therefore, glycolytic ATP production may provide some degree of resistance of MTAL cells to hypoxic circumstances. However, during ischemia, it is unlikely that MTAL cells will be protected by this mechanism. The idea that MTAL cells are not protected by glycolytic ATP production is supported by the observation that in the erythrocyte-free perfused kidney, extensive and selective MTAL damage is observed, despite the presence of glucose (5 mM) in the perfusate (Alcorn et al., 1981).

1.2.2.5 The ISOM as critical zone in ischemia-reperfusion injury

Renal IRI is associated with an acute inflammatory response that occurs in waves: early induction of adhesion molecules, cytokines, and chemokines in the first hour that induce neutrophil accumulation starting at 2 to 4 hours. This is followed by later accumulation of macrophages and T-cells at about 24 to 48 hours, and numbers start to decrease by 72 hours (Rabb & Star, 2001; Bonventre & Weinberg, 2003). Until recently, this leukocyte infiltrate, particularly the neutrophils among them, was considered as a cause of damage, exacerbating renal injury in the reperfusion phase by releasing reactive oxygen species (ROS) and enzymes that can directly injure cells (Lameire & Vanholder, 2001). On the other hand, infiltrating leukocytes may act as scavengers of apoptotic cells and necrotic cellular debris, and may be a source of growth factors, and therefore may take part in the repair process (Degreef et al., 2003). Yokota et al. (Yokota et al., 2000) recently demonstrated that Interferon-γ production by T-lymphocytes during ischemia-reperfusion injury is deleterious for renal function, whereas IL-4 production by T-lymphocytes improved functional outcome.

The expression of JE, a growth-factor-responsive gene that codes for a small secreted glycoprotein with cytokine-like properties, which may play a role in inflammation, was found to be increased in the reperfusion period in the TAL (Safirstein et al., 1991). Sublethal damaged epithelial cells in proximal tubules and thick ascending limbs have the capacity of liberating chemotactic substances which, through upregulation of adhesion molecules at the site of endothelial cells, may facilitate a leukocyte adhesion/infiltration (Ysebaert et al., 2000). Interestingly, as mentioned in paragraph1.2.1.1, ICAM-1 expression and leukocyte infiltration early after ischemia-reperfusion is most pronounced in the ISOM (Degreef et al.,

2003). In this region of the kidney, medullary thick ascending limb segments, but no straight proximal tubules are present (see Fig. 3.1). This may indicate that sublethal changes in MTAL cells play a crucial role in the pathophysiology of renal IRI and this is, in addition to the anatomo-pathological findings in human ARF, a second major reason for investigating MTAL cells in the present work.

1.2.2.6 Early gene expression

In addition to inflammation, mitogenic phenomena accompany the renal response to ischemic injury. Ischemia induces alterations in the expression of a multiplicity of genes, a response that is similar to that induced in cultured cells by growth factors. Expression of the "early immediate response genes" such as *c-fos* an *egr-1* increases almost immediately after renal ischemia and precedes increased protein or DNA synthesis. Interestingly, most genes induced by ischemia-reperfusion are expressed predominantly in the MTAL segment (Safirstein et al., 1998; Brady et al., 2000). Also, in the RAO model, the MTAL responds with up-regulation of anti-apoptotic Bcl-2 genes (Gobé et al., 1999). Cell cycle inhibitors (the cyclin-dependent kinase inhibitors such as p21 and 14-3-3σ) are also induced after ischemic injury to the kidney, primarily in the TAL, distal convoluted tubules and collecting ducts. Their combined activities check the cell cycle at the G_1-to-S and G_2-to-M transitions. Cell cycle arrest is a prerequisite for renal cell repair and/or regeneration after injury, and the inhibition of the cell cycle allows the repair of cellular damage to occur before cell replication (Megyesi et al., 2002). Therefore, the TAL epithelial cells may, in some instances, be adaptively resistant to IRI and function as a reservoir for the production of growth factors critical to the maintenance and/or regeneration of their own cell population (autocrine action) and also the proximal tubular cells that abut on them (paracrine action) (Gobé et al., 1999; Brady et al., 2000).

1.3 Pathophysiology of ARF at the cellular level: tubular cell ischemia

The changes in tubular epithelial cell function that lead to renal dysfunction and ultimately to obstruction of the tubular lumen and backleak of ultrafiltrate, can be understood only by defining the alterations in cell physiology that result from ischemia. Even though great progress has been made in the last decade in understanding the molecular mechanisms of apoptosis, the biochemical pathways leading to necrotic cell death remain poorly understood (Martin, 2001).

Only a very limited number of studies on the cellular pathophysiology of ischemia in MTAL cells or distal tubular cells in general, has been published. Therefore this general introduction to the cellular pathophysiology of renal ischemia is based on data derived from proximal renal cells or in some cases non-renal cells, if no data on renal cells are available. An overview of the limited available data on ATP, pH_i and Ca^{2+} measurements performed on distal tubular cells during ischemia will be presented in the introduction to chapter 5.

1.3.1 Cellular energy metabolism

A fall in cell ATP levels is an early event following oxygen deprivation due to ischemia and is believed to be the proximate event responsible for cell dysfunction and death. Prolonged ischemia will ultimately result in irreversible loss of mitochondrial function, which impairs rapid regeneration of ATP following reperfusion. Thus, the rate of cell ATP recovery following reperfusion, along with the ability of the cell to survive ischemia, is therefore dependent upon the duration of the ischemic period (Brady et al., 2000). Using ^{31}P NMR, a rapid and complete normalization of intracellular ATP was observed if renal ischemia lasted no longer than 15 minutes. If renal ischemia was prolonged, the regeneration of ATP was less complete (Chan & Shapiro, 1989).

Ischemic renal injury leads to a rapid decrease in the level of the adenine nucleotide pool (ATP, ADP and AMP). The adenine nucleotides are degraded to the purine nucleosides adenosine and inosine (Padanilam, 2003). The catabolism of AMP to adenosine appears to be the primary pathway for nucleotide degradation. Adenosine is metabolized to hypoxanthine. In the rabbit kidney, in contrast to the rat kidney, no further catabolism to xanthine or uric acid occurs because of the absence of xanthine oxidase in the rabbit kidney (Burke & Schrier, 1997).

The fate of intracellular nucleotides was investigated in suspensions of rabbit proximal tubular cells. During 30 minutes of hypoxia, intracellular ATP levels fell and AMP levels increased. In the extracellular space, AMP, inosine and

hypoxanthine were detected. Hypoxanthine was the predominant purine present. Recovery of cell ATP during reoxygenation was from remaining cell nucleotides rather than from the nucleosides and bases (Weinberg, 1988). However, since the purine metabolites are more membrane permeable due to well defined mechanisms for their membrane transport, prolonged ischemia will lead to the continued loss of these precursor nucleosides and will make the cells dependent on the precursor compounds that become available during reperfusion for ATP re-synthesis (Padanilam, 2003). The improved proximal tubule viability associated with the administration of ATP-$MgCl_2$ in vitro appears to be due to adenosine itself, which is generated extracellularly from catabolism via ecto-ATPase of the added ATP. Adenosine then enters the cells in order to enhance ATP production (Burke & Schrier, 1997).

The fate of inorganic phosphate (P_i) has been investigated with ^{31}P NMR: when clamp ischemia is applied to the rat kidney, ATP concentration decreases dramatically and at the same time, P_i concentration increases (Chan & Shapiro, 1989). This experiment however provides no information on further changes in P_i concentration during ischemia and reperfusion.

Structural, functional and biochemical abnormalities of mitochondria are widely believed to be important pathogenic factors that underlie ischemic cell injury. Two defects recently have captured attention. One is characterized by pore formation in the inner mitochondrial membrane, de-energization and swelling (mitochondrial pore transition, MPT). MPT precedes and triggers nuclear apoptosis whereas the stabilization of MPT by anti-apoptotic proteins (Bcl-2 or Bcl-X_L) or cyclosporine A rescues apoptosis. The second involves leakage of cytochrome *c* from the inner membrane space into the cytosol, which activates caspase-9 by forming a complex with Apaf-1, procaspase-9 and dATP. Cytochorome *c* leakage may follow the MPT or occur independently. There is general agreement that these dramatic alterations result in cell death by necrosis and/or apoptosis. However, the proximate events that lead to the MPT and loss of cytochrome *c* are unclear and are subjects of ongoing investigation (Ueda et al., 2000; Weinberg et al., 2000).

1.3.2 Cell death by apoptosis or necrosis

In humans and experimental models of renal ischemia, tubular cells in various nephron segments undergo necrotic and/or apoptotic cell death. In isolated perfused rat kidneys, signs of apoptosis were detected selectively in thick ascending limbs after 10 minutes of hypoxia (Beeri et al., 1995). Apoptosis is defined by cytoplasmic and nuclear shrinkage, chromatin margination and

fragmentation, and breakdown of the cell into multiple spherical bodies that retain membrane integrity (Padanilam, 2003).

Unlike apoptosis, that occurs in normal and disease states, necrosis is induced only when cells are exposed to severe, acute injury. Severe depletion of ATP leads to failure of the pump-leak balance mechanism, leading to an influx of Na^+ and H_2O that results in cytoplasmic swelling. The latter feature leads to cellular fragmentation and release of lysosomal and granular contents into the surrounding extracellular space, with subsequent inflammation (Carini et al., 1995).

The perception that apoptosis and necrosis are functionally opposed forms of cell death is fading, and a consensus has developed that both phenotypes of cell death constitute two extremes of a continuum (Padanilam, 2003; Gobé et al., 1999; Wiegele et al., 1998; Lieberthal et al., 1998).

In primary cell cultures of mouse proximal tubular cells, the effect of a graded ATP depletion ranging from 2 to 70% of control levels was studied. Cells subjected to ATP depletion below 15% of control died uniformly of necrosis. Cells subjected to ATP depletion between 25 and 70% of control all died by apoptosis. Therefore, a narrow range of ATP depletion between 15 and 25% of control seems to represent a threshold that determines whether cells die by necrosis or apoptosis. This observation falls within the accepted paradigm of apoptosis, having an absolute requirement for ATP (Lieberthal et al., 1998).

Dagher (Dagher, 2000) demonstrated in LLC-PK cells that during 45 minutes of ischemia, GTP levels decreased in parallel with ATP levels. He observed a similar pattern of parallel ATP and GTP depletion in cells from the renal cortex, which had been subjected to *in vivo* ischemia by artery occlusion. GTP is synthesized from GDP and ATP by the nonspecific enzyme nucleoside diphosphate kinase. This reaction is driven by the depletion of GTP through its exergonic hydrolysis in the biosynthetic reactions in which it participates (Voet & Voet, 1990). Of more interest is the observation that a selective GTP depletion (with mycophenolic acid) resulted in significant apoptosis in LLC-PK cells, whereas selective ATP depletion (with alanosine) caused mostly necrosis (Dagher, 2000). The apoptosis during states of GTP depletion seems to be mediated by p53 and its downstream targets p21 and Bax (Kelly et al., 2003). Further *in vivo* studies revealed that selective GTP re-pletion during the reperfusion phase was accompanied by a significant reduction in medullary apoptosis and a remarkable protective effect on GFR (Kelly, 2001). Also different methods to prevent apoptosis (the use of the caspase inactivator ZVAD-fmk and inhibition of complement factor C5) during renal ischemia-reperfusion injury, proved to be strongly protective against renal dysfunction (Daemen et al., 1999; De Vries et al., 2003).

1.3.3 Acidosis

Two cardinal features of ischemia are hypoxia and up to a 100-fold increase of H^+ concentration (Herman & Gores, 1990). Studies on kidneys and renal cells consistently report intra and/or extracellular acidosis during ischemia (Chan & Shapiro, 1989; Dittert et al., 1997; Môller et al., 2000; Hropot et al., 2001), with the exception of freshly isolated proximal tubules (Weinberg et al., 1994; Rose et al., 1995) and the rejecting renal allograft in which, despite a marked decrease in ATP concentration, no change in intracellular pH was demonstrable (Chan & Shapiro, 1989).

Acidification during ischemia is believed to be the consequence of glycolytic lactate production (glucose $\rightarrow$ 2 lactate$^-$ + H^+), CO_2 accumulation, hydrolysis of ATP (ATP + $H_2O \rightarrow n.H^+ + P_i$ + ADP, where *n* varies with pH and Mg^{2+} concentration) and inhibition of transport processes that maintain acid-base balance in physiological conditions (e.g. Na^+/H^+ exchanger (NHE), H^+-ATPase, Cl^-/HCO_3^-) (Katsura et al., 1992; Brady et al., 2000).

Severe intracellular acidosis can contribute to ischemic cell injury, although only pH values below 6.3 cause irreversible morphological alterations (Bretschneider et al., 1988; Dittert et al., 1997). Acidosis can be detrimental because of the decrease of enzyme activities, the decrease of lysosomal membrane stability, the disruption of the binding of transition metals (e.g., iron) to carrier proteins (Môller et al., 2000), and the self-inhibition at the phosphofructokinase step of anaerobic glycolytic ATP production (Dittert et al., 1997).

Although severe intracellular acidosis can clearly contribute to ischemic cell injury, there is convincing evidence that a decrease in cellular pH in the range observed during ischemia *in vivo* is more likely to protect cells from the damaging effect of oxygen deprivation. Shanley et al. (Shanley et al., 1988). demonstrated that mild *extracellular* acidosis (pH 7.0) is cytoprotective for the TAL segment in the isolated perfused rat kidney. Similarly, *extracellular* acidification (pH 6.9) strongly protected against lactate dehydrogenase release during hypoxia in freshly isolated proximal tubules (Weinberg, 1988) and during chemical ischemia (iodoacetate and KCN) in suspensions of distal tubular cells (Lash et al., 1996). Some years later, Weinberg et al. (Weinberg et al., 1994) demonstrated that in freshly isolated proximal tubules, *intracellular* pH readily equilibrated with the cytoprotective decreases of medium pH during chemical ischemia.

The mechanisms responsible for the protective effect of acidosis are likely to be multifactorial. Acidosis does not result in a better preservation of ATP levels although it is possible that total cellular nucleotide content is better preserved

under acidic conditions due to the reduction in AMP metabolism by inhibition of cytosolic 5'-nucleotidase (Weinberg, 1988; Lash et al., 1996; Burke & Schrier, 1997). Acidosis may preserve ionic gradients by reducing plasma membrane permeabilities for K^+ and Ca^{2+} (McNicholas et al., 1988; Zeiske et al., 1999). Acidosis stabilizes cell membranes (Bell et al., 1971). Acidosis directly inhibits Na^+,K^+-ATPase activity (Eaton et al., 1984), so it is possible that acidosis reduces transport activity resulting in less energy demand. Finally, acidosis may reduce the activity of some isoforms of phospholipase A_2 that act optimally at physiologic pH. Phospholipase A_2 may contribute to IRI by cleaving phospholipids, resulting in free fatty acid and lysophospholipid. Both have a direct toxic effect on plasma membrane integrity (Sheridan & Bonventre, 2000).

1.3.4 Intracellular free calcium concentration ($[Ca^{2+}]_i$)

The cytosolic and organellar Ca^{2+} concentration within cells requires tight regulation by active transport because the concentration of Ca^{2+} in extracellular fluid exceeds the intracellular concentration (approximately 100 nM) approximately 10,000 fold. This gradient is maintained by Ca^{2+} ATPases of the plasma mebrane and the endoplasmatic reticulum and by a plasma membrane Na^+/ Ca^{2+} exchanger (Brady et al., 2000).

Substantial evidence now suggests that an increase in $[Ca^{2+}]_i$ plays an important role in necrosis (Edelstein et al., 1997; Levine & Lieberthal, 2001). In rat proximal tubules, clear evidence exists that during hypoxia, a significant rise in $[Ca^{2+}]_i$ precedes evidence of membrane damage as assessed by propidium-iodide staining (Kribben et al., 1994). Using the same model system, Peters et al. (Peters et al., 1996). demonstrated that the increase in total cell calcium was correlated with the severity of hypoxia. In rabbit proximal tubular cells, anoxic incubation increases $[Ca^{2+}]_i$ from 100 to 400 nM. After addition of verapamil, $[Ca^{2+}]_i$ only increased to 120 nM during anoxia, and this was associated with an increased survival of the proximal tubular cells (Rose et al., 1994). In rat proximal tubular cells, Peters et al. (Peters et al., 1996) demonstrated that the increase of total cell calcium was correlated to the severity of hypoxia. The Ca^{2+} channel blocker verapamil also protected (functionally and morphologically) the kidneys during *in vivo* renal ischemia in the rabbit (Alvarez et al., 1994). In human renal transplantation however, two randomized, placebo-controlled studies could not demonstrate a beneficial effect of the use of calcium channel blockers (Ladefoged & Andersen, 1994).

An early rise in the concentration of intracellular free Ca^{2+} following ATP depletion has the potential to cause cell injury and death by different mechanisms.

Intracellular protein degradation is increased by a rise in $[Ca^{2+}]_i$, since a group of cytosolic proteases, whose activities depend on micromolar concentrations of $[Ca^{2+}]_i$, does exist. Activation of such proteases may alter the structure of the subplasmalemmal cytoskeleton, resulting in plasma membrane blebbing, an often observed consequence of cell injury (Herman et al., 1990; Garza-Quintero et al., 1993).

In glomerular mesangial cells, *phospholipase A_2* activity (see previous paragraph) was potentiated in the range of calcium levels from 100 nM to .9 µM, which may explain the activation of phospholipase A_2 in the face of the relatively small increases in $[Ca^{2+}]_i$, observed following injury to cells (Bonventre & Swidler, 1988; Herman et al., 1990).

An increase in $[Ca^{2+}]_i$ can facilitate *the generation of oxygen free radicals* by accelerating the conversion of xanthine dehydrogenase to xanthine oxidase through a calmodulin-calcium dependent protease. This is the enzyme that during reperfusion, generates superoxide ions due to the conversion of hypoxanthine to xanthine and further to uric acid. This is especially true during reperfusion in rat tubules. Since this reaction requires the presence of oxygen, ROS could also be formed during the "ischemic" phase of chemical ischemia, since the ambient atmosphere contains O_2. It is important to note however, that rabbit (species used in our study) kidney, like human kidney, in contrast to rat kidney, contains little xanthine oxidase activity (Burke & Schrier, 1997; Brady et al., 2000). This might explain why allopurinol (a xanthine oxidase inhibitor) has no beneficial effect in renal IRI in the rabbit (Hansson et al., 1986).

In *mitochondria*, isolated from rat renal cortical tissue, it was shown that especially the combination of an increased calcium concentration and the presence of ROS is deleterious for mitochondrial function: a pronounced increase in mitochondrial membrane permeability and a major functional defect in the electron transport chain resulted in a complete uncoupling of respiration (Malis & Bonventre, 1986).

Although the precise role of calcium is still being evaluated (see next paragraph), these data suggest that an increased $[Ca^{2+}]_i$ is an important event in the evolution of ischemia-reperfusion injury.

1.3.5 Correlation between changes in $[Ca^{2+}]_i$ and pH_i during IRI

In the isolated perfused rat kidney, an opposing effect was observed of extracellular calcium concentration and extracellular pH with respect to the extent of hypoxic damage in the TAL: the protection afforded by extracellular acidosis (pH 7.0) was overcome by increasing perfusate calcium concentration and the injury

caused by Ca^{2+} at these higher concentrations was again reduced by further decreasing pH (Shanley & Johnson, 1991).

Weinberg et al. (Weinberg et al., 1991) have shown that acidosis exerts its protective effect despite a very impressive elevation of cytosolic free Ca^{2+} which was achieved by the use of an ionophore. This study suggests that (part of) the protective effects of acidosis in renal ischemia seem to exert themselves at sites distal to the increase in $[Ca^{2+}]_i$. One such site may consist of an acidosis-induced reduction in affinity of calmodulin for Ca^{2+} and thereby impairment of multiple calcium-calmodulin regulated events such as calpain activation (Edelstein et al., 1996; Brady et al., 2000).

However, extracellular acidosis may exert its protective effect proximal of the increase in $[Ca^{2+}]_i$ by limiting the magnitude of the Ca^{2+} influx. Different hypotheses on the underlying mechanism have been proposed. Acidosis may limit Ca^{2+} influx by inhibition of Ca^{2+} fluxes between the cytosol and the extracellular space, as it does in normoxic states (Studer & Borle, 1979). Extracellular acidosis may inhibit the Na^+/H^+ exchanger thereby preventing Na^+ and thus Ca^{2+} overload (through the diminished forward or even the backward action of the Na^+/Ca^{2+} exchanger) (Karmazyn, 1988; Meng et al., 1991; Burke & Schrier, 1997). This backward action has been demonstrated in monkey kidney cells (Snowdowne & Borle, 1985). Na^+/Ca^{2+} exchange activity has also been demonstrated in basolateral membrane vesicles from rat kidney cortex (van Heeswijk et al., 1984).

1.3.6 The Na^+/H^+ exchanger and NHE inhibition during IRI.

If inhibition of Na^+/H^+ exchange during ischemia by extracellular acidosis is protective, then pharmacological NHE inhibition might be useful to prevent organ damage in IRI.

The *in vivo* ischemic reperfused myocardium can be protected when NHE-1 (the "housekeeping" NHE isoform, see introduction to chapter 4) is inhibited before or at the onset of ischemia (Hendrikx et al., 2001; Knight et al., 2001). The protective mechanisms of NHE inhibition have been investigated especially in myocardial cells (more than 100 publications in 2002), but also in hepatocytes (Gores et al., 1989), endothelial cells (Symons & Schaefer, 2001; Gumina et al., 2001), kidney cells (Hropot et al., 2001) and neuronal cells: in cultured neuronal cells, NHE inhibitors during reperfusion after metabolic inhibition were protective (Vornov et al., 1996) and during *in vivo* experiments in rats, NHE inhibition during acute cerebral ischemia reduced infarct size and brain edema (Kitayama et al., 2001).

The cellular mechanism(s) that underlie this protection by NHE inhibitors during ischemia and/or reperfusion is unclear. As proposed in the previous paragraph, NHE inhibition is believed to limit Ca^{2+} overload by first decreasing Na^+ overload, which will prevent backward action of the Na^+/Ca^{2+} exchanger and thereby prevent Ca^{2+} accumulation in the ischemic cell. In isolated hearts from guinea pig, NHE inhibitors given before ischemia or on reperfusion diminished both Na^+ and Ca^{2+} loading (An et al., 2003). In isolated rabbit hearts, blockade of the Na^+/Ca^{2+} exchanger was shown to be even more efficient than NHE blockade for protection from reperfusion injury (Matsumoto et al., 2002).

However, also conflicting results have been published. In cardiomyocytes, NHE inhibition during simulated IRI was shown to be protective independently of cytosolic acidification and Ca^{2+} overload (Schäfer et al., 2000). In isolated rat cardiomyocytes, NHE inhibition did not attenuate Ca^{2+} overload (Russ et al., 1996). In freshly isolated cardiomyocytes from guinea pigs, NHE inhibition reduced the Na^+ overload but had no effect on $[Ca^{2+}]_i$ (Salameh et al., 2001).

An alternative mechanism by which NHE inhibition may be protective, is the maintenance of intracellular acidosis during the reperfusion phase (Russ et al., 1996; Bak & Ingwall, 2003). Indeed, if acidosis is protective during ischemia (see 1.3.3), then a rapid return to normal pH values during reperfusion might be harmful: in cultured rat cardiomyocytes, the increase in pH_i during reperfusion precipitated cell death independently of the changes in $[Ca^{2+}]_i$ during reperfusion. This observation was referred to as the "pH paradox" (Bond et al., 1993).

Other mechanisms may be involved in NHE-dependent organ protection. Leukocyte adhesion and emigration were markedly reduced by NHE inhibitors in ischemic rat muscle, possibly because of increased L-selectin shedding of activated leukocytes. This may attenuate the post-ischemic inflammatory response (Redlin et al., 2001).

1.3.7 The protective effect of glycine

Recently, Yin et al. (Yin et al., 2002) observed an *in vivo* protective effect of a bolus injection of glycine given before reperfusion together with dietary glycine supplementation in the rat renal artery occlusion model. This protective effect was observed only when the cross-clamping of the renal artery lasted no longer than 15 minutes.

The cytoprotective effect of glycine during IRI was discovered in the isolated proximal tubule preparation (Weinberg et al., 1991) and was further investigated in kidney cells and hepatocytes. The protective effect offered by glycine was shown to be independent of changes in pH_i (Weinberg et al., 1994;

Sakaida et al., 1996), ATP (Sakaida et al., 1996; Weinberg et al., 1989), Ca^{2+} (Rose et al., 1994a) and also independent of fatty acid accumulation (Weinberg et al., 1995). Observations in ATP-depleted MDCK cells suggest that the cellular abnormality that is suppressed by glycine involves rearrangement of plasma membrane proteins to form water-filled pores large enough to enable the permeation of macromolecules (Dong et al., 1998).

Since glycine is abundant in renal tissue under normal conditions, it is most appropriately considered a "natural modifying factor" (Weinberg et al., 1994). However, during the reperfusion period, glycine content was significantly reduced both in the outer medulla and in the cortex from rat kidneys that had been subjected to 60 minutes of renal artery clamping (Beck et al., 1995).

To avoid an artificially increased sensitivity to IRI during *in vitro* experiments, all experimental solutions should contain glycine.

1.4 The use of cell cultures in the study of renal IRI

The complex composition of the kidney, in terms of morphology and physiological and biochemical functions, necessitates detailed investigations of responses of the various nephron segments to ischemia. There has been an evolution over the past decades to go from whole animal, isolated organ to cellular (either freshly isolated or cultured) cells. Most of the efforts have been directed at isolated cell systems using freshly prepared tissue, primary tissue culture, or established cell lines (Burke & Schrier, 1997).

Immortalized cell lines derived from proximal tubular cells (LLC-PK_1) and distal tubular cells (MDCK and A6) have been widely used to investigate the cellular pathophysiology of ARF. Their routine use in cell culture labs provides numerous, especially practical advantages. Several factors have to be kept in mind when conducting experiments with immortalized cell lines. Apart from loss of cell differentiation and development of ambiguous hybrid phenotypes (Helbert et al., 2001), cell lines have been reported to be more resistant to the effects of oxygen deprivation than primary cell cultures. This has been attributed to relative preservation of ATP stores because of glycolytic adaptation and anaerobic ATP production (Ardaillou et al., 2000). This may be overruled by blocking both aerobic and glycolytic pathways of ATP production (metabolic inhibition). However, other factors contribute to the resistance of cell lines to anoxia: MDCK cells were shown to release less free fatty acids (FFA) in comparison to primary cell cultures of mouse proximal tubular cells. It may therefore be that differences in anoxia-induced PLA_2 activity between the two cell types may play a role in the resistance of MDCK cells to injury (Sheridan et al., 1993).

Primary cultured cells derived from different nephron segments of rabbit kidneys were shown to have different susceptibilities to anoxia and ischemia: 45 minutes exposure to N_2 in either cell culture medium (anoxia) or phosphate buffered saline (ischemia) showed differential cell killing (statistically significant) dependent on the segment of origin: MTAL = S3 > S2 = CCT > S1. These results indicate that cultured cells from different nephron segments have different intrinsic susceptibilities to ischemia (Wilson & Schrier, 1986). Lash et al. (Lash et al., 1995) examined the susceptibility of proximal and distal tubular (PT and DT) cells to chemically induced toxicity. Both freshly isolated nephron segments and primary cell cultures from rat kidneys were used. DT cells were significantly more susceptible to injury from both *tert*-butyl hydroperoxide and methyl-vinyl-ketone, but the two cell populations were equally susceptible to injury from *p*-aminophenol, which is the same susceptibility pattern seen in freshly isolated cells. These results suggest that primary cultures of rat renal PT and DT cells reflect similar

biochemical properties as freshly isolated cells and are, therefore, useful models for the study of chemically induced injury. Therefore, it seems useful to culture renal cells from different parts of the nephron to investigate their specific responses to IRI.

1.5 Aims of the present study

Since existing methods for obtaining primary cell cultures from MTAL segments have the disadvantage of yielding a mixture of different cell types, the *first goal* of this study is to develop a new method for obtaining 100% pure primary cell cultures from MTAL segments of rabbit kidneys. This will allow us to evaluate whether cells within the same monolayer behave homogeneously.

A *second goal* is to characterize these primary cell cultures with respect to their phenotype as MTAL cells. This will include the investigation of their morphology, electrophysiological characteristics and hormone responsiveness. These characteristics can then be compared with those from an immortalized cell line of the same origin (TALH-SVE) (Scott et al., 1986), which will be used in parallel studies.

Since changes in intra- and extracellular pH play a crucial role in IRI, a *third goal* of this work consists of the extensive characterization of the pH regulatory mechanisms of these primary cell cultures. Apart from Na^+/H^+ exchangers and H^+ pumps, NH_4^+ transport pathways will be investigated since NH_4^+ reabsorption by the MTAL has a profound impact on its intracellular pH.

The *fourth goal* of this study is to investigate the cellular pathophysiology of metabolic inhibition in these primary cultured MTAL cells. The discovery of the important role of glycine as a protective agent during ischemia, emphasizes the importance of working in physiologically relevant conditions. Therefore all experiments will be performed at 37° C and a balanced salt solution containing phosphate, magnesium and small amino acids will be used.

The focus will be on sublethal injury to the cells. Therefore, first the ischemia and reperfusion time interval that leads to sublethal injury in these cells will be determined. To further validate this model of sublethal ischemic damage, changes in ATP during this time interval will be measured.

For reasons outlined in the introduction, a detailed description of the parallel changes in $[Ca^{2+}]_i$ and pH_i during ischemia and reperfusion will be realized. By using digitized microfluorescence, the correlations between different parameters (for example pH_i and cell death) can be investigated at the single cell level. Possible protective mechanisms and/or interventions, such as NHE inhibition, also belong to the scope of this study.

A *final goal* of this study is to compare the results obtained during IRI in these primary cell cultures to the results that were obtained on immortalized cell lines of the distal nephron such as A6, MDCK and TALH-SVE cells.

Chapter 2

Materials and methods

2.1 Cell-culture

Methods and materials for obtaining primary cell cultures from rabbit MTAL segments are described in detail in chapter 3.

An immortalized cell line derived from rabbit MTAL cells (TALH-SVE) was kindly supplied by prof. dr. R.K.H. Kinne (Max-Planck-Institute für Molekulare Physiologie, Dortmund, Germany). For further characterization passages 39 to 49 are used. The culture medium consists of Dulbecco's modified Eagle's (DME) medium supplemented with 10% Fetal Calf Serum (FCS) (heat inactivated), L-glutamine 2 mM, Minimal Essential Medium (MEM) Non-Essential Amino Acids Solution 1X, sodium pyruvate 1 mM, 2-mercaptoethanol 50 µM, bovine thyrocalcitonin 0.1 µM and arginin-vasopressin (AVP) 0.1 µM. The cells are inoculated in 25 cm^2 tissue culture flasks and are maintained in a standard humidified incubator (95% air - 5% CO_2) at 37° C. The medium is replaced every 48 hours. Confluent cultures are trypsinized with PBS containing 0.25% trypsin and 0.2% EDTA. For experiments cells are grown in cell culture inserts with 0.33 cm^2 collagen-coated (equimolar mixture of types I and III collagen derived from bovine placentae) polytetrafluoroethylene (PTFE) membranes, pore size 0.4 µm (Transwell-COL™, Costar™, Corning Inc., USA) and in 24 well cell culture clusters (tissue culture treated, Costar™, Corning Inc., USA) (Jans et al., 2000).

2.2 Metabolic inhibition

Metabolic inhibtion is a pharmacological approach to mimic the effects of ischemia. Cells are able to produce ATP via two distinct pathways: first, anaerobic ATP production by cytosolic glycolysis with conversion of pyruvate to lactate, and second, the mitochondrial oxidative phosphorylation. In *in vitro* cell culture models ischemia can be simulated by inhibition of both metabolic pathways (Canfield et al., 1991; Sheridan et al., 1993; Doctor et al., 1994). Respiration can be blocked by the addition of mitochondrial inhibitors (Fig. 2.1). Glycolysis can be inhibited through the removal of glucose and addition of 2-deoxyglucose (DOG).

The glucose-derivative, 2-deoxy-glucose, is phosphorylated to DOG-6-phosphate (DOG-6-P) by the intracellular glycolytic hexokinase. DOG-6-P competitively inhibits the conversion of glucose-6-posphate (G-6-P) to fructose-6-phosphate by G-6-P isomerase (metabolization of DOG-6-P by G-6-P isomerase occurs very slowly) and therefore effectively inhibits glycolysis (DOG-6-P cannot leave the cell) (Wick al., 1957). By undergoing extensive phosphorylation DOG depletes

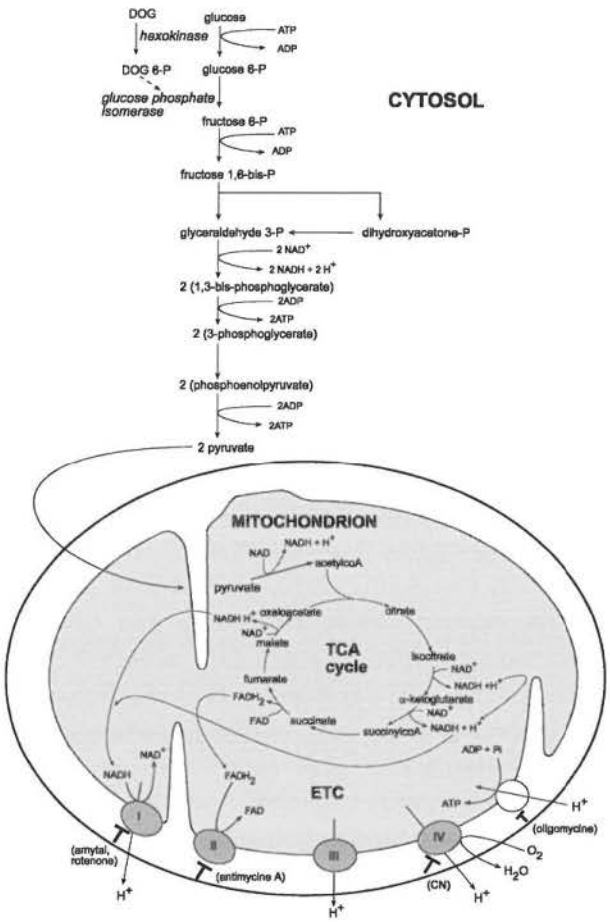

Figure 2.1 *Schematic presentation of cellular metabolic pathways. The upper part of the figure illustrates the cytosolic glycolysis. The interference of 2-deoxyglucose (DOG) with the glycolytic enzyme glucose phosphate isomerase is indicated. The end-product of aerobic glycolysis, pyruvate, enters mitochondria and, after conversion to ac-CoA, serves as a substrate for the tricarboxylic acid cycle (TCA cycle). The supply of substrate to the TCA cycle promotes the reduction of NAD^+ to NADH and of FAD to $FADH_2$. As these are re-oxidized, they supply electrons to the electron transport chain (ETC). In the process of electron transfer to O_2, protons are translocated across the inner mitochondrial membrane, generating a potential gradient of –150 to –180 mV. ATP synthesis takes place at a separate site, the ATP synthase (F_1F_0-ATP synthase). The enzyme is driven by the downhill movement of H^+ and phosphorylates ADP, producing ATP, which is transported out of the matrix by the adenine nucleotide translocase in exchange for ADP. The blockers for the different sites of the ETC are indicated between brackets (adapted with permission from Smets, 2001).*

existing ATP stores (Lieberthal et al., 1998). Accumulation of DOG-6-P is self-limiting because DOG-6-P is competitive versus ATP for hexokinase (feedback inhibition of hexokinase). In the presence of glucose and in the absence of CN^- this causes the DOG-6-P formation to stop at 50 mM (Chen & Guéron, 1992). Therefore, when using DOG in combination with a mitochondrial inhibitor and in the absence of glucose, formation and thus accumulation of DOG-6-P will be limited since ATP stores will be rapidly depleted. Although DOG-6-P is a competitive inhibitor of G-6-P isomerase, in the whole animal model the DOG effect seems "irreversible" since even low plasma DOG concentrations are capable of blocking glycolysis at a high and constant level (Wick et al., 1957). The whole animal model is however different from an *in vitro* cell culture model where DOG can be added in the absence of glucose and where, on reperfusion, DOG can be completely removed and replaced by glucose. It seems that with this type of protocol, the DOG effect is, at least partially, reversible (Doctor et al., 1994).

The mitochondrial oxidative phophorylation is blocked by cyanide (CN^-). Hydrocyanic acid (HCN) has a pK_a of 10. Therefore at physiological pH_i, only a small fraction of the incoming HCN dissociates into CN^- and H^+. CN^- binds irreversibly at the binuclear cytochrome a_3 - Cu_B center of cytochrome *c* oxidase. This is a multi-subunit enzyme of the mitochondrial respiratory chain that transfers electrons from cytochrome *c* to O_2. It is coupled to translocation of protons across the inner membrane (Panda & Robinson, 1995). Although many textbooks refer to the CN^- binding as an irreversible interaction with the cytochrome *c* oxidase, in conditions of high oxygen concentration, oxygen may "loosen" CN^- from the metal center. In addition, pyruvate *in vivo* is known to be protective against CN^- toxicity when administered simultaneously with CN^- because pyruvate and CN^- react to form cyanohydrin. In this way, CN^- is "trapped". Therefore, the combination of high oxygen tension and presence of pyruvate may partially reverse cytochrome *c* oxidase inhibition (Delhumeau et al., 1994). However, a major disadvantage of using pyruvate under these conditions, is that it will be converted at a high rate to lactate by lactate dehydrogenase (LDH) and thereby convert all NADH to NAD^+ (Stalmans W, *personal communication*).

2.3 Measurement of transepithelial potential difference (V_{te}) and resistance (R_{te})

These two electrophysiological parameters of confluent cultured monolayers, grown on permeable filter supports, are measured routinely in the cell culture lab every 48 hours with an EVOM-G potentiometer (World Precision Instruments, Sarasota, USA), using sterile "chopstick" electrodes. For experiments examining the effect of bumetanide and amiloride on V_{te}, cell culture inserts with confluent monolayers are placed in a home-built Ussing-type chamber (chamber opening 0.33 cm^2 (Fig. 2.2, insert)) and are continuously superfused on both sides with warm (37°C) 20 N-2-hydroxyethylpiperazine-N'-2-ethanesufonic acid (HEPES)-buffered balanced salt solution (HB-BSS). The perfusion speed is adjusted in such a way that the apical and basolateral volume is completely exchanged in one minute. Electronically controlled valves (080T4 Mixing Valve, Bio-Chem Valve™ Inc., Boonton, NJ, USA) are used to change between gravity-fed solutions. An end-mounted vacuum line removes excess perfusate. V_{te} is measured using Ag/AgCl voltage electrodes that are connected to the bath solutions with agar bridges containing 2% agarose in 1.5 M KCl medium. The Ussing-type chamber, the perfusion solutions, perfusion tubing and mixing valves are all located inside a transparent box in which the temperature is kept at 37° C (Jans et al., 2000).

2.4 Transmission electron microscopy

Confluent primary cell cultures, grown on permeable filter supports, are fixed with a solution of 2% glutaraldehyde in 0.05 M cacodylate buffer (pH = 7.3) and washed in 0.05 M cacodylate buffer for 10 minutes. Then the PTFE-filter is carefully cut out of the plastic insert and cut into small fragments. These fragments are postfixed in 2% osmium tetroxide in 0.05 M sodium cacodylate buffer (pH = 7.3) for 1 hour. Following dehydration through graded concentrations of acetone, the filter fragments are embedded in Araldite. Semithin sections are cut on a Reichert Ultracut E microtome and stained with thionin-methylene blue (0.15 % (weight/volume) aqueous solution) for light microscopy. Serial ultrathin sections (0.06 µm) from selected fragments are mounted on 0.7% formvar-coated grids, contrasted with uranyl acetate followed by lead citrate and examined in a Philips EM 400 electron microscope (Jans et al., 2000).

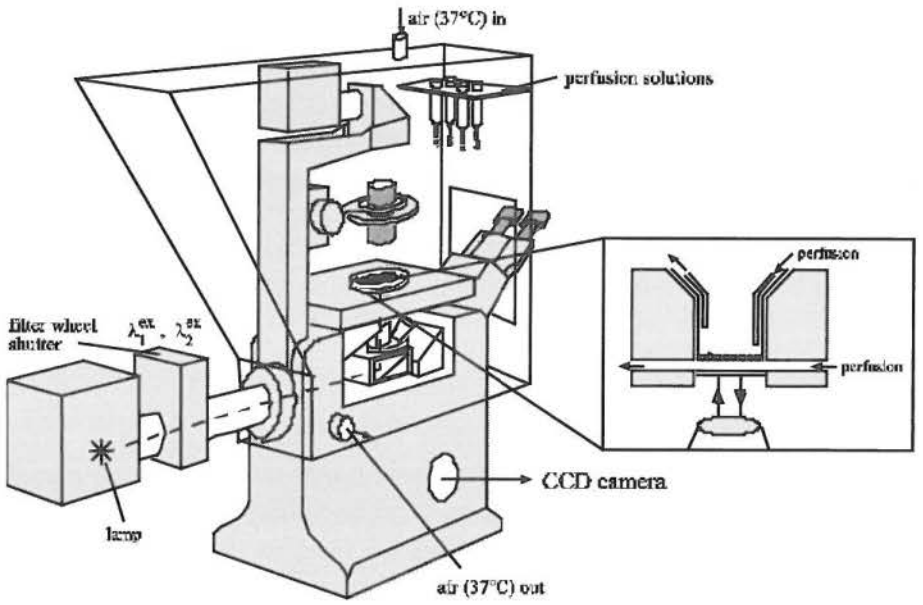

Figure 2.2 *Schematic representation of the experimental microfluorescence set-up. The expanded part shows the perfusion chamber containing the cell culture insert with a confluent monolayer. The fluorescence collected by the objective was transmitted through a dichroic mirror and an emission filter to either a Quantix CCD camera or a photomultiplier tube.*

2.5 Immuno-staining

2.5.1 Immunohistochemistry for detecting Tamm-Horsfall protein (THP)

To study the expression of THP-antigen in our primary cultures immunoperoxidase staining was performed on 7- and 12-day old confluent primary cultures that are fixed by incubation for 10 minutes in a 1% $CaCl_2$ Na-cacodylate buffer containing 4% formaldehyde (pH = 7.4). After washing three times with tri(hydroxymethyl)aminomethane base (TRIS)-buffered saline (TBS, pH = 7.6), the primary cultures are incubated for 30 minutes with 20% (volume/volume) goat-serum TBS, the same species in which the secondary antibody was made. Endogenous peroxidase activity is blocked by incubation in TBS containing 0.03% (volume/volume) H_2O_2 for 30 minutes. This is followed by incubating the cultures for 120 minutes with the primary antibody, a biotinylated goat-anti-human-THP-Ab (Organon, Oss, The Netherlands), and after washing three times with TBS, incubating for 30 minutes with avidin/biotin/peroxidase complex (ABC) (Vector

Laboratories, Burlingame, Canada). After final washing with TBS, peroxidase staining is developed using aminoethylcarbazole (AEC) as staining reagent (Jans et al., 2000)

2.5.2 Indirect immunofluorescence for detecting Na-P_i cotransporter type I and type II

From the laboratory of H. Mürer (Institute of Physiology, University of Zurich, Switzerland), polyclonal antibodies raised in rabbits against a C-terminal peptide of Na-P_i type I and type II cotransporters, were obtained. These antibodies were shown to cross-react with the rabbit isoform of type I (Na-P_i 1 protein) for immunohistochemistry and for Western blotting (Biber et al., 1993; Verri et al., 1995), and with the rabbit isoform of type II (NaP_i-6 protein) for Western blotting (Custer et al., 1994; Verri et al., 1995), respectively. Confluent primary cell cultures were washed with phosphate-buffered saline (PBS) and fixed with methanol (100%) during 15 min at room temperature. After washing with PBS, the cells were permeabilized and blocked by incubation for 20 min at room temperature with PBS containing Triton X100 (0.2%) and Normal Goat Serum (NGS, 10%). After washing, the cells were incubated during 1 hour at room temperature with the primary antibody at various dilutions in PBS containing 1% NGS and 0.025% sodium-azide. After washing three times with PBS, cells were incubated during 1 h at room temperature with the secondary antibody (goat-anti-rabbit IgG) conjugated with Alexa Fluor 488™ (20 µg/ml) in PBS containing 1% NGS and 0.025% sodium-azide. After washing and mounting in glycerol 100%, the filter-cups were placed on coverslips and examined on the stage of the microfluorescence microscope (see 2.8) using a narrow-band filter system for Alexa Fluor 488™ (excitation 495 nm, emission > 515 nm) from Omega Optical (Vermont, USA).

2.6 Measurement of hormone stimulated cAMP accumulation

To assess the effect of hormones on adenylyl cyclase activity, primary cultures were pre-incubated for 30 minutes in HB-BSS at 37° C with 100 µM isobutylmethylxanthine (IBMX, a phosphodiesterase inhibitor), after which hormones at a concentration of 1 µM were added to both sides of the epithelium, still in the presence of IBMX. After 30 minutes, the incubation was stopped and the cellular cAMP was extracted by removal of the HB-BSS and addition of 200 µl of ice-cold ethanol (65%) to the apical side. After 10 minutes, this was repeated once. The 400 µl of ethanol solution was centrifuged for 10 minutes at 2000 rpm and the supernatant was lyophilized for 4 hours. After appropriate dilution, cAMP was

assayed immediately with the use of an ^{125}I radio immunoassay kit (Biotrak™ acetylation protocol, Amersham Pharmacia Biotech, Buckinghamshire, UK) and ^{125}I was counted on a Packard 5330 gamma counter (Meriden, CT, USA) (Jans et al., 2000).

2.7 ATP measurements

Confluent monolayers of cells grown on permeable filter supports were washed and equilibrated in HB-BSS solution for 1 hour. Subsequent incubation with metabolic inhibitors was performed in non-perfusion conditions. At the start of the recovery phase cell layers were washed three times with HB-BSS, containing glucose or pyruvate or both. Control cells were incubated for the same amount of time in BSS. ATP measurements were performed with a luciferin-luciferase based assay kit (Molecular Probes, Eugene, OR, USA). The assay is based on luciferase's requirement for ATP in producing light (emission maximum ~560 nm at pH 7.8) according to the reaction:

$$\text{luciferin} + \text{ATP} + O_2 \xrightarrow[\text{luciferase}]{Mg^{2+}} \text{oxyluciferin} + \text{AMP} + \text{pyrophosphate} + CO_2 + \text{light}$$

The reaction buffer contained 150 µg ml^{-1} luciferin, 1.25 µg ml^{-1} luciferase, 5 mM $MgSO_4$, 1 mM dithiothreitol (DTT), 25 mM Tricine buffer, 0.1 mM ethylenediaminetetraacetic acid (EDTA) and 0.1 mM azide, pH=7.8. The cells were solubilized in 650 µl of somatic cell ATP-releasing agent (Sigma, St Louis, MO) for 30 seconds. 50 µl of cell extract was added to 450 µl reaction buffer. ATP levels were measured with a luminometer type 1250 from Wallac (Turku, Finland). At the start of each new series of ATP measurements, a calibration curve was obtained with standard ATP solutions (Molecular Probes, Eugene, OR, USA) in the concentration range 10^{-8}-10^{-4} M (Fig. 2.4). The dilution of the sample was choosen to result in a luminescence signal on the linear part of the calibration curve. In this way the luminescence signal from the luminometer (expressed in mV) could be converted to the ATP concentration of the sample. Converting the ATP concentration of the sample to intracellular ATP concentration would require a very rough estimation of the total cell volume of one primary cell culture. Since this could result in erroneous estimations of the ATP concentration, and since total cell volume of one primary cell culture is constant, the results are presented as a percentage change compared to control (control is a primary cell culture that is kept in HB-BSS for the same time as the ischemia(-reperfusion) time of the

sample). To exclude the possibility that trace amounts of CN^- and DOG could influence the luciferin-luciferase reaction, a control experiment was performed with NaCN (2.5 mM) and DOG (10 mM) present in the standard ATP solutions. As shown in Figure 2.3, this did not change the luminescence signal.

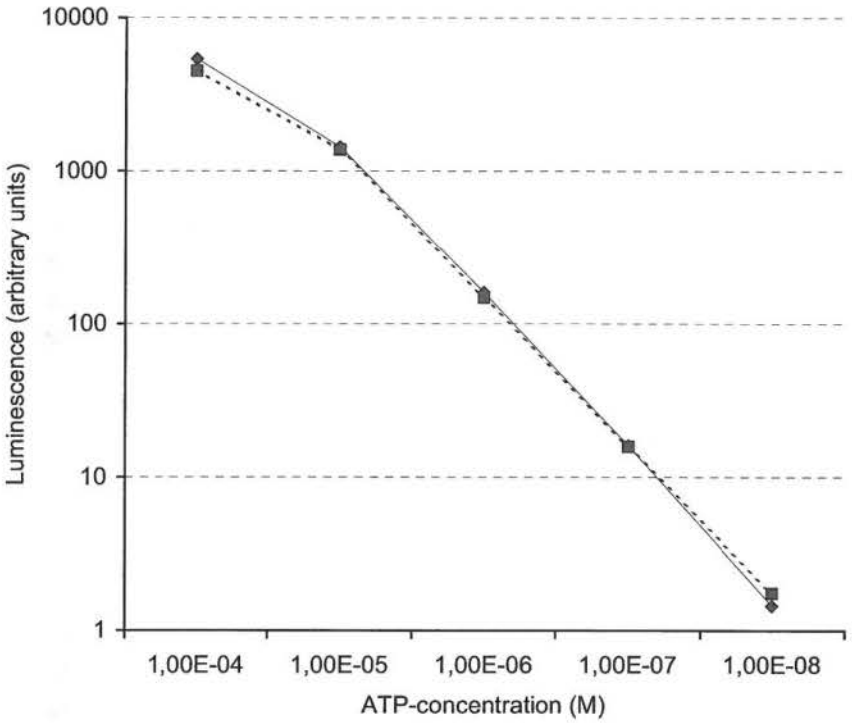

Figure 2.3 *Typical calibration curve for ATP measurements (▲). The presence of NaCN (2.5 mM) and DOG (10 mM) in the ATP standard solutions did not influence the luminescence signal (■)*

2.8 Fluorescence microscopy

2.8.1 Fluorescent probes Fura-2, BCECF, calcein and EtHD-1

A fluorescent probe is a fluorophore designed to localize biomolecules within a specific region of a biological specimen or to respond to a specific stimulus. The fluorescent probes BCECF and Fura-2 respond to changes in intracellular pH and calcium concentration, respectively. EtHD-1 and calcein are fluorescent probes that can respectively detect necrotic and viable cells. The

process responsible for the fluorescence of fluorescent probes is the result of a three-stage process. First, a photon, supplied by an external source such as an incandescent lamp, is absorbed by the fluorophore, creating an excited electronic singlet state. Second, during this excited state which exists for typically 10^{-9} to 10^{-8} s, the fluorophore undergoes conformational changes. As a consequence, the energy is partially dissipated, yielding a relaxed excited singlet state. Finally, a photon is emitted, returning the fluorophore to its ground state. Due to energy dissipation during the excited-state lifetime, the energy of this photon is lower, and therefore of longer wavelength, than the excitation photon. This shift of wavelengths (the so-called Stokes shift) is fundamental to the sensitivity of fluorescence techniques because it allows emission photons to be detected isolated from excitation photons (Ameloot M, Introduction to Fluorescence techniques, p 11-12).

Indicators that show an excitation or emission spectral shift upon ion binding can be calibrated using a ratio of the fluorescence intensities measured at two different wavelengths, resulting in the cancellation of artifactual variations in the fluorescence signal that might otherwise be misinterpreted as changes in ion concentration. The ratio of two intensities with opposite ion-sensitive responses gives the largest possible dynamic range of ratio signals for a particular indicator. Alternatively, the ratio of an ion-sensitive intensity to an ion-insensitive intensity (measured at a spectral isosbestic point) can be used (Fig. 2.4). Ratiometric measurements reduce or eliminate variations of several determining factors in the measured fluorescence intensity, including indicator concentration, excitation path length, excitation intensity and detection efficiency. Artifacts that are eliminated include photobleaching and leakage of the indicator, variable cell thickness, and non-uniform indicator distribution within cells (due to compartmentalization) or among populations of cells (due to loading efficacy variations).

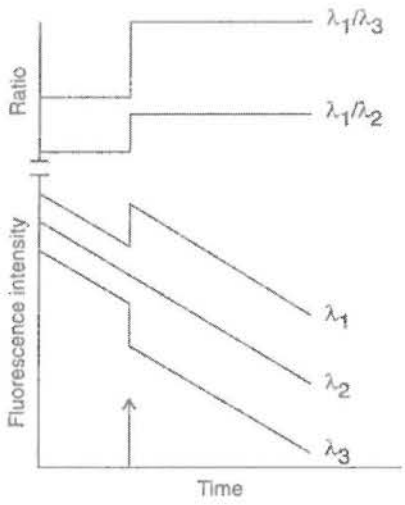

Figure 2.4 *Simulated data demonstrating the practical importance of ratiometric fluorescence techniques. The figure represents an ion indicator that exhibits a fluorescence intensity increase in response to ion binding at wavelength λ_1 and a corresponding decrease at λ_3. Fluorescence measured at an isosbestic point (λ_2) is independent of ion concentration. The intracellular indicator concentration diminishes rapidly due to photobleaching, leakage (assuming the extracellular indicator is not detectable) or some other process. The change of intracellular ion concentration due to a stimulus applied at the time indicated by the arrow is unambiguously identified by recording the fluorescence intensity ratios λ_1/λ_3 or λ_1/λ_2 (adapted from Molecular Probes Handbook, Web Edition, 2002 (www.molecularprobes.com)).*

Fura-2 is an ultra violet (UV) light–excitable, ratiometric Ca^{2+} indicator that has become the dye of choice for ratio-imaging microscopy, in which it is more practical to change excitation wavelengths than emission wavelengths. Upon binding Ca^{2+}, Fura-2 exhibits an absorption shift that can be observed by scanning the excitation spectrum between 300 and 400 nm, while monitoring the emission at ~ 510 nm. Fura-2 may be subject to compartmentalization, whereas it is resistant to photobleaching. Fura-2 exhibits a K_d value that is close to typical basal Ca^{2+} levels in mammalian cells (~100 nM), and displays high selectivity for Ca^{2+} binding relative to Mg^{2+} (Molecular Probes Handbook Section 20.2, 2002).

Since its introduction by Roger Tsien (Tsien et al., 1982), the polar fluorescein derivative 2',7'-bis(carboxyethyl)-5(6)-carboxyfluorescein (BCECF) and its membrane-permeant acetoxymethyl (AM) ester (BCECF-AM) has become the most widely used fluorescent indicator for estimating intracellular pH. The four to

five negative charges of BCECF at pH 7–8 improve its retention in cells. The pK_a of 6.98 is ideal for typical intracellular pH measurements. Absorption of the phenolate anion (basic) form of BCECF is red-shifted and has increased molar absorptivity relative to the protonated (acidic) form; there is little, if any, pH-dependent shift in the fluorescence emission spectrum of BCECF upon excitation at 505 nm. BCECF is typically used as a dual-excitation ratiometric pH indicator. Intracellular pH measurements with BCECF are made by determining the pH-dependent ratio of emission intensity (detected at 535 nm) when the dye is excited at ~490 nm versus the emission intensity when excited at its isosbestic point of ~440 nm (Molecular Probes Handbook Section 21.2, 2002).

Calcein-AM can serve as an indicator of cell viability because it measures both the non-specific esterase activity (a characteristic of living cells), which is required to activate the fluorescence, and the cell-membrane integrity of living cells, which is required for intracellular retention of the fluorescent product. Calcein, which is the hydrolysis product of calcein-AM, is a polyanionic fluorescein derivative that has about six negative charges and two positive charges at pH 7. Calcein is better retained in viable cells than is BCECF and tends to have brighter fluorescence (Molecular probes Handbook Section 15.2, 2002).

The red-fluorescent, cell-impermeant ethidium-homodimer-1 (**EtHD-1**) has large Stokes shifts and may be used in combination with fluorescein-based probes (such as calcein) for two-color applications. With its high affinity for DNA and low membrane permeability, EtHD-1 is often the preferred red-fluorescent dead-cell indicator. EtHD-1 binds to nucleic acids 1000 times more tightly than does ethidium bromide and undergoes about a 40-fold enhancement of fluorescence upon binding (Molecular probes Handbook Section 15.2, 2002).

2.8.2 Microfluorescence set-up

The fluorescence measurements are performed with a home-built microfluorimeter under computer control (Fig. 2.2). Cell culture inserts with confluent monolayers are placed in a home-built Ussing-type chamber (see 2.1.2) that is mounted on the stage of a Nikon TMD 35 inverted microscope (Tokyo, Japan) and are continuously superfused on both sides with warm (37°C) HB-BSS. The perfusion speed is adjusted in such a way that the apical and basolateral volume of the bath is completely exchanged in one minute. Electronically controlled valves (080T4 Mixing Valve, Bio-Chem Valve™ Inc., Boonton, NJ, USA) are used to change between gravity-fed solutions. An end-mounted vacuum line removes excess perfusate. The Ussing-type chamber, the perfusion solutions, perfusion tubing and mixing valves are all located inside a home-built transparent box that is

constructed around the stage of a Nikon TMD 35 inverted microscope (Tokyo, Japan). The air inside the box is kept at 37° C by constant ventilation through an external circuit containing a heating element under control of a configurable loop controller (Gefran 1000, Provaglio d'Iseo, Italy) connected to a thermocouple inside the box.

A 40X/0.60 objective (LD Achroplane™, Carl Zeiss, Oberkochen, Germany) is used. The light of a 100 W Xe-lamp (Nikon, Tokyo, Japan) is filtered for excitation by interference filters and is reflected towards the cells by a dichroic mirror. The filters are placed in a computer-controlled filter wheel, Lambda-10 (Sutter Instrument Company, Novato, USA). Neutral density filters inserted between the microscope and the filter wheel reduce the intensity of the source. The fluorescence emission, after passing through an interference filter, is detected with a photomultiplier tube 9124A (Thorn-EMI, Middlesex, England) operating in photon counting mode. The pulses are transferred to the computer through a counter/timer board C660 (Thorn-EMI, Middlesex, England). The data are collected within a dwell time of 1 s at each wavelength and corrected for the dead time of the counting system. The background due to scattering and autofluorescence is subtracted subsequently from each of the signals.

In the second part of the experiments a charge coupled device (CCD) camera was used for detection of fluorescence emission. The use of a camera allows to compare the loading and behaviour of different cells within one monolayer. The Quantix CCD camera (Photometrix, Tucson, Arizona, USA) was equipped with a Kodak KAF 1400 CCD (grade 2, MPP) with 1317x1035 pixels and cooled to -25°C by a thermoelectric cooler. The exposure time was 5 s. The acquisition of pairs of images was performed every minute and was controlled by a homemade program based on the V for Windows software (Digital Optics, Auckland, New Zealand). The signals were obtained by spatially integrating the pixels over the cells. The background image was automatically subtracted, pixel-by-pixel, from the image of the loaded cells.

2.8.3 Measurement of intracellular pH (pH_i)

Confluent primary cell cultures are placed in a home-built Ussing-type chamber. After measuring the background signals, the cells are loaded from the apical and the basolateral side by exposure to the membrane permeant form of the fluorescent pH indicator BCECF at a final concentration of 10 µM using a stock solution of 5 mM in dimethylsulfoxide (DMSO). Loading is performed for 15 minutes at 37°C and for an additional 75 minutes at room temperature in HB-BSS

containing 1% bovine serum albumin (BSA). After loading, excessive dye in the apical and basolateral solution is washed out for at least 10 minutes.

The excitation light is filtered at 440 nm and 490 nm by the interference filters 440DF20 and 490DF20 from Omega Optical (Vermont, USA) and is reflected towards the cells by the dichroic mirror 515DRLPXR from Omega Optical (Vermont, USA). The fluorescence emission is monitored at 535 nm using the interference filter 535DF25 from Omega Optical (Vermont, USA).

Calibration of the BCECF fluorescence ratio $r = F_{490}/F_{440}$ *versus* a given pH_i is performed at the end of each experiment, using the nigericin/high K^+ technique (Thomas et al., 1979). Cells were clamped at three different pH's (6.5, 7.0 and 7.5) using calibration solutions at 37° C containing 13 µM nigericin and 140 mM K^+. This K^+ concentration closely approximates the reported cytosolic K^+ concentration of rabbit TALH cells (Eveloff et al., 1980). For the considered pH range a linear calibration function was used (Jans et al., 2000).

2.8.4 Measurement of intracellular calcium ($[Ca^{2+}]_i$)

Confluent primary cell cultures are placed in a home-built Ussing-type chamber. After measuring the background signals, the cells are loaded from the apical and the basolateral side by exposure to the membrane permeant form of the fluorescent Ca^{2+} indicator Fura-2 at a final concentration of 10 µM using a stock solution of 5 mM in DMSO. Loading is performed for 15 minutes at 37°C and for an additional 75 minutes at room temperature in HB-BSS containing 1% bovine serum albumin. After loading, excessive dye in the apical and basolateral solution is washed out for at least 10 minutes.

The excitation light is filtered at 340 nm and 380 nm by the interference filters 340DF10 and 380DF13 from Omega Optical (Vermont, USA) and is reflected towards the cells by the dichroic mirror 400DCLP from Omega Optical (Vermont, USA). The fluorescence emission is monitored at 510 nm using the interference filter 510WB40 from Omega Optical (Vermont, USA) (Jans et al., 2000).

2.8.5 EtHD-1 and calcein staining

For viability testing, the microfluorescence set-up described in 2.8.2 was used, without continuous perfusion. Experimental solutions were changed manually. In order to remove metabolic inhibitors completely, monolayers were washed three times with HB-BSS after exposure to CN^- and/or DOG. After the ischemia/reperfusion or time-control period, cells were loaded from their apical side

with HB-BSS containing Calcein-AM 4 µM (stock solution 4 mM in DMSO) and EtHD-1 2 µM (stock solution 2 mM in DMSO/H_2O 1/4 (volume/volume)).

The excitation light was filtered at 495 nm by the interference filter 495DF10 from Omega Optical (Vermont, USA) and was reflected towards the cells by the dichroic mirror 515DRLPXR for Calcein-AM, and 565DRLPXR for EtHD-1. The fluorescence emission was detected by the CCD camera at 530 nm using the interference filter 535DF50 (bandpass) for Calcein-AM and at 590 nm using the interference filter 590DF55 (longpass) for EtHD-1. Exposure times from 1 to 3 s were used. Images were obtained from 2 to 15 minutes after addition of the Calcein-AM/EtHD-1 to the cells.

2.9 Statistical analysis

Data from electrophysiological, pH_i, calcium and cAMP measurements are reported as mean ± standard error of the mean (SE). Initial acidification-alkalinization rates were obtained from fitting linear equations to the recorded pH_i time courses. Data from intracellular pH measurements were converted to proton concentrations in order to calculate the mean ± SE and for statistical analysis. For uniformity, all graphical data were presented as pH_i and not $[H^+]_i$. Statistical significance was judged from a one- or two-sided Wilcoxon test. Paired and unpaired Student's *t* test was used only after checking for normality assumptions, as indicated in the text. Significance was accepted at $p < 0.05$.

All tests are performed with the statistical package StatXact (version 3.0.1) (Cytel Software, Cambridge, MA, USA).

Chapter 3

A simple method for obtaining functionally and morphologically intact primary cultures of the medullary thick ascending limb of Henle's loop (MTAL) from rabbit kidneys

3.1 Introduction

3.1.1 Existing techniques for obtaining primary cell cultures from MTAL cells

Several different techniques for starting primary cell cultures from MTAL segments have been described in the past: microdissection of individual nephron segments (Burg et al., 1982), macroseparation by differential sieving (Trinh-Trang-Tan et al., 1986) or centrifugation on a continuous Percoll gradient (Chamberlin et al., 1984) of enzymatically digested pieces of kidney outer medulla and finally immunodissection with plate-sieving (Allen et al., 1988; Rose et al., 1994b) or with fluorescence-activated cell sorting (FACS) (Helbert et al., 2001). Their respective disadvantages are low yields of starting material (for microdissection), contamination with other nephron segments (for macroseparation after enzymatic digestion) and aggressive disruption of intercellular communications (for immunodissection). With FACS, a purity of approximately 80% can be obtained for harvesting TAL cells (Helbert et al., 2001).

In 1997 Schafer described a simplified method for isolating large numbers of defined nephron segments. The authors proposed this method to obtain enough starting material for immunoblotting or RT-PCR of mRNA from individual nephron segments (Schafer et al., 1997). This method was used to start primary cell cultures because of the following reasons: first, a minimal amount of equipment is required; second, since each nephron segment is identified individually, a high-grade purification and therefore a maximal homogeneity of the primary cultures can be expected; third, once established for one nephron segment, it should be easy to extend it to other segments as well.

3.1.2 Morphology and function of the MTAL cell

The TAL corresponds to the last segment of the loop of Henle. It extends from the boundary between inner and outer medulla up to or just beyond the macula densa in the cortex. The TAL, therefore, includes a medullary portion (MTAL) and a cortical portion (CTAL) (Fig. 3.1). The general cell organization and ultrastructure as well as the main transport properties are roughly similar in TAL from rabbit, rat and mouse (Fig. 3.2). There is a single type of cell in each TAL portion. The apical membrane bears stubby microvilli of irregular shape. Apically, the intercellular space is sealed from the luminal space

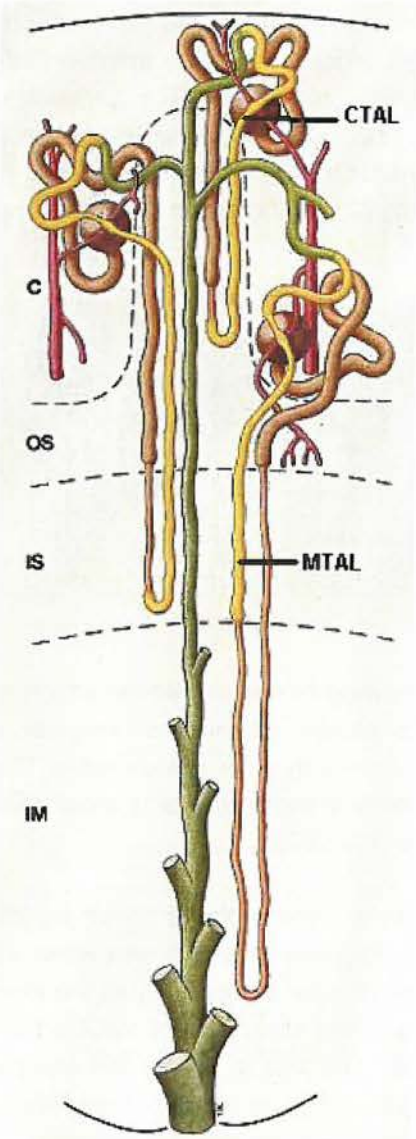

Figure 3.1 *Structural organization of the nephrons and collecting ducts of the kidney. The renal parenchyma is divided into the cortex (C), the outer stripe (OS), the inner stripe (IS), and the inner medulla (IM). The renal corpuscles and the proximal tubules are shown in brown. The thin limbs are shown in pale brown. The thick ascending limb (straight part of the distal tubule including the macula densa) and the distal convoluted tubule are shown in yellow. The connecting tubules are shown in light green. Finally, the collecting duct system is shown in dark green (adapted from Koushanpour & Kriz, 1986, p xi).*

by a tight junctional band. Gap junctions do not exist between cells of the distal segments. The lateral cell processes are occupied entirely by large mitochondria. The nucleus spans the total cell height. The perinuclear region contains small mitochondria. Lipid droplets and some glycogen can be present anywhere in the cell. The THP protein, which is synthesized by the TAL cells, has been localized along the cell membranes, but with stronger staining along the luminal membrane. (Kaissling & Kriz, 1992).

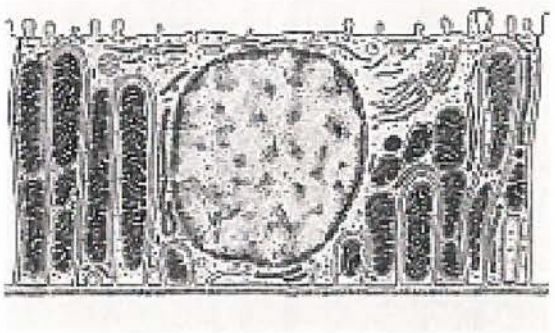

Figure 3.2 *Schematic drawing of the subcellular structures of an MTAL cell. The apical membrane bears stubby microvilli of irregular shape. The lateral cell processes are occupied entirely by large mitochondria. The nucleus spans the total cell height and the perinuclear region contains small mitochondria (adapted from Kaissling & Kriz, 1992, pp 109-167).*

The loop of Henle is responsible for absorbing 25% to 40% of the filtered Na^+ load. Moreover, the dissociation of salt and water absorption by the loop of Henle is ultimately responsible for the capacity of the kidney either to concentrate or to dilute the urine. The active absorption of NaCl in the water-impermeable TAL serves both to dilute the urine and to supply the energy for the single effect of countercurrent multiplication. The osmotic permeability to water is very low in apical membranes and junctions, so that the epithelial layer can sustain a large osmotic pressure difference. Intercellular junctions, however, are highly permeable to ions, and more permeable to cations than to anions, so that the paracellular route is of a low ohmic resistance (Reeves & Andreoli, 2000).

As shown in Figure 3.3, net Cl^- absorption by the TAL is a secondary active process. Luminal Cl^- entry into the cell is mediated by an electroneutral (bumetanide sensitive) $Na^+/K^+/2Cl^-$ cotransport process (NKCC2) driven by the favorable electrochemical gradient for Na^+ entry. In contrast to the

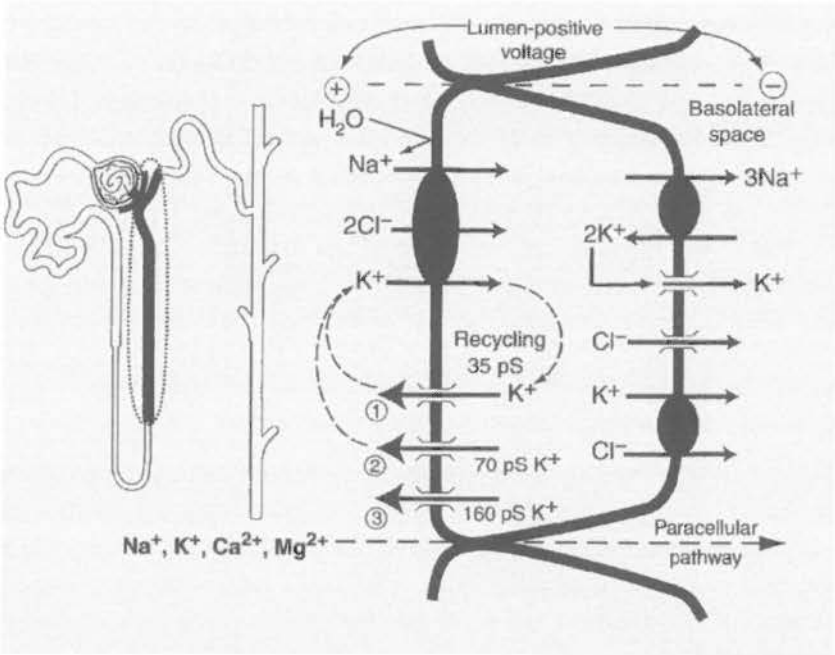

Figure 3.3 *A model depicting the major elements of the mechanism of NaCl absorption by the (rat) thick ascending limb (Giebisch & Wang, 2000).*

electroneutral entry of Cl^- across the apical membrane, the majority of Cl^- efflux across the basolateral membrane proceeds through conductive pathways. In rabbit, also a component of electroneutral KCl cotransport has been proposed (Greger & Schlatter, 1983). Intracellular Cl^- is maintained at concentrations above electrochemical equilibrium by the continued entry of Cl^- through the apical NKCC2 cotransporter. The K^+ that enters the cells through the NKCC2 cotransporter recycles across the apical membrane by way of a K^+ conductive pathway (for a detailed overview on apical K^+ channels in MTAL, see discussion chapter 4). This apical K^+ recycling ensures a continued supply of luminal K^+ to sustain $Na^+/K^+/2Cl^-$ cotransport and provides a pathway for net potassium secretion by the TAL. Furthermore, the K^+ current from cell to lumen polarizes the lumen and causes an equivalent current to flow from lumen to bath through the paracellular pathway. Because the paracellular pathway is cation selective, the majority of the current is carried by sodium, calcium and magnesium. This paracellular absorption of sodium increases the efficiency of sodium transport by the TAL and allows to reabsorb approximately 25% and 70% of the filtered load of calcium and magnesium, respectively (Reeves & Andreoli, 2000; Giebisch & Windhager, 2003(b)). When perfused *in vitro* with identical solutions on both sides, the TAL generates a lumen-

positive transepithelial voltage. A diffusion potential due to the efflux of chloride depolarizes the basolateral membrane, whereas the diffusion potential due to the efflux potassium hyperpolarizes the apical membrane. According to the equivalent circuit for the TAL tubule cell, constituting the overall epithelial tubular wall (Fig. 3.4), the membrane potential differences of the apical (V_2) and basolateral (V_1) membrane are a function of all electromotive forces (E_1, E_2, E_3) and all resistances (R_1, R_2, R_3) of the transcellular and paracellular ion pathways across the tubular wall. An important consequence of the fact that the resistance of the paracellular pathway (R_3) is small compared to the resistances of both membranes of the polarized cell (R_1=apical, R_2=basolateral) leads to electrical "cross-talk". Both membrane potential differences will influence each other. For example, a depolarization of the basolateral membrane leads to a depolarization of the apical membrane. Based on the complement of channels and ion gradients at the basolateral membrane, i.e. efflux of chloride and potassium, the apical membrane, which is characterized by potassium channels and thus a membrane voltage that is negative due to the efflux of potassium, will have a less negative voltage than the Nernst equilibrium diffusion potential for potassium (Ek_2) due to the electrical "cross-talk". Nevertheless, the transepithelial potential (V_3) is positive in the lumen versus blood (Fig. 3.4). On the other hand, when bumetanide blocks the electrically silent luminal Cl^- entry into the cell, the conductive Cl^- efflux across the basolateral membrane will decrease. Due to the electrical cross-talk, the hyperpolarized basolateral membrane will increase the negative voltage (elevated by the diffusion potential of potassium) at the luminal membrane and at the same time the positive transepithelial potential will diminish (Morel & Doucet, 1992; Giebisch & Windhager 2003 (a)).

Numerous transducing pathways are involved in the modulation of NaCl reabsorption in the TAL. The stimulation of this function is mainly due to the cAMP cascade, whereas its down-regulation is accounted for by several signaling pathways. These act either by inhibiting the hormonally-induced cAMP accumulation (inhibitory G protein or increases in $[Ca^{2+}]_i$) or independently of cAMP (cGMP, phopholipase A_2, protein kinase C) (Bailly, 1992). It must be noted that inhibition of the reabsorptive function of MTAL, especially via phospholipase A_2 derivatives, may have a pathophysiological relevance in preserving the epithelium from damages during energy depletion (Brezis & Rosen, 1995).

TALs also constitute an important site of ammonia transport. The NH_4^+ transporters are still under investigation (for review see Attmane-Elakeb, 2001).

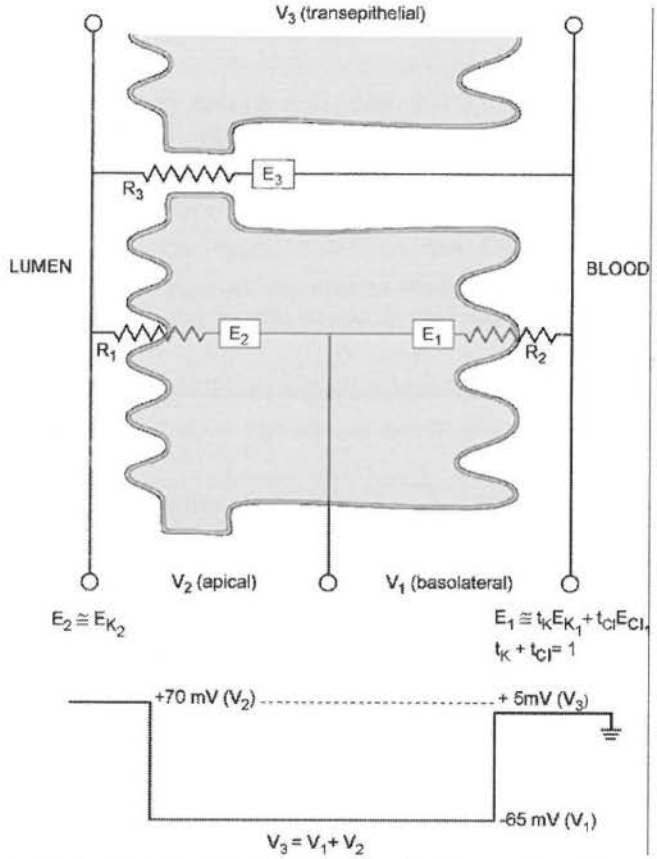

Figure 3.4 *The equivalent circuit of the TAL cell. For explanation of symbols, see text (adapted from Giebisch & Windhager, 2003(a)).*

Ammonium (NH_4^+) is the main component of urinary net acid excretion by which the kidney regulates acid-base balance. After being metabolized from glutamine by proximal tubule cells and secreted into the tubular fluid, ammonium must be reabsorbed by the MTAL to be accumulated in sufficient amounts in the renal medulla via a countercurrent mechanism. From there NH_3 diffuses into the collecting ducts, where it is trapped and excreted as NH_4^+. Thus ammonium reabsorption by the MTAL is a key step in the renal tubular handling of ammonia, especially since this reabsorption process is subjected to regulation (Attmane-Elakeb, 2001). Ammonium may be reabsorbed by paracellular diffusion (driven by the apical side positive transepithelial potential difference) or by transcellular transport.

Although the MTAL is impermeable to urea and does not contribute to the generation of a high urea concentration in the medulla, specific urea-transporters

may be present in rabbit MTALs and play a role in their volume regulation (Grunewald et el., 1998).

The TAL reabsorbs 8% and 12% of the filtered Ca^{2+} and Mg^{2+} load, respectively. In 1980, Suki et al. (Suki et al., 1980). used isolated perfused MTAL segments from rabbit kidneys and measured a net Ca^{2+} flux under basal conditions of about 1.3 $pmol.mm^{-1}.min^{-1}$. As the Mg^{2+} and Ca^{2+} reabsorption in the TAL is entirely dependent on the lumen-positive transepithelial voltage the majority, if not all, of the transport of both cations occurs via the paracellular pathway. A mutation in paracellin-1 located in the tight junction of TAL impairs this passive transport of Mg^{2+} and Ca^{2+} (Simon et al., 1999; Monnens et al., 2000). The recently cloned Ca^{2+} channel TRPV5, which is responsible for transcellular Ca^{2+} reabsorption in the distal nephron, was shown to be absent in TAL from rabbit kidneys (Hoenderop et al., 2003).

Rocha et al. (Rocha et al., 1977) showed that phosphate permeability was exceedingly low bidirectionally across in vitro perfused rabbit TAL segments. They observed no net transport of phosphate in the loop of Henle.

The acid/base transporters in the MTAL and the regulation of pH_i will be discussed in detail in the introduction to chapter 4.

3.2 Solutions and chemicals

For optimal control of extracellular pH, HEPES buffered (bicarbonate-free) balanced salt solutions were used (composition in mM : 128 NaCl, 5 KCl, 1 $CaCl_2$, 1.2 $MgSO_4$, 2 $NaH_2PO_4.H_2O$, 1 L-alanine, 5 glycine, 10 glucose, 20 HEPES, final pH brought to 7.4 with TRIS and osmolality to 320 mosm/kg H_2O with mannitol).

The cell culture medium for primary cell cultures of MTAL cells consisted of DME/Ham's F12 (DME/F12) medium without phenol red, containing FCS, heat inactivated, 5% (volume/volume), L-glutamine 2 mM, tri-iodothyronin 5 pM, prostaglandin E_1 70 ng/ml, hydrocortisone 50 nM, spermine 30 nM, spermidine 250 nM, EGF 10 ng/ml, insulin 5 µg/ml, transferrin 5 µg/ml, selenium 50 nM, AVP 0.1 µM, bovine thyrocalcitonin 0.1 µM, MEM Non Essential Amino Acids 1X, penicillin 100 I.U./ml and streptomycin 100 µg/ml. For the first 48 hours amphotericin B was added at a concentration of 1 µg/ml.

DME/F12 medium without phenol red, DMEM, MEM Non-Essential Amino Acids solution (liquid, 100X), 2-mercaptoethanol, sodium pyruvate, trypsin/EDTA, L-glutamine and penicillin/streptomycin were from Life Technologies™, Gibco BRL, Paisley, Scotland. Earle's MEM without phenol red was from Biochrom KG, Berlin. Insulin-transferrin-sodium selenite supplement (ITS) and epidermal growth factor (EGF) were from Boehringer Mannheim GmbH, Germany. Iso-butyl-methyl-

xanthine (IBMX) and methyl-sulfoxide (DMSO) were from Acros Organics, Geel, Belgium. Collagenase type 2 was from Wothington Biochemical, Lakewood, NJ, USA. Soybean Trypsin Inhibitor (SBTI) was from Fluka, Buchs, Switzerland. BCECF-AM and Fura-2-AM were from Molecular Probes, Leiden, The Netherlands. Cell-Tak™ was from Collaborative Biomedical Products, Bedford, MA, USA. FCS was from Sigma Chemical Company, St Louis, MO, USA. Cell culture inserts were 0.33 cm^2 collagen-coated PTFE membranes, pore size 0.4 µm from Costar™, Corning Inc., USA and 24 well cell culture clusters were tissue culture treated from Costar™, Corning Inc., USA. Tissue culture flasks 25 cm^2 were from Falcon™, Becton Dickinson Labware Europe, France. All other hormones and chemicals were from Sigma Chemical Company, St Louis, MO, USA.

Blockers were dissolved in ethanol or DMSO, the final concentration of these solvents never exceeded 1 pro mille.

3.3 Specific materials and methods

3.3.1 Collection of MTAL segments

The method for collecting large amounts of MTAL segments was learned at the laboratory of prof. dr. E. Schlatter (Westfalische Wilhems-Universität, Münster, Germany). The method described below is essentially the same with some modifications for adaptation to primary cultures (Schafer et al., 1997). A brief description of the whole method follows. Young white rabbits (body weight 1200-1500 g) were killed by cervical dislocation and carotid exsanguination. Using a sterile technique, both kidneys were excised rapidly and transferred into ice-cold HB-BSS. The kidneys were decapsulated with fine forceps (Dumont n° 5). With a bistoury they were cut longitudinally through the hilus in two identical pieces and then coronally into slices of approximately 1 mm thickness. These slices were transferred to a large Petri dish containing fresh ice-cold HB-BSS. With a bistoury the inner stripe of the outer medulla was dissected and further cut into small pieces. This procedure could be carried out without the use of a microscope. These small pieces were transferred with a 3 ml polyethylene Pasteur pipette into a 20 ml scintillation vial where the tissue was digested with 2 ml of a collagenase containing solution at 37° C. This collagenase solution was the same as in Schafer et al. (1997), but containing type 2 collagenase 0.1% (weight/volume), SBTI 96 µg/ml and no deoxyribonuclease. The 2 ml of collagenase solution was changed every 15 minutes. From the moment the supernatant contained large amounts of long nephron segments, the supernatant was filtered through a 50 µm nylon mesh to get rid of blood cells, cellular debris and small nephron segments. The filtrated

solution was discarded, and the longer tubule segments, which were retained on the mesh, were resuspended by flushing the sieve in opposite direction with warm (37° C) Earle' s MEM containing BSA) 1% (weight/volume) and glycine 5 mM. This suspension was collected in a large Petri dish. Because the time between sieving the supernatant and transferring the tubules to the culture medium was 10 minutes at the most, the collection was done in warm (37° C) medium in order to avoid additional temperature shocks. The apparatus to collect nephron segments consisted of a micropipette connected via polyethylene tubing to a 1 ml syringe. The barrel of this syringe was fixed and the plunger was operated with a micromanipulator (Narishige type MO-11, Tokyo, Japan). The whole system was filled with HB-BSS. The micropipette was a sodalime glass capillary with an internal diameter of 1.6 mm (Hilgenberg, Malsfeld, Germany) of which one end was pulled (Puller-steuergerät KHB 6), cut and polished, so that the diameter of the micropipette opening approximated 20 µm. The Petri dish was placed on the stage of an inverted microscope (Telaval 31, Carl Zeiss, Oberkochen, Germany) and under a magnification of 100 times in bright field illumination each nephron segment was identified visually before being sucked into the micropipette tip.

3.3.2 Primary cell cultures

After collecting 100 MTAL's, which took 5 to 10 minutes, the micropipette tip was transferred into 150 µl of cell culture medium on the apical side of the cell culture inserts (0.33 cm^2 collagen-coated PTFE membranes, pore size 0.4 µm (Transwell-COL™, Costar™, Corning Inc., USA)) and with a fast rotation of the micromanipulator the MTAL segments were blown out of the micropipette tip and were distributed evenly on the collagen coated membrane. The volume the nephron segments were collected in, was very small (less than 10 µl). This allowed direct transfer of the collected nephron segments to the cell culture inserts without the need for centrifugation and resuspension, which in our hands always led to significant loss of nephron segments. To the basolateral side of the cell culture inserts 650 µl of cell culture medium was added. The cell culture medium was based on DME/F12 medium without phenol red, containing FCS, heat inactivated, 5% (volume/volume), L-glutamine 2 mM, tri-iodothyronin 5 pM, prostaglandin E_1 70 ng/ml, hydrocortisone 50 nM, spermine 30 nM, spermidine 250 nM, EGF 10 ng/ml, insulin 5 µg/ml, transferrin 5 µg/ml, selenium 50 nM, AVP 0.1 µM, bovine thyrocalcitonin 0.1 µM, MEM Non Essential Amino Acids 1X, penicillin 100 I.U./ml and streptomycin 100 µg/ml. For the first 48 hours amphotericin B was added at a concentration of 1 µg/ml. The cultures were left unstirred for 72 hours at 37° C in a

standard humidified incubator (95% air - 5% CO_2), after which the medium was changed for the first time. The medium was then replaced routinely every two days.

3.4 Results

3.4.1 Collection of MTAL segments

After changing the collagenase solution four to five times, the supernatant contained large amounts of MTAL segments, thin descending limbs and some S3 segments with their transition to thin descending limb. At that time, outer medullary collecting ducts (OMCD) which seem more resistant to enzymatic digestion also appeared in the supernatant and increased in number from then on. However, MTAL segments were the most abundant throughout the whole procedure. S3 segments were characterized by their attachment to the thin descending limb and their "milky" appearance. The thin descending limbs were characterized by their small diameter. The OMCD had a typical "cobblestone" appearance with fuzzy borders. MTAL segments could easily be recognized by their smooth appearance, with two outer dense borders, a transparent inner line and a diameter that was smaller than the diameter of the S3 segment and the OMCD (Chini & Dousa, 1996) (Fig. 3.5). Photographs of these nephron segments from rat kidney have been published by Schafer et al. (Schafer et al., 1997). With this method, it was possible to collect 100 MTAL segments in 5 to 10 minutes. The time the tubules had been in collagenase solution seemed to correlate negatively with the amount of cellular outgrowth from the tubules. Moreover, after approximately 180 minutes in collagenase solution, the morphology of the nephron segments became distorted. So in general, collection of nephron segments was stopped after three hours of enzymatic digestion. This time interval was usually sufficient to start 8 primary cell cultures from the kidneys of one animal.

3.4.2 Light microscopy

After leaving the MTAL segments undisturbed for 48 hours, cellular outgrowth could be seen from the majority of nephron segments. The donor segments became disorganized and were washed away when the medium was

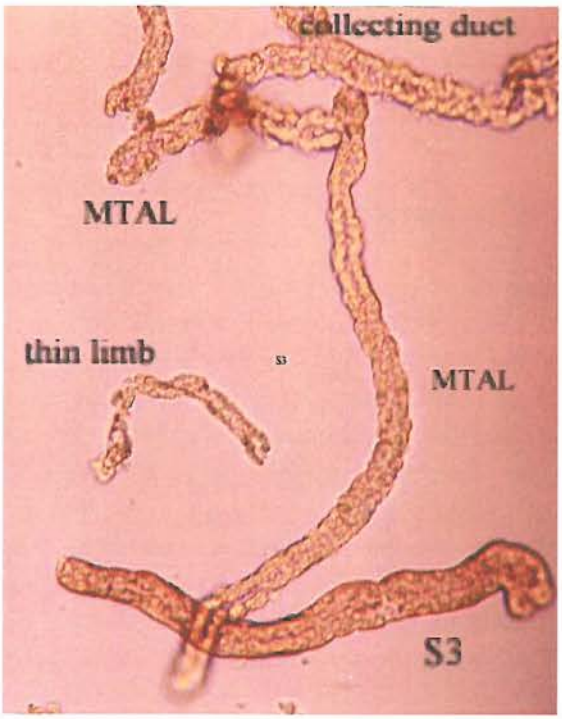

Figure 3.5 *Photograph of the different nephron segments obtained after enzymatic digestion of the inner stripe of the outer medulla. Proximal straight tubule segments (S3) are characterized by their attachment to the thin descending limb and their "milky" appearance. The thin descending limbs are characterized by their small diameter. The collecting ducts have a typical "cobblestone" appearance with fuzzy borders. MTAL segments can easily be recognized by their smooth appearance, with two outer dense borders, a transparent inner line and a diameter that is smaller than the diameter of the S3 segment and the OMCD.*

changed for the first time. Different supports have been tested (cover glasses, tissue culture treated plastic wells, uncoated permeable supports, Cell-Tak^{TM} coated supports), but only collagen coated supports were able to support cellular outgrowth. When glycine was omitted from the HB-BSS, the number of tubule segments from which cells started to grow was dramatically diminished. The "islands" of cellular growth increased progressively in diameter until they fused with other "islands" and the 0.33 cm^2 insert became completely covered with cells. Confluence was reached on average on day 7 in culture. Light microscopic evaluation showed cells with epithelial (polygonal) morphology and on all transverse sections of the cell culture inserts (Fig. 3.6) a nice monolayer could be

observed. After trypsinization of these primary cultures and seeding the cells onto collagen coated supports, the cells attached to the surface and proliferated. So in principle subculturing was possible. However, the cell cultures obtained in this way were never characterized.

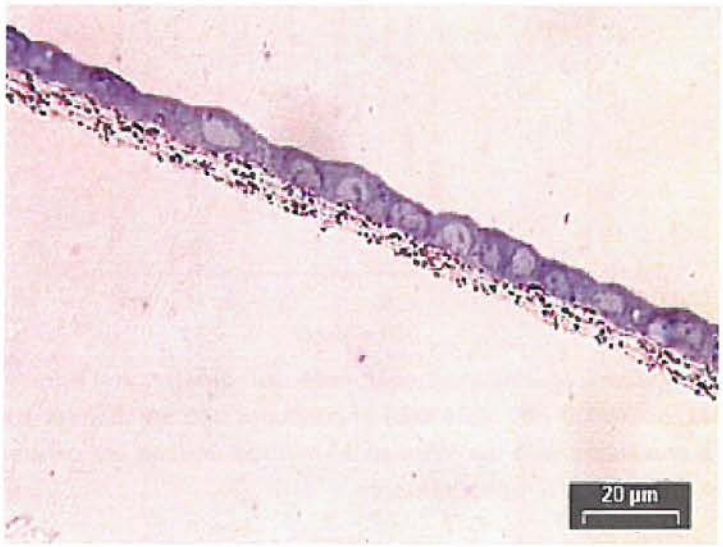

Figure 3.6 *Light-microscopic photograph of transverse section of confluent primary culture of MTAL (magnification X900). A monolayer of epithelial cells as well as the PTFE-permeable filter support can be observed.*

3.4.3 Electrophysiology

As shown in Figure 3.7, the R_{te} on day 7 was on average 212 Ohm.cm^2 and increased with ageing of the cultures. A V_{te} of 6 to 8 mV, apical side positive, could be measured during one week after the primary cultures had reached confluency. The effect of bumetanide 100 µM or amiloride 100 µM on the V_{te} when measured during apical and basolateral perfusion with HB-BSS in an Ussing-type chamber is shown in Figure 3.8. Addition of bumetanide 0.1 mM to the apical perfusion solution caused a sudden drop in V_{te}, with recovery after removal of bumetanide. Addition of amiloride 0.1 mM to the apical perfusion solution had almost no effect on the V_{te}. The median decrease in potential was significantly higher using bumetanide versus amiloride ($p=0.004$). Bumetanide when added to the basolateral perfusion solution caused only a very small decrease in V_{te}.

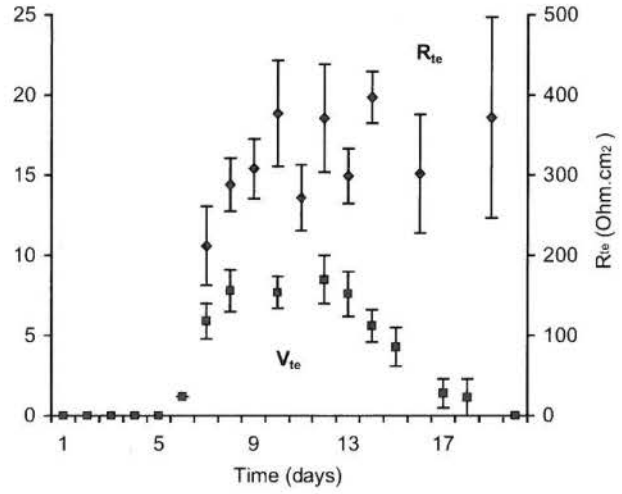

Figure 3.7 *Evolution of transepithelial potential difference (■, left axis) and transepithelial resistance (◆, right axis) in confluent primary cultures as measured in cell culture conditions with the "chopstick"-method. Values are mean ± SE. Each value represents at least 5 measurements.*

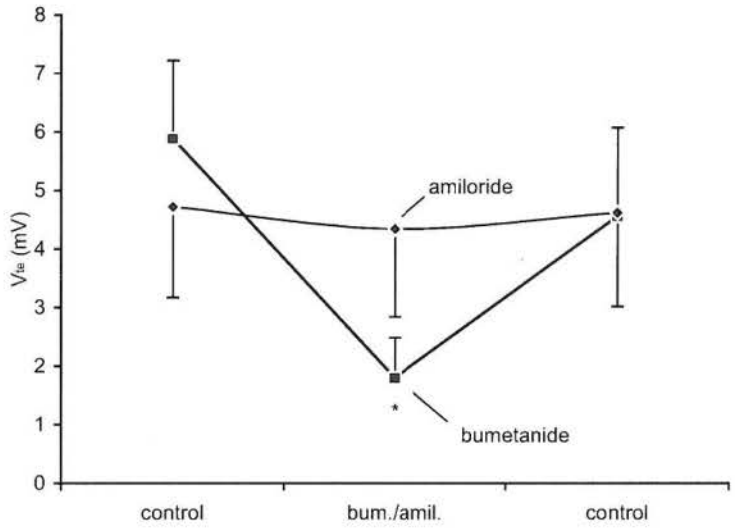

Figure 3.8 *Effect of addition of bumetanide 100 µM(■) or amiloride 100 µM(◆) to apical perfusate on the transepithelial potential difference of primary cultures measured in a modified Ussing-chamber with apical and basolateral perfusion. Values are mean ± SE (n=5), (*) indicates that the median decrease in potential is significantly higher using bumetanide versus amiloride (p=0.004, one-sided Wilcoxon test).*

TALH-SVE cells, when grown on permeable filter supports, developed no measurable R_{te}, even after prolonged time in culture. As a consequence, no electrophysiological studies could be performed on this cell line.

3.4.4 Electron microscopy

Electron microscopic evaluation of the primary cultures revealed cells with numerous blunt apical microvilli, a large nucleus, tight junctions at the apical part of the cells, some basolateral infoldings and mitochondria which were preferentially distributed over the apical part of the cells (Fig. 3.9).

TALH-SVE cells formed mainly monolayers, but polylayer formation was observed in several sections. Only a few apical microvilli and no basolateral infoldings were observed. The nucleus comprised the largest part of the cytoplasm. At the apical part of the cells, tight junctions were formed and as for the primary cultures the mitochondria seemed to be preferentially located in the apical part of the cytoplasm.

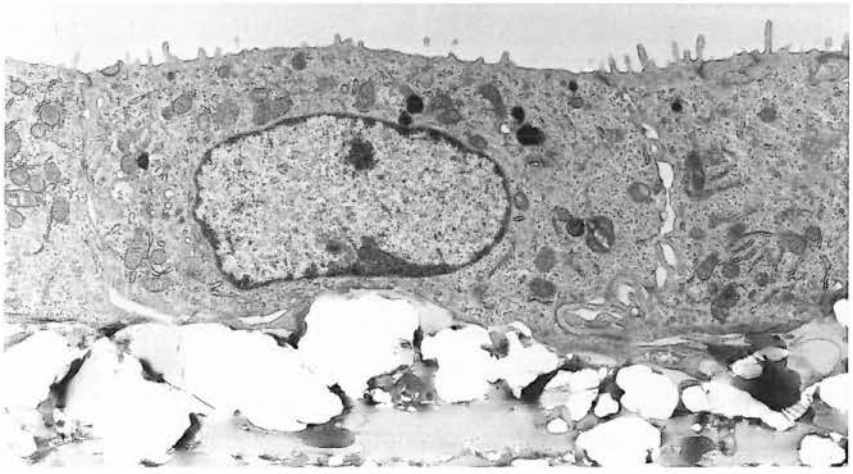

Figure 3.9 *Electron-microscopic photograph of transverse section of confluent primary culture of MTAL.*

3.4.5 Immunostaining for THP

This TAL-specific antigen (Hoyer & Seiler, 1979) was shown to be expressed in the primary cell cultures on day 7 and 12 in culture (Fig. 3.10). Although all cells stained positive, there was a marked difference in staining intensity between different cells within the same monolayer. The control primary

cell cultures underwent the same immunoperoxidase staining, but the primary antibody was omitted.

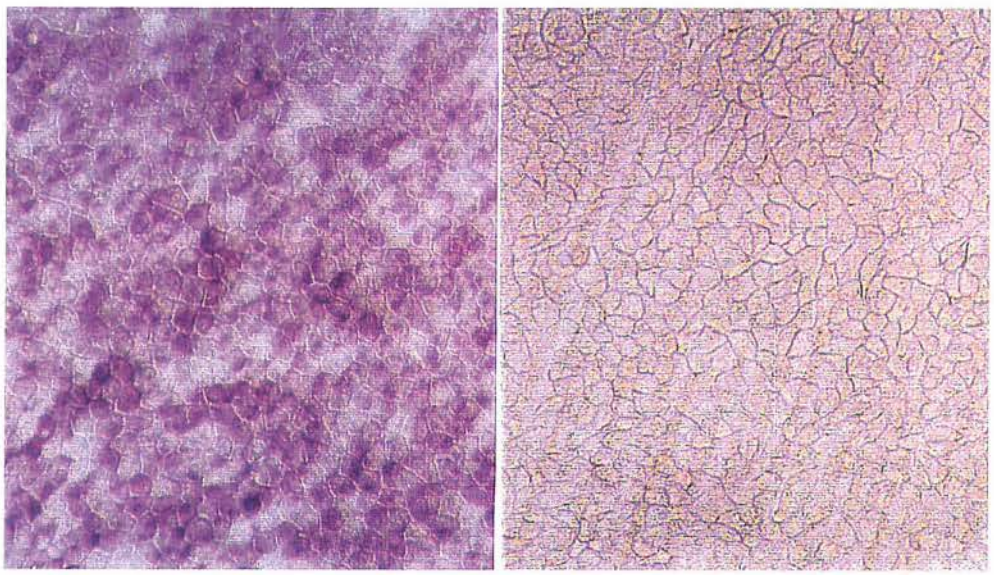

Figure 3.10 *12-Day-old confluent primary cultures: immunostaining for Tamm-Horsfall protein (left) and control (right).*

3.4.6 Ammonium transport

The changes in pH_i due to the addition of NH_4Cl 20 mM (replacing mannitol, glucose, glycine and alanine, resulting in an osmolality of 330 mosm/kg H_2O) to the basolateral or the apical perfusion solution were investigated. Addition of NH_4Cl to the basolateral perfusion solution first caused a transient intracellular alkalinization, followed by a slow intracellular acidification When the apical membrane of the primary cell cultures was exposed to NH_4Cl, a rapid and pronounced intracellular acidification was observed (Fig. 3.11). During basolateral NH_4^+-exposure, pH_i first increased from 7.22 ± 0.07 to 7.42 ± 0.06, then decreased to 7.00 ± 0.04 (n=5). During apical NH_4^+-exposure, pH_i sharply decreased from 7.22 ±0.07 to 6.65 ± 0.04 (n=5).

This pattern of a low permeability of the apical membrane to NH_3 relative to the basolateral membrane is typical for the TAL (Good, 1994) and is necessary to build up a medullary NH_4^+ gradient.

In TALH-SVE cells ammonium-pulses from both sides of the epithelium caused an intracellular alkalinization. Thus in this cell line, the changes in pH_i are identical to those seen in numerous other cell types.

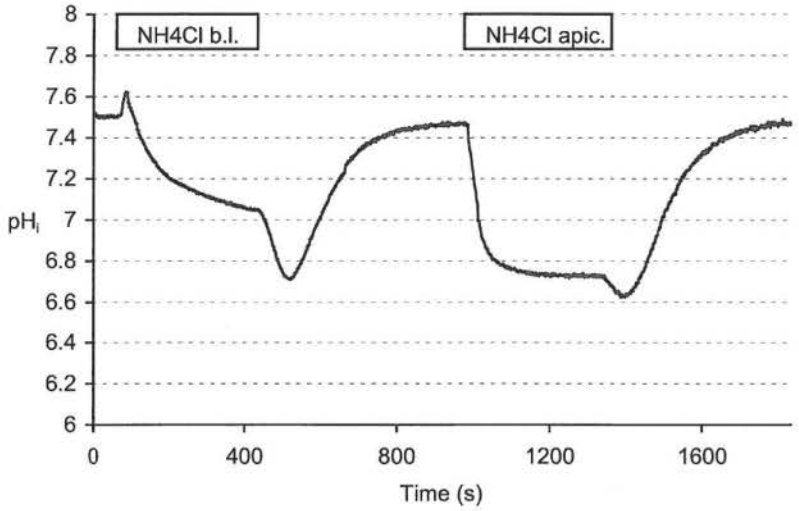

Figure 3.11 *Representative trace of intracellular pH measurement during basolateral and apical NH_4^+-pulse (20 mM of NH_4Cl in HB-BSS) in primary cell cultures.*

3.4.7 Intracellular Ca^{2+} signaling

Transient increases in $[Ca^{2+}]_i$ in response to the addition of hormones to the perfusion solution were investigated. For the primary cell cultures, we observed a response of the cells when bradykinin (10 nM), ATP (1 µM) or adenosine (1 µM) were added to the basolateral perfusion solution. For ATP and adenosine a response was also observed after addition to the apical perfusion solution (n=3). No rise in $[Ca^{2+}]_i$ was observed after addition of angiotensin II (1 µM), endothelin-1 (0.1 µM), salmon calcitonin (10 nM), parathyroid hormone (10 nM), AVP (0.1 µM), isoproterenol (1 µM) or prostaglandin E_2 (PGE_2) (1 µM) to either the apical or the basolateral perfusion solution.

For TALH-SVE, bradykinin (10nM) (Fig. 3.12) and adenosine (1 µM), but not ATP (1 µM), angiotensin II (1 µM) and endothelin-1 (0.1 µM) evoked transient rises in $[Ca^{2+}]_i$ when added to the basolateral perfusion solution. When added to the apical perfusion solution, only adenosine had an effect on $[Ca^{2+}]_i$ (n=3).

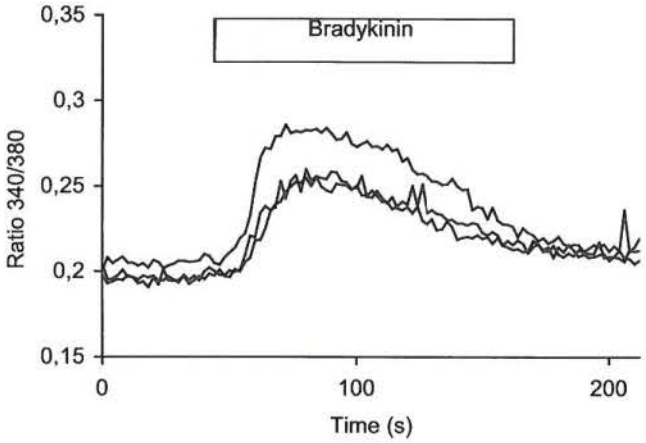

Figure 3.12 *Transient rise of intracellular calcium concentration in TALH-SVE cells after addition of bradykinin 10 nM to the basolateral perfusion solution. The figure depicts the traces of three independent experiments. The fluorescence ratio increases from 0.203 ± 0.003 to 0.263 ± 0.009.*

3.4.8 Measurements of hormone induced cAMP accumulation

In the presence of IBMX, the accumulation of cAMP was measured during hormonal stimulation (pmol cAMP.filter^{-1}.30 min^{-1}). Figure 3.13 shows the results of the stimulation of the primary cell cultures with 1 µM of AVP, salmon calcitonin or isoproterenol. All three hormones stimulated adenylyl cyclase activity significantly. The difference in cAMP accumulation after stimulation with AVP and calcitonin was also statistically significant.

The TALH-SVE cell line only seemed to respond to isoproterenol, but this was not statistically significant (p=0.18) (Fig. 3.14). For the TALH-SVE cell line, cAMP measurements were performed both on permeable supports and when grown on a solid substrate (24 well cell culture cluster), but this did not affect the result.

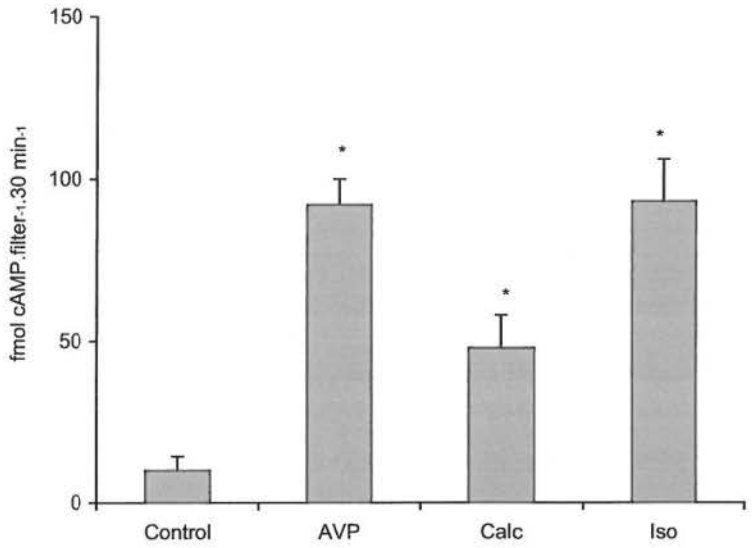

Figure 3.13 *Stimulation of cAMP production in confluent primary cell cultures (expressed as fmol cAMP produced by one confluent monolayer in a cell culture insert of 0.33 cm^2 in 30 minutes) by 1 µM of arginine-vasopressin (AVP), thyrocalcitonin (Calc) and isoproterenol (Iso). (*) Indicates value significantly different from control ($p<0.05$).*

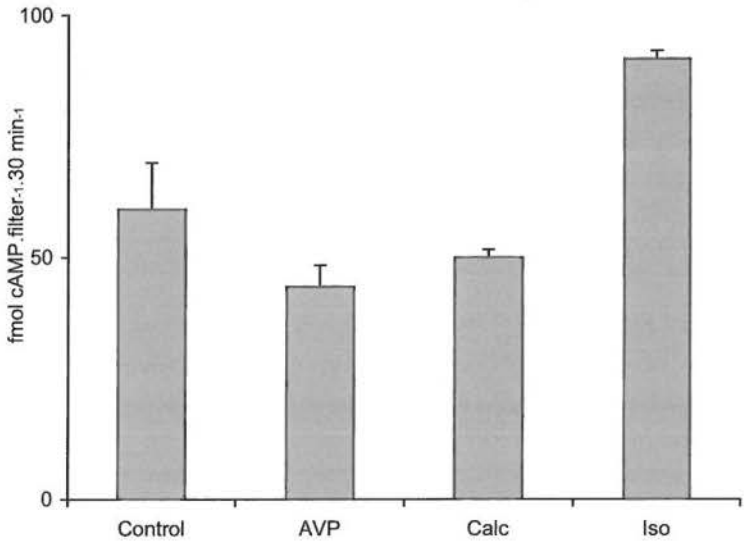

Figure 3.14 *Stimulation of cAMP production in TALH-SVE cells grown on permeable filter supports by 1 µM of arginine-vasopressin (AVP), thyrocalcitonin (Calc) and isoproterenol (Iso).*

3.5 Discussion

Since in the L.U.C. laboratory experiments on isolated autologous-blood perfused rabbit kidneys are performed, the same species was chosen as starting material for the primary cell cultures. Some preliminary experiments were done with kidneys from young and newborn rats, but these seemed to be less capable of giving rise to cellular outgrowth. In contrast to individually microdissected nephron segments, where cellular proliferation can be seen only at the open ends of the nephron segments (Horster et al., 1979), cellular proliferation along the whole length of the nephron segments was observed. This may have been due to partial enzymatic degradation of the basal membrane surrounding the nephron segments. Horster described formation of polylayers after treating the kidneys with collagenase (Horster et al., 1979). Although the same concentration of collagenase was used in the present experiments, monolayer formation was always observed.

FCS is essential for cellular outgrowth of TAL segments. 1% (volume/volume) is reported to be the minimum requirement (Horster & Sone, 1990), 5% seems optimal (Drugge et al., 1989). Our experience is in accordance with these findings. Fibroblast overgrowth was never observed, which is an indication of the purity of the starting material. The relatively high number (100) of collected MTAL segments per cell culture filter was necessary to obtain a confluent monolayer within a reasonable amount of time. If it took too long to reach confluence, it usually was not possible to measure a V_{te}, probably because of dedifferentiation (Valentich & Stokols, 1984). Whereas in the original method, the emphasis lies on collecting long nephron segments, in the present investigation we were particularly interested in high numbers of shorter segments. With some practice, nephron segments of 100 µm in length can already be identified by their morphological criteria.

The electrophysiological characteristics of the primary cell cultures corresponded well to the *in vivo* situation, as judged by the *in vitro* perfused TAL tubules (Greger & Schlatter, 1983). The apical side positive V_{te} is the result of a depolarization of the basolateral cell membrane relative to the apical cell membrane. The decrease in V_{te} in response to bumetanide indicates that the NaCl transport pathways in these primary cell cultures may be similar to the *in vivo* situation. The apical side positive V_{te} may theoretically have been the result of the generation of a transepithelial NaCl concentration difference resulting in "backflux" of NaCl through the paracellular pathway. Since this paracellular pathway is more permeable to Na^+ ions than to Cl^- ions, this passive movement of ions may have generated a "dilution potential". Two observations however are not in agreement with this hypothesis. First, during the experiments performed in the Ussing-type

chamber, the fluid-exchange rate was sufficiently rapid to prevent the generation of transepithelial concentration differences. Second, for the steady-state experiments with the chopstick electrodes, the apical and basolateral solutions were exchanged before performing the measurements. Therefore the observed transepithelial potential difference must have been the result of active, transcellular NaCl transport thereby generating a "transport potential". With an average value of 212 Ohm.cm^2 on day 7, the R_{te} corresponds to epithelia with an intermediate resistance.

Electron microscopic examination demonstrated that these cells in primary culture are well polarized and show several characteristics of distal nephron epithelia. Atypical is the distribution of the mitochondria. In the primary cell cultures the mitochondria are not localized in the basolateral infoldings, but are spread out over the cytoplasm. This might be due to the fact that oxygen supply to the cells is maximal at the apical side, and not as *in vivo* at the basolateral side. Aw et al. (Aw et al., 1987) showed that the distribution of the mitochondria within renal cells is an important determinant of the cellular O_2 dependence.

THP is a glycoprotein produced by cells of the TALH and the early distal convoluted tubule and is a marker of tubular maturation (Zimmerhackl et al., 1996). The expression of THP in these primary cell cultures is a strong indication of their origin specific differentiation. Helbert et al. (Helbert et al., 1999) have demonstrated that the expression of THP in primary cell cultures derived from human immunodissected kidneys decreased with increasing time in culture. Therefore it is conceivable that the heterogeneity of THP expression in our primary cell cultures reflects the "age difference" of the cultured cells.

The MTAL is an important site for active ammonium reabsorption. The changes in pH_i that were observed during an ammonium-pulse either at the apical or the basolateral side of the primary cultures are very typical for the MTAL cells (Good, 1994). This is an additional indication for the high degree of polarized differentiation of the primary cell cultures.

Ca^{2+} signaling was demonstrated in these primary cell cultures after stimulation with adenosine, ATP and bradykinin. Freshly immunodissected and cultured immunodissected rabbit MTAL cells show transient increases in calcium concentrations in response to 1 µM of the adenosine analogues N^6-cyclohexyladenosine (CHA) and 5'-(*N*-ethylcarboxamido)adenosine (NECA) (Burnatowska-Hledin & Spielman, 1991). In the kidney, adenosine induces both cortical vasoconstriction and medullary vasodilatation with inhibition of tubular transport, which suggests that it has an intrarenal homeostatic role that attenuates medullary hypoxia (Brezis & Rosen, 1995). For ATP and bradykinin no data was found in the literature concerning their effect on calcium concentrations in rabbit

MTAL, but in rat MTAL, increases in intracellular calcium mediated by bradykinin inhibit NaCl transport (Bailly, 1998). In rat kidney, ATP induced calcium signaling is observed in S1 and OMCD, but not in TAL segments (Cha et al., 1998). In isolated perfused rabbit *cortical* TAL, AVP increases intracellular calcium levels through a V_1-receptor (Nitschke et al., 1991) and in a suspension of rabbit MTAL tubules calcitonin doubles intracellular calcium concentration over a time range of minutes (Murphy et al., 1986). We do not observe calcium signaling with AVP or calcitonin in TAL cells from medullary origin. PGE_2 inhibits transport dependent oxygen consumption in rabbit MTAL (Lear et al., 1990). In rabbit MTAL, mRNAs for EP_3 receptor have been found (Breyer et al., 1993) which indicates that PGE_2 exerts its inhibitory effect via G_i activation. This is supported by the observation that PGE_2 fails to increase basal adenylyl cyclase activity and $[Ca^{2+}]_i$ in rat TAL. However, in rabbit MTAL, PGE_2 did increase cAMP levels by approximately 100% (Lear et al., 1990).

Hormonal stimulation of cAMP production in the nephron is segment specific and it is routinely used as a marker for the origin of primary cultures. Because we had no indication of the degree of polarization of the TALH-SVE cell-line, we added the hormones simultaneously to both sides of the epithelium. The same protocol was used for the primary cell cultures. AVP and calcitonin are known to stimulate adenylyl cyclase activity in rabbit MTAL (De Rouffignac et al., 1991). AVP exerts this effect through a V_2-receptor (Knepper et al., 1999). This important characteristic was preserved in the present primary cell cultures. Although stimulation of adenylyl cyclase activity by calcitonin is reported to be more pronounced relative to stimulation by AVP in the rabbit MTAL (Nitschke et al., 1991), cAMP accumulation in the present primary cell cultures is higher after stimulation with AVP. Stimulation by isoproterenol is reported not to influence cAMP levels in this nephron segment *in vivo* or in freshly immunodissected MTAL cells (Allen et al., 1988; Nitschke et al., 1991; Morel, 1981) and was included in our experiment as a negative control. In the present primary cell cultures however, a significant stimulation of the cAMP production was also observed with isoproterenol. The aspecific presence of this receptor is also observed in primary cell cultures that were started with immunodissected rabbit MTAL cells (Burnatowska-Hledin & Spielman, 1991). This may have been the result of the use of FCS in the culture medium.

TALH-SVE cells were shown to produce THP, to express the Na/K/2Cl-cotransporter and a barium-sensitive potassium channel (Scott et al., 1986). This cell-line was subcultured for 92 passages without a sign for chromosomal instability and is considered to be immortal (MacDonald et al., 1991). The absence of development of an R_{te} and thus a measurable V_{te} by the TALH-SVE cells was

probably the most important distinction with the MTAL cells in primary cell culture. Electron microscopic examination of the TALH-SVE cells showed a tendency for polylayer formation. AVP, thyrocalcitonin or isoproterenol did not significantly stimulate cAMP accumulation in TALH-SVE cells. It must be noted however that control cAMP levels in our experiments were high in comparison to the primary cell cultures. Intracellular Ca^{2+} signaling was observed after exposure to bradykinin and adenosine, but not ATP. In contrast to our findings, Tinel et al. (Tinel et al., 2002) recently reported ATP (100 µM) induced Ca^{2+} signaling in TALH-SVE cells grown on collagen-coated Petri-dishes. The authors did not mention the passage-numbers that were used in their study. In lower passage numbers, addition of ammonium to the extracellular fluid caused an intracellular acidification as monitored by ^{31}P NMR (von Recklinghausen et al., 1992). The TALH-SVE cells from the passage numbers we used (39 to 49) alkalinized upon apical exposure to ammonium. So apparently they had lost their specific apical ammonium transport pathways. Although the characterization we performed on this immortalized cell line reveals some degree of dedifferentiation in comparison with lower passage numbers, we plan to use this cell line in parallel studies with the primary cell cultures to investigate the effects of long-term subculturing on the cellular responses to ischemia.

In conclusion, a simple method for obtaining pure primary cell cultures of rabbit MTAL that are functionally and morphologically well differentiated during at least one week following confluency, is described. The fact that with this method intercellular contacts are preserved during the whole procedure and cells are not adherent to a plastic surface may account for these results (Valentich & Stokols, 1984).

Chapter 4

Intracellular pH in physiological conditions

4.1 Introduction

A comprehensive review on H^+ and HCO_3^- transporters in the MTAL was published by Paillard (Paillard, 1998). Since data on acid/base transporters in rabbit MTAL are incomplete, most conclusions were derived from observations made in rat and mouse nephron segments. In contrast to the rat and mouse TAL segment, rabbit TAL does not reabsorb HCO_3^- from the luminal fluid (Iino & Burg, 1981). Therefore, in these species, acid-base transport by the MTAL is more complex, because both HCO_3^- and NH_4^+ are being reabsorbed from the luminal fluid.

4.1.1 HCO_3^- transporters in the MTAL

The lack of HCO_3^- reabsorption in the rabbit TAL correlates with the absence of carbonic anhydrase activity in rabbit TAL (Dobyan & Bulger, 1982; Schwartz et al., 2000). Therefore the use of HCO_3^- free, HEPES buffered, solutions when studying rabbit TAL cells will simplify experimental procedures and interpretation of results, without interfering with physiologically relevant transepithelial transport processes. In mouse and rat, TAL reabsorbs most of the bicarbonate present in Henle's loop *in vivo* (10 to 15% of the filtered load). In the basolateral cell membrane of rat MTAL, different HCO_3^- transport mechanisms are functional under physiological circumstances: a Na^+/HCO_3^- cotransporter, a Ba^{2+} sensitive $K^+/Cl^-(HCO_3^-)$ cotransporter and an electroneutral Cl^-/HCO_3^- exchanger are present. It is likely that the Na^+-coupled pathway operates as HCO_3^- loader and is therefore involved in the control of pH_i. The Cl^-/HCO_3^- exchange and the $K^+/Cl^-(HCO_3^-)$ cotransport are expected to drive HCO_3^- out of the cell and thus are involved in the active, transcellular HCO_3^- reabsorption (Paillard, 1998; Bourgeois et al., 2002). No data on HCO_3^- transporters in the rabbit TAL have been published.

4.1.2 Na^+/H^+ exchangers in the MTAL

NHE extrude protons from, and take up sodium ions into the cells. Eight isoforms have been described (Aronson et al., 2003). The NHE-1 isoform is expressed in virtually all cells and tissues and is considered to be the "house-keeping" isoform. NHE-3 is expressed in the proximal tubule, the thin limbs of Henle's loop and the TAL segment and is specifically targeted to the apical cell membrane. In comparison to the other isoforms, NHE-3 mediates the great majority of Na^+ and HCO_3^- reabsorption in the kidney. NHE-2 has been detected in kidney and is, like NHE-3, targeted to the apical cell membrane of epithelial cells.

NHE-4 is mostly present in the inner medulla collecting duct and has also been found on the basolateral membrane of cortical tubule cells. The function of both NHE-2 and NHE-4 is unclear, although it has been suggested that NHE-4 may play a role in cell volume regulation. NHE-5 is not expressed in the kidney. NHE-6 is expressed in the mitochondria and has a wide tissue distribution (Counillon & Pouysségur, 2000; Burckhardt et al., 2002).

In the apical cell membrane of (rat and mouse) MTAL cells, the Na^+/H^+ exchanger is the major pathway for H^+ excretion (HCO_3^- reabsorption) (Reeves & Andreoli, 2000). In contrast to the other isoforms, the pH_i-dependence curve of the apical Na^+/H^+ exchanger in rat and mouse MTAL is positioned toward the alkaline direction and therefore will be maximally activated at pH_i 7.15 (Counillon & Pouysségur, 2000; Paillard, 1998). This is important for transepithelial NH_4^+ reabsorption since in this way the intracellular acidification resulting from transcellular NH_4^+ reabsorption will not stimulate the apical Na^+/H^+ exchanger. This was confirmed by the observation in freshly isolated rat MTAL tubules, that luminal ethyl-isopropyl-amiloride (EIPA) did not diminish transepithelial NH_4^+ reabsorption (Good & Watts, 1996). Immunolocalization studies showed that Na^+/H^+ exchanger isoforms NHE-2 and NHE-3 were present in the apical cell membrane of rat TAL, which is similar to the apical cell membrane of the proximal tubule (Peti-Peterdi et al., 2000). Immunolocalization of NHE-3 in the rabbit nephron showed its absence in the MTAL tubules (Biemesderfer et al., 1993) and in the CTAL (Peti-Peterdi et al., 2000). The rabbit CTAL cells were positive for NHE-2 at their apical membranes (Peti-Peterdi et al., 2000).

In, mouse, rat and rabbit TAL a Na^+/H^+ exchanger is present in the basolateral membrane, which has been identified by immunostaining as Na^+/H^+ isoform NHE-1. This isoform is present in almost all animal cells where it functions in hypertonic cell volume regulation and cell pH regulation ("housekeeping") (Biemesderfer et al., 1992; Peti-Peterdi et al., 2000; Paillard, 1998).

4.1.3 H^+-ATPase in the MTAL

In rat TAL, a Na^+ independent, ATP dependent, bafilomycin-A_1 sensitive H^+ extrusion mechanism is present, consistent with the presence of a H^+-ATPase. This H^+-ATPase is responsible for approximately 20% of the H^+ secretion (HCO_3^- reabsorption) into the luminal fluid (Paillard, 1998; Glück et al., 1996).

4.1.4 NH_4^+ transport pathways in the MTAL

The MTAL segment reabsorbs 40 to 80% of the amount of NH_4^+ (the main component of the acids excreted in the urine) delivered by the proximal tubule. Since NH_4^+ reabsorption is also subjected to regulation in the MTAL, this nephron segment plays a key role in the regulation of acid-base balance by the kidney (Attmane-Elakeb et al., 2001) (see 3.1.2).

In steady-state conditions, resting intracellular pH in MTAL cells is very low due to the symmetrical presence of ammonium (Watts & Good, 1994). The apical pathways for transcellular ammonium reabsorption have been extensively studied. Three types of apical NH_4^+ transport pathways have been described so far. The best documented pathway is the bumetanide sensitive $Na^+/K^+/2Cl^-$ co-transporter, which can accept NH_4^+ at its K^+ binding site (Kinne et al., 1986). An amiloride sensitive NH_4^+ conductance was demonstrated in suspension from rat MTAL fragments (Amlal et al., 1994). The third pathway is a Ba^{2+} sensitive pathway, which is responsible for 30 to 60% of apical NH_4^+ entry (Attmane-Elakeb et al., 2001). Because apical TAL membranes are characterized by their high K^+ conductance and since Ba^{2+} is a K^+ channel blocker, it was assumed that the Ba^{2+} sensitive component of NH_4^+ entry occurred via apical K^+ channels (Kikeri et al., 1989; Watts &Good, 1994; Good, 1994; Garvin et al., 1988; Kikeri et al., 1992). Some publications during the past decade however provided some evidence against the role of apical K^+ channel(s) in NH_4^+ reabsorption (Bleich et al., 1995; Amlal et al., 1994; Laamarti & Lapointe, 1997). Finally, Amlal et al. have described a Ba^{2+} sensitive apical $K^+/H^+(NH_4^+)$ exchanger and suggested this could represent the Ba^{2+} sensitive pathway (Amlal et al., 1994; Attmane-Elakeb et al., 2001).

In contrast to the apical transport pathways, the basolateral pathways for NH_4^+/NH_3 transport in the MTAL have not been extensively investigated. However, Blanchard et al. (Blanchard et al., 1998) demonstrated in membrane vesicles from rat TAL, that the basolateral Na^+/H^+ and the apical Na^+/H^+ were capable of functioning as Na^+/NH_4^+ exchangers. They concluded that basolateral Na^+/NH_4^+ activity would contribute to transepithelial NH_4^+ transport, whereas apical Na^+/NH_4^+ activity might provide a feedback mechanism that limits net NH_4^+ absorption as the interstitial NH_4^+ concentration increases.

4.2 Solutions and chemicals

The **standard** perfusion solution was HB-BSS as described in chapter 3. Solutions containing 4 and 10 mM **NH_4Cl** had the same composition only less or no mannitol was added to reach 320 mosm/kg H_2O. **Ba^{2+}** containing solutions were without $MgSO_4$, and $NaH_2PO_4.H_2O$. **Na^+ free** solutions contained (in mM):100 N-methyl-D-Glucamine ($NMDG^+$), 100 HCl, 5 KCl, 1 $CaCl_2$, 1.2 $MgSO_4$, 2 KH_2PO_4, 1 L-alanine, 5 glycine, 10 glucose, 20 HEPES. **Cs^+** solution contained (in mM): 108 NaCl, 5 KCl, 1 $CaCl_2$, 1.2 $MgSO_4$, 2 KH_2PO_4, 1 L-alanine, 5 glycine, 10 glucose, 20 HEPES, 20 CsCl. **High K^+** solution contained (in mM): 113 NaCl, 20 KCl, 1 $CaCl_2$, 1.2 $MgSO_4$, 2 KH_2PO_4, 1 L-alanine, 5 glycine, 10 glucose, 20 HEPES. **Propionate** solution contained (in mM): 98 NaCl, 5 KCl, 30 NaPropionate, 1 $CaCl_2$, 10 glucose, 1 L-alanine, 5 glycine, 20 HEPES. **Tetraethylammonium** (TEA^+) solution contained (in mM): 118 NaCl, 5 KCl, 10 $TEACl.H_2O$, 1 $CaCl_2$, 1.2 $MgSO_4$, 2 $NaH_2PO_4.H_2O$, 1 L-alanine, 5 glycine, 10 glucose, 20 HEPES. Final pH of all these solutions was brought to 7.4 with (solid) TRIS and osmolality to 320 mosm/kg H_2O with mannitol. rCharybdotoxin and Tertiapin were from Alomone Labs Inc. (Jerusalem, Israel), CsCl was from Acros Organics (Geel, Belgium). All other hormones and chemicals were from Sigma Chemical Company (St. Louis, MO, USA).

Blockers were dissolved in ethanol or DMSO, the final concentration of these solvents never exceeded 1 pro mille.

4.3 Results

4.3.1 Na^+/H^+ exchange

Resting pH_i in BCECF-loaded primary cell cultures, when perfused on both sides with HCO_3^- free, HEPES buffered solutions at 37° C, was 7.22 ± 0.07 (n=5). Addition of EIPA (10 µM) to the apical perfusion solution acidified the cells from pH_i 7.15 ± 0.04 to 7.09 ± 0.03. When added to the basolateral perfusion solution pH_i decreased from 7.21 ± 0.06 to 7.10 ± 0.05 (n=3) (Fig. 4.1). To provide further evidence that a Na^+/H^+ exchanger is present and functional both in the apical and the basolateral cell membrane, Na^+ dependent acidifications or alkalinizations at both sides of the epithelium were investigated. Replacing all Na^+ by $NMDG^+$ (iso-osmotically) in the basolateral perfusion solution acidified the cells. Steady-state pH_i in these circumstances was 6.81 ± 0.03 (n=5). Re-addition of Na^+ to the basolateral side of the epithelium rapidly alkalinized the cells to pH_i 7.03 ± 0.04 (n=5). When the same experiments were repeated with EIPA (10 µM) present in

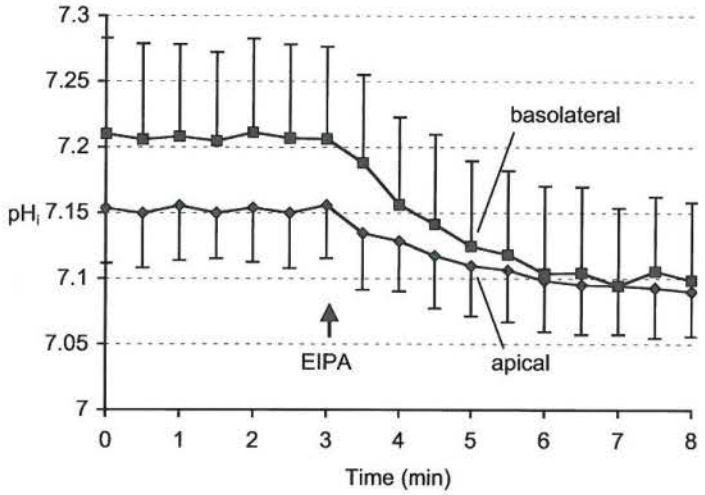

Figure 4.1 *Effect of EIPA 10 µM on pH$_i$: at the time point indicated by the arrow, EIPA was added to either the apical (◆) or the basolateral(■) perfusion solution (mean ± SE, n=3).*

the basolateral perfusion solutions, no Na^+ dependent alkalinization could be observed (Fig. 4.2). During superfusion of the apical side of the epithelium with Na^+ free Ringer solution, the cytosol acidified to pH_i 6.75 ± 0.08. Re-addition of Na^+ to the apical solution rapidly alkalinized the cells to 7.09 ± 0.06 (n=8). When the same experiments were repeated in the presence of EIPA (10 µM) in the apical superfusion solutions, the cytosol again rapidly alkalinized from 6.77 ± 0.04 to 7.04 ± 0.08 (n=7) (Fig. 4.3). Thus, the total Na^+ dependent increase in pH_i was not different either in the presence or the absence of EIPA. However, the initial rate of alkalinization (obtained from fitting linear equations to the recorded pH_i time courses, see paragraph 2.9) was significantly diminished from 0.14 ± 0.03 pH units/min (n=8) in the absence of EIPA to 0.07 ± 0.01 pH units/min (n=7) in the presence of EIPA ($p < 0.05$, student-t test). This indicated that either the Na^+ dependent alkalinization was only partially attributable to a Na^+/H^+ exchanger, or that all Na^+ dependent alkalinization was attributable to a Na^+/H^+ exchanger that was only partially blocked by 10 µM EIPA. Since the acidification that was observed during Na^+-free perfusion at the apical side of the cells was probably caused by the reversal of Na^+/H^+ exchange activity (Alpern, 2000), we investigated whether this acidification itself could be prevented by EIPA. Therefore, three control experiments were performed in which Na^+ free apical superfusion caused

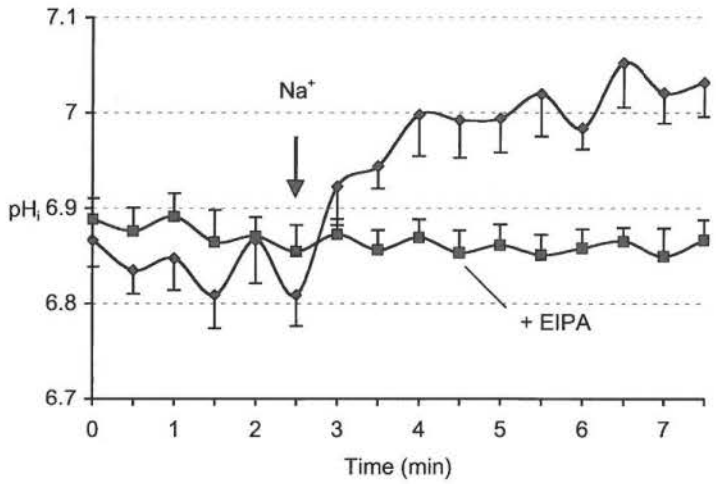

Figure 4.2 *Primary cell cultures were acidified by perfusion with sodium-free basolateral solution. At time 2.5 min (arrow), sodium was re-introduced in the basolateral solution (◆) (mean - SE, n=5). The same protocol was repeated with EIPA (10 µM) present in all basolateral solutions (■) (mean + SE, n=5).*

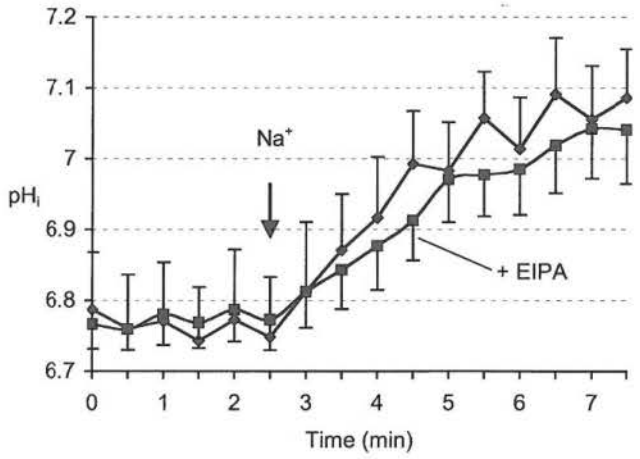

Figure 4.3 *Primary cell cultures were acidified by superfusion with sodium-free apical solution. At time 2.5 min (arrow), sodium was re-introduced in the apical solution (◆) (mean + SE, n=5). The same protocol was repeated with EIPA (10 µM) present in all apical solutions (■) (mean - SE, n=5).*

an intracellular acidification from 7.20 ± 0.05 to 6.53 ± 0.16 (n=3), whereas the presence of EIPA 10 µM completely prevented this acidification (Fig. 4.4).

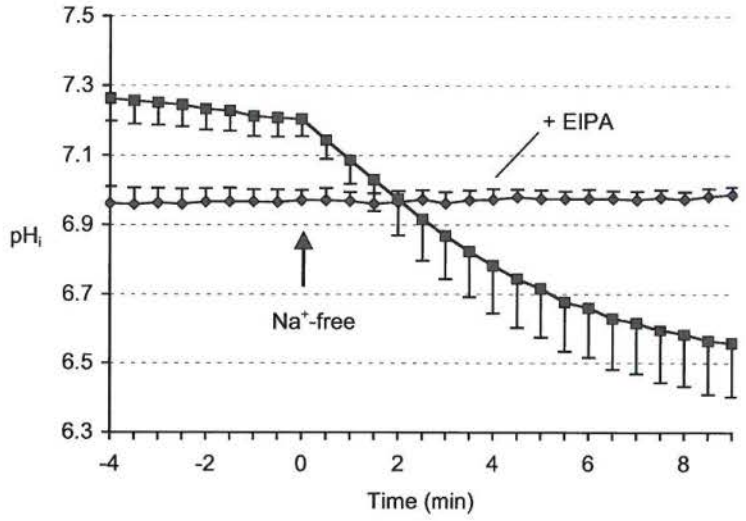

Figure 4.4 *At time 0 s (arrow), the apical superfusion solution was replaced by sodium-free solution (■) (mean - SE, n=3). The same protocol was repeated with EIPA 10 µM present in all apical solutions (◆) (mean + SE, n=3).*

4.3.2 Na-P$_i$ cotransporter

To investigate further the nature of the "amiloride-resistant" Na^+-dependent pH_i recovery at the apical cell membrane, the same type of experiments were performed in the absence of phosphate. Sudden re-addition of Na^+ in the absence of phosphate had only a minimal alkalinizing effect on the cells (n=5) (Fig. 4.5). This very limited pH_i-recovery during the initial 30 to 60 seconds upon re-addition of Na^+, was followed in some experiments by a slight decrease in pH_i. In a next series of experiments, the addition of phosphate 2 mM to the apical perfusion solution was shown to alkalinize the cells from pH_i 6.84 ± 0.09 to pH_i 7.18 ± 0.08 (n=10) (Fig. 4.6). The initial alkalinization rate was 0.09 ± 0.03 pH units/min. Although not statistically different from the Na^+-dependent alkalinization in the absence of EIPA (0.14 ± 0.03 pH units/min), this value is almost identical to the Na^+-dependent alkalinization rate in the presence of EIPA (0.07 ± 0.01 pH units/min) (Fig. 4.3). Addition of phosphate in the absence of Na^+ did not result in an intracellular alkalinization (n=5) (Fig. 4.6). Since these results indicated that a Na-P_i cotransporter was present in the apical cell membrane, indirect

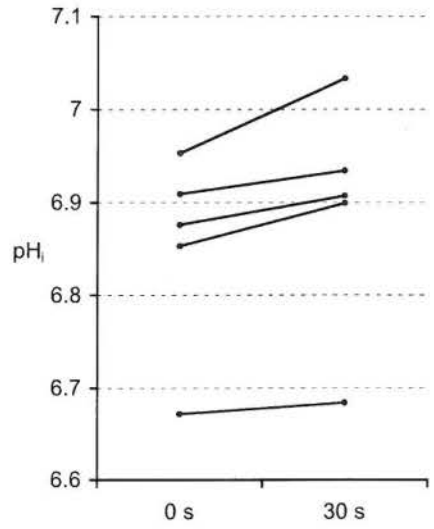

Figure 4.5 *Results of pH_i measurements in 5 primary cell cultures that were acidified by superfusion with sodium-free apical solutions. All apical solutions were phosphate-free. At time 0 s, sodium (but not phosphate) was re-introduced in the apical solutions. Intracellular pH values measured at time 30 s are shown.*

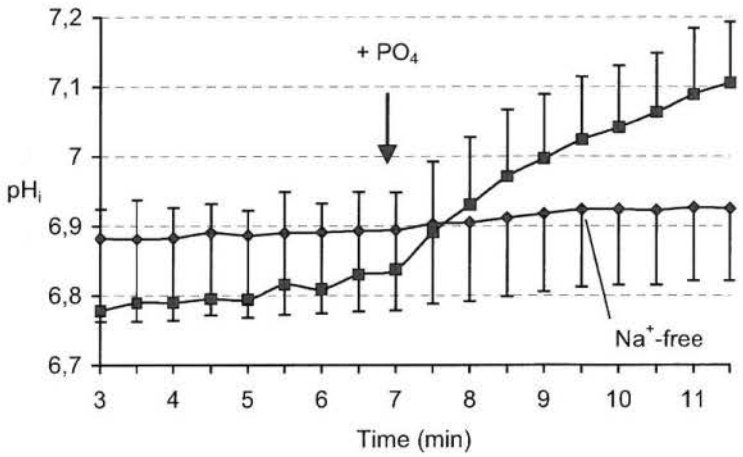

Figure 4.6 *At time 7 min (arrow), phosphate (2 mM) was added to the apical superfusion solution (■) (mean + SE, n=10). At time 7 min (arrow), phosphate (2 mM) was added to the sodium-free apical superfusion solution (◆) (mean - SE, n=5).*

immunofluorescence was performed for the Na-P_i co-transporters type I and type II. A fluorescent cellular staining pattern was obtained only with anti-type I antibodies (dilution 1/200) (Fig. 4.7). Control experiments in which the primary antibody were omitted, were negative.

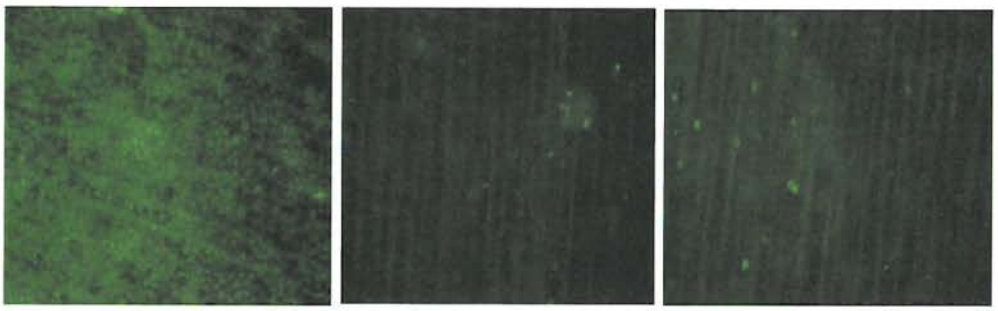

Figure 4.7 *Indirect immunofluorescence with α-Na-P_i type I (**left**) and α-Na-P_i type II (**middle**) (dilution 1/200). Control experiment in which the primary antibody was omitted (**right**).*

4.3.3 H^+-ATPase

Addition of 10 nM (n=4) or 100 nM (n=4) bafilomycin A_1 to the apical or basolateral perfusion solution did not change pH_i in acid loaded cells. Furthermore, the absence of depolarization induced alkalinizations in acid-loaded cells (Fig. 4.11) is also compatible with the absence of an electrogenic acid/base transporter in the apical cell membrane.

4.3.4 Ammonium

NH_3/NH_4^+ transport pathways were investigated indirectly by measuring changes in pH_i. With a pK_a value of approximately 9 at 37°C, the calculated ratio between NH_4^+ and NH_3 at pH 7.4 is 97.5/2.5. If membrane permeability for NH_3 exceeds permeability for NH_4^+ (which is the case for most cell types), the cells will alkalinize upon addition of NH_4Cl to the extracellular fluid. They will acidify if the membrane is highly permeable to NH_4^+. The initial rate of acidification is determined almost exclusively by the rate of NH_4^+ entry that causes H^+ accumulation within the cells because the intracellular NH_3 amount that tends to rise above the NH_3 equilibrium value leaves the cell as fast as NH_4^+ enters (no NH_3 is present in the basolateral solution) ("ammonium-pulse experiments") (Amlal et al., 1996). To study ammonium transport in more physiologically relevant conditions, experiments can be performed in the symmetrical presence of 4 mM

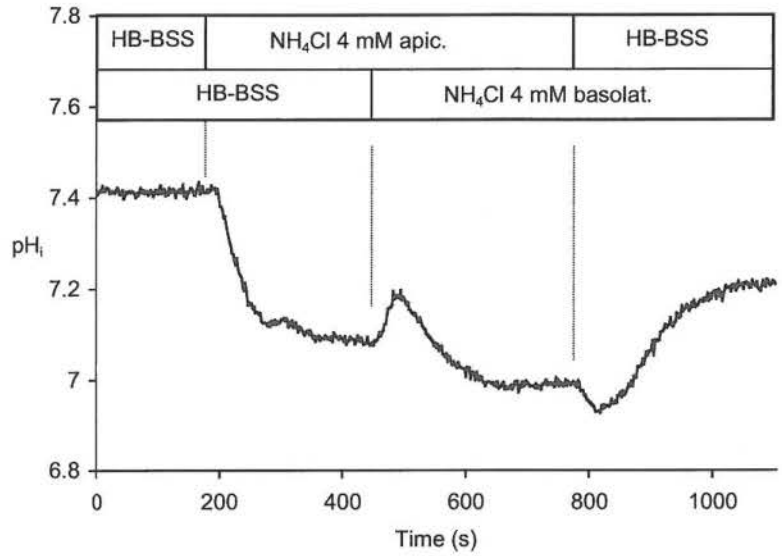

Figure 4.8 *Representative experiment for pH_i response to bilateral (sequential) exposure to 4 mM NH_4Cl.*

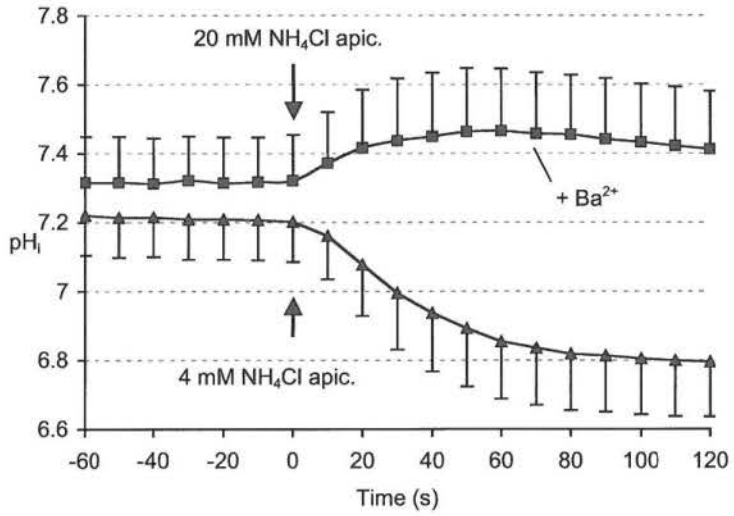

Figure 4.9 *At time 0 s (arrow), ammonium 20 mM was added to the apical superfusion solution in the continuous presence of Ba^{2+} 2 mM (■) (mean + SEM, n=3). At time 0 s, ammonium 4 mM was added to the apical superfusion solution (◆) (mean-SEM, n=5).*

NH_4^+. This is the average concentration to which rat MTAL cells are exposed *in vivo* (Eveloff et al., 1980). When under these conditions a blocker of apical NH_4^+ entry is applied, we expect to see an intracellular alkalinization due to the suppression of the sustained component of NH_4^+ entry within the cells ("resetting of steady-state pH_i"). This type of experiments was previously described by Watts et al. (Watts & Good, 1994) in rat TAL cells ("steady-state experiments").

In the symmetrical presence of 4 mM NH_4Cl steady-state pH_i decreases from 7.22 ± 0.07 (n=5) to 6.89 ± 0.03 (n=12) (the pH_i recording of one representative experiment is shown in Fig. 4.8). This marked intracellular acidification associated with ammonium indicates that the acid loading effects of NH_4^+ transport predominate over the acid-extruding mechanisms responsible for pH_i regulation. Since the high permeability of the apical membrane to NH_4^+ is attributed to the activity of the $Na^+/K^+(NH_4^+)/2Cl^-$ co-transporter and a second, Ba^{2+}-sensitive component, we investigated the effect of bumetanide and Ba^{2+} on the NH_4^+-induced intracellular acidification ("ammonium-pulse experiments"). The acidification rate after addition of NH_4^+ 10 mM to the apical perfusion solution was 0.38 ± 0.04 pH units/minute (n=5). In the presence of bumetanide (100 µM), this acidification rate was significantly decreased to 0.30 ± 0.01 pH units per minute (n=4) ($p < 0.05$, student-t test). In the presence of Ba^{2+} (2 mM), the addition of NH_4^+ (20 mM) to the apical superfusion medium induced an intracellular alkalinization (Fig. 4.9), unmasking the permeability of the apical cell membrane for NH_3. Therefore, the Ba^{2+}-sensitive pathway for apical NH_4^+ clearly is predominant over the bumetanide-sensitive cotransporter in these primary cell cultures.

We subsequently performed a series of experiments to investigate the effect of different (K^+-channel) blockers on apical NH_4^+ entry in the symmetrical presence of 4 mM NH_4^+ ("steady-state experiments"). In Figure 4.10 experimental data, expressed as maximum change in pH_i, are summarized. The effect of Ba^{2+} (2 mM) is significantly larger than the effect of bumetanide (100 µM). In fact, application of Ba^{2+} restores pH_i to a value close to the resting pH_i in the absence of NH_4^+. Cs^+ (20 mM) has exactly the same effect as Ba^{2+}, but TEA (10 mM) did not change pH_i.

Since the pharmacological profile of sensitivity to Ba^{2+} and Cs^+ but insensitivity to TEA has been described for the cloned renal outer medullary K^+ channel (ROMK) (see discussion), we used the ROMK specific blocker Tertiapin. Tertiapin alkalinized the NH_4^+-loaded cells to a level intermediate between bumetanide and Ba^{2+} (Fig. 4.10). Another rather specific blocker for K_{ATP}-channels is glibenclamide (200 µM decreases channel activity by 70%) (Wang, 1994). At this concentration, glibenclamide ($pK_a = 5.3$) acidified the cells in control conditions (i.e. in the absence of NH_4Cl). Therefore it could not be used in this type of

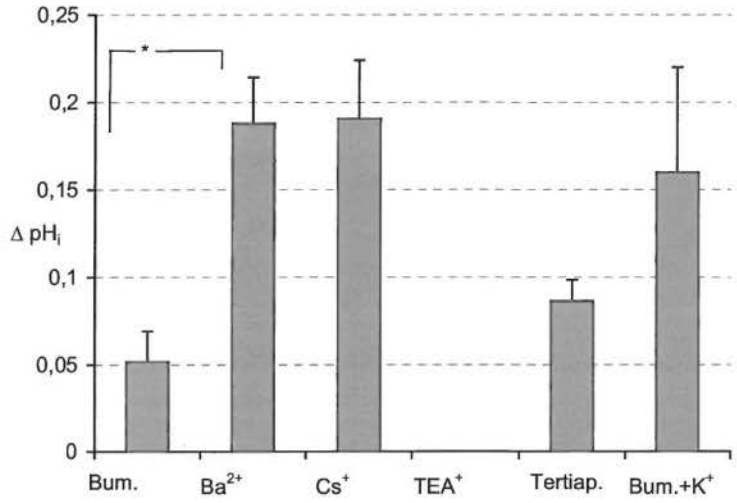

Figure 4.10 *Summary of maximum changes in pH_i after addition of different blockers to the apical superfusion solution in steady-state experiments (i.e. symmetrical presence of ammonium 4 mM). Bumetanide 0.1 mM alkalinized the cells by 0.05 ± 0.02 pH units (n=6), Ba^{2+} 2 mM by 0.19 ± 0.03 pH units (n=8), Cs^+ 20 mM by 0.19 ± 0.03 pH units (n=8), TEA^+ 10 mM had no effect on pH_i (n=3), Tertiapin 1 µM by 0.09 ± 0.01 pH units (n=4) and K^+ 20 mM (in the presence of bumetanide 0.1 mM) by 0.16 ± 0.06 pH units (n=4) (* p<0.05).*

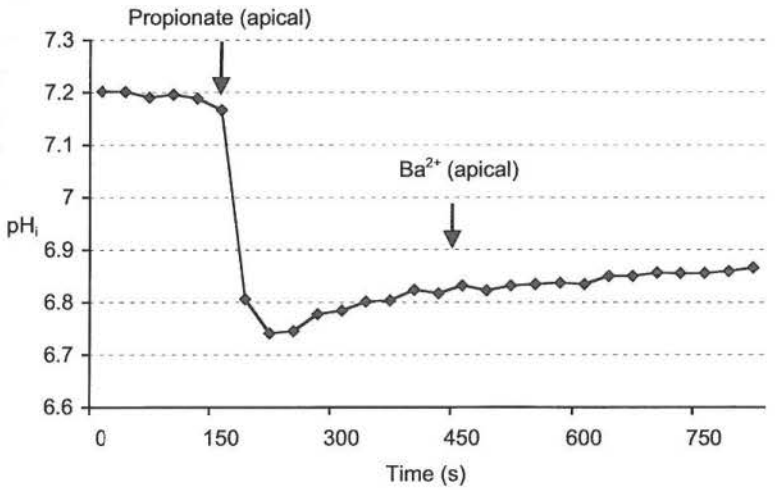

Figure 4.11 *Effect of apical addition of Ba^{2+} 2 mM on pH_i of cells that were acidified by incubation with propionate 30 mM in the presence of EIPA 10 µM. Trace of one representative experiment (n=4).*

experiments. 100 µM Verapamil had a small and variable effect on pH_i (increase of 0.04 ± 0.03 pH units (n=4)). Amiloride 1 µM had no effect on pH_i (n=2) (data not shown).

Three types of control experiments were performed. First, all substances used were tested for their effect on pH_i in the absence of ammonium. At the concentrations used, all control experiments (except for glibenclamide) were negative. For control of the Ba^{2+} effect, also $MgSO_4$ free and NaH_2PO_4 free Ringer solutions in the presence of NH_4^+ were used, but this did not change pH_i either. Second, for excluding the possibility of depolarization-induced alkalinizations (e.g. due to an increased H^+-ATPase activity, although it can be presumed that no H^+-ATPase is active in this preparation, see previous experiments), the cells were acidified with propionate 30 mM (in the symmetrical presence of EIPA 10 µM) to pH_i 7.03 (n=4). Under these conditions Ba^{2+} 2 mM did not change pH_i (Fig. 4.11) So the changes in pH_i observed in the presence of NH_4^+ were dependent on ammonium transport. Third, in steady-state experiments, blockers were applied to the basolateral side of the cells. Except for Ba^{2+}, which caused a small alkalinization in comparison to its effect at the apical cell membrane, none of the blockers affected pH_i from the basolateral side of the monolayer (data not shown).

Depolarizing the apical cell membrane by increasing K^+ concentration in the apical perfusion solution to 20 mM after blocking the $Na^+/K^+(NH_4^+)/2Cl^-$ cotransporter with 100 µM bumetanide alkalinized the cells by 0.16 units (Fig. 4.10). This concentration of K^+ was used in the apical superfusate because in rabbit TAL, increasing K^+ concentration from 4 to 19 mM depolarizes the apical cell membrane to the same extent (+20 mV) as Ba^{2+} (3 mM) does (Greger & Schlatter, 1983). Although this observation indicates that the apical cell membrane potential is an important driving force for NH_4^+ entry into the cells, it also means that the effect observed with Ba^{2+}, Cs^+ and Tertiapin might be attributed to a decrease in driving force for the entry of NH_4^+ through nonspecific cation channels. To differentiate between both possibilities, "ammonium pulse experiments" were performed. When ammonium is abruptly added to the apical perfusion solution, not only the membrane potential, but also the concentration gradient serves as a driving force for NH_4^+ entry. In Figure 4.12, data expressed as initial acidification/alkalinization rates are summarized. In control experiments, application of 4 mM of NH_4^+ acidifies the cells at 0.17 ± 0.01 pH units per minute (n=5), and this is significantly decreased in the presence of bumetanide and 20 mM K^+ (minus 0.11 ± 0.02 pH units per minute, n=5, $p<0.05$), but in both circumstances the apical cell membrane is primarily permeable to NH_4^+. We already described that Ba^{2+} converts this situation to a high NH_3-permeability (Fig. 4.9), and Cs^+ and tertiapin do the same (both plus 0.09 ± 0.03 pH units per minute, n=3 and n=4

respectively). This means that NH_4^+ must permeate the pathway(s) blocked by Ba^{2+}, Cs^+, and Tertiapin rather than permeating nonspecific cation channels. However, the initial alkalinization in the presence of 1 µM Tertiapin was followed by an acidification (minus 0.12 ± 0.01 pH units per minute (n=4)), which was significantly smaller than control acidification rates ($p<0.05$, student-t test) (Fig. 4.13). The combination of Tertiapin and bumetanide induced an effect comparable to that of Ba^{2+} and Cs^+, i.e. the apical cell membrane became primarily permeant to NH_3 with only a residual acidification (Fig. 4.14).

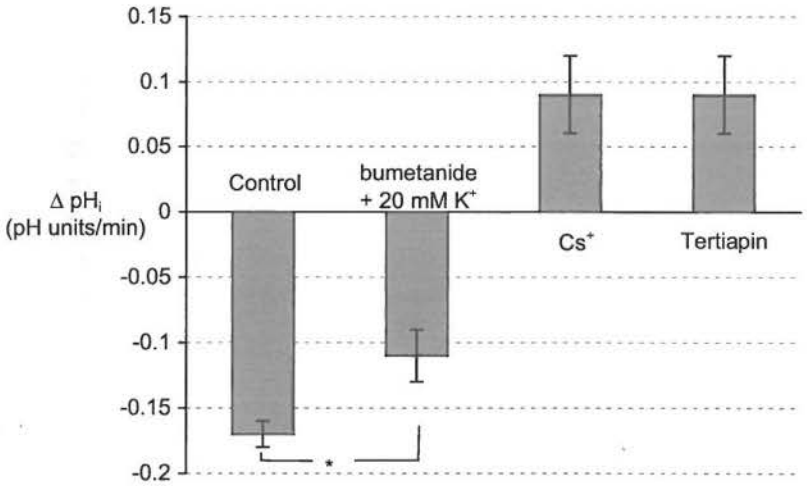

Figure 4.12 *Summary of initial acidification/alkalinization rates during ammonium (4 mM) pulse experiments. In control experiments, the initial acidification rate was 0.17 ± 0.01 pH units/minute (n=5) and this was significantly reduced to 0.11 ± 0.02 pH units/minute (n=5) in the presence of bumetanide 0.1 mM and K^+ 20 mM. In the presence of Cs^+ 20 mM and Tertiapin 1 µM, an initial alkalinization was observed at 0.09 ± 0.03 pH units/minute (n=3 and n=4, respectively) (* p<0.05).*

Since in preliminary experiments, cells grown on PTFE-collagen-coated filter supports were unsuitable for patch-clamp experiments, we cultured the cells on glass coverslips. However, addition of NH_4^+ (4 mM) to these cells induced an intracellular alkalinization, indicating the loss of the differentiated apical membrane transporters. Therefore, no patch-clamp experiments were performed.

With indirect immunofluorescence using anti-ROMK antibodies (dilution 1/10) directed to the COOH-end of the channel protein (identical for ROMK1 and ROMK2), a fluorescent image of the primary cultured cells in the confluent

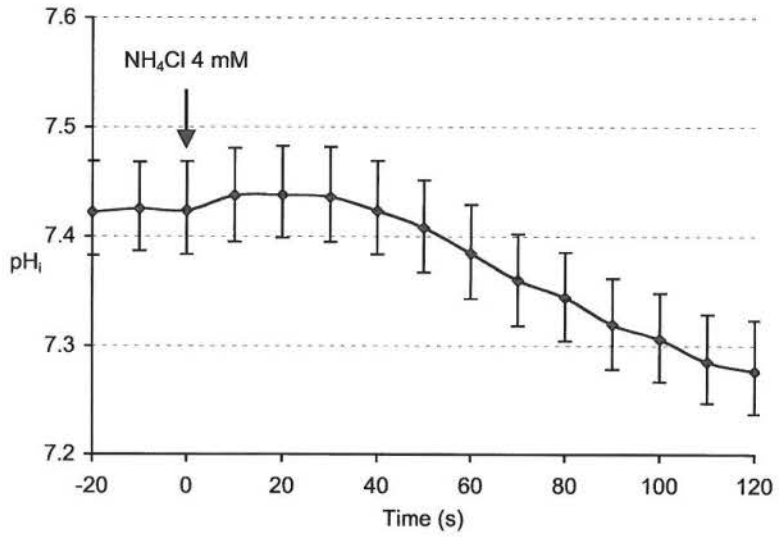

Figure 4.13 *Ammonium-pulse experiment in the presence of Tertiapin. At time 0 s (arrow), ammonium 4 mM was added to the apical superfusion solution. All apical solutions contained Tertiapin 1 µM (mean ± SEM, n=4).*

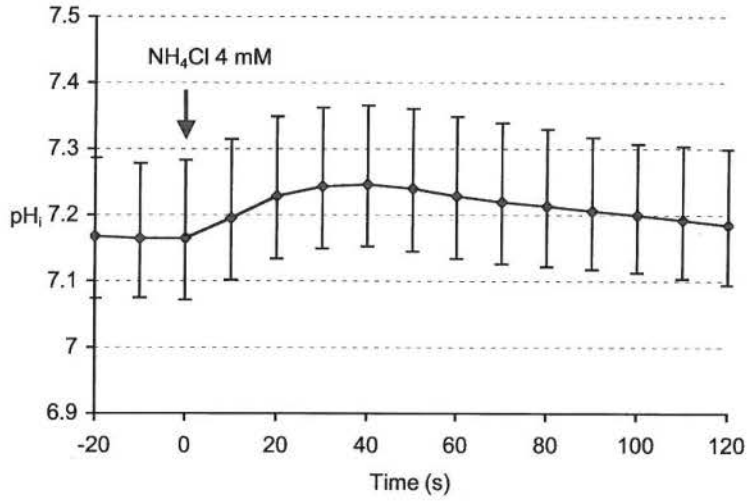

Figure 4.14 *Ammonium-pulse experiment in the presence of Tertiapin and bumetanide. At time 0 s (arrow), ammonium 4 mM was added to the apical superfusion solution. All apical solutions contained Tertiapin 1 µM and bumetanide 0.1 mM (mean ± SEM, n=3).*

monolayer was obtained. In the control experiment, the primary antibody was left out, and no fluorescent signal was obtained (Fig. 4.15).

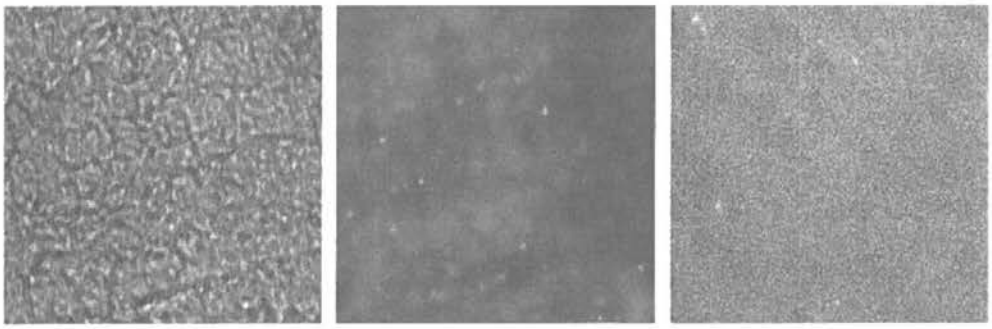

Figure 4.15 *Indirect immunofluorescence using anti-ROMK antibodies (dilution 1/10) directed to the COOH-end of the channel protein.* ***Left****: brightfield image.* ***Middle****: a fluorescent image of the same cells obtained after staining with anti-ROMK.* ***Right****: in the control experiment, the primary antibody was left out, and no fluorescent signal was obtained (**B**).*

4.4 Discussion

4.4.1 Na^+/H^+ exchange

NHE activity was assessed by monitoring Na^+ dependent pH_i recovery from an acid load imposed by Na^+ removal. The Na^+ dependent alkalinization in each experiment was always examined from the same starting pH_i value because Na^+/H^+ exchange rate is influenced by resting pH_i value (Counillon & Pouysségur, 2000). Measurements consisted of the change in pH_i from control (ΔpH_i). In most studies on NHE activity, the ammonium-pulse technique is used to provide an acid-load to the cells. There are two reasons why we did not use this technique. First, ammonium rapidly enters the cells through the apical membrane, so the changes in pH_i during the ammonium-pulse are very different from those observed in most other cell types. Second, the time-characteristics ($t_{1/2}$ of mixing is 10 s if apical perfusion speed is 36 ml/min and apical compartment contains 200 µl) of our perfusion system is much slower than in the isolated-tubule setup. The total exchange of solutions takes probably 30 seconds, and therefore the initial rate of pH_i recovery is not a good measure for acid extruding mechanisms. Therefore we investigated whether we could completely block Na^+ dependent pH_i recovery with EIPA.

In these primary cell cultures, pH_i is maintained at a neutral range in the absence of bicarbonate and ammonium in the extracellular solutions. Since the calculated pH_i, assuming that intra- and extracellular H^+ distribution follows purely its electrochemical gradient, is approximately 6.2, plasma membrane H^+ extrusion systems must be present, such as Na^+/H^+ exchangers and H^+-ATPases (Wakabayashi et al., 1997).

As outlined in the introduction, we expected to find a Na^+/H^+ exchanger (NHE-1) in the basolateral membrane. The observation that EIPA, a specific blocker of Na^+/H^+ exchangers, caused a small acidification (0.11 pH units) when added to the basolateral solution is best explained by the presence of NHE-1 in the basolateral membrane. This isoform is completely blocked by 10 μM of EIPA (IC_{50} is 20 nM) and has a pH_i threshold near 7.2, thus probably not very active at the resting pH_i value in these primary cell cultures. However, the observation that a lower steady-state pH_i is reached, implicates that other acid-extruders can not fully compensate for the inactivation of the basolateral Na^+/H^+ exchanger.

The acidification with 0.06 pH units observed after addition of EIPA to the apical perfusion solution indicates that a Na^+/H^+ exchanger is present in the apical cell membrane as well. It is unlikely that EIPA has exerted this effect at the basolateral membrane since Good et al. have demonstrated that in isolated perfused rat TAL tubules EIPA, when added to the bath, does not directly inhibit the apical Na^+/H^+ exchanger (Good et al., 1995). However, since no functional information on the presence or absence of an apical Na^+/H^+ exchanger in rabbit MTAL cells is available, we directly investigated Na^+ dependent alkalinizations at each side of the epithelium. In these experiments Na^+ was only removed from one side of the epithelium, so the effects observed upon re-addition of Na^+ can not be attributed to effects at the contralateral membrane.

This type of experiments confirmed the presence of an EIPA-sensitive basolateral Na^+/H^+ exchanger. At the apical side, removal of Na^+ elicited a profound acidification, whereas the alkalinization upon re-addition of Na^+ (in the absence of inorganic phosphate) was very small. However, the observation that the acidification upon removal of apical Na^+ could be completely prevented by 10 μM of EIPA, indicated that an apical Na^+/H^+ exchanger (operating in reverse mode) must be responsible for this acidification. From these experiments it seems that the reverse mode of the apical Na^+/H^+ exchanger is more effective in acidifying the cells, than its "forward" activity in alkalinizing the cells. Interestingly, the opposite observation was made in freshly isolated rabbit S3-fragments, where removal of Na^+ from the perfusion solution and subsequent re-addition caused a Na^+ dependent pH_i recovery primarily at the apical membrane, whereas basolateral Na^+ dependent pH_i recovery was smaller than the acidification upon removal of

basolateral Na^+ (Nakhoul et al., 1988). The best explanation for the discrepancy between the high rate of "reverse" mode and low rate of "forward" mode of apical Na^+/H^+ activity in these primary cell cultures, is the influx of Na^+ by sudden re-activation of the $Na^+/K^+/2Cl^-$ co-transporter. By increasing intracellular NaCl concentration (or increasing cell volume) Na^+/H^+ exchange activity both at the apical and basolateral membrane might have been inhibited. Basolateral Na^+/H^+ exchanger must have been inhibited as well, since we have shown that its normal activity will restore pH_i towards a neutral value. This may also explain the secondary decrease in pH_i after an initial, small alkalinization that was observed in some experiments: during the acid-loading process of reverse apical Na^+/H^+ activity, basolateral Na^+/H^+ must have been maximally activated. If now the acid loading at the apical cell membrane stops, the cells will start alkalinizing until basolateral (and apical) Na^+/H^+ exchange activity is inhibited by the increasing intracellular NaCl concentration.

No further experiments for determining the isoform of the apical Na^+/H^+ exchanger in these primary cell cultures were performed. From the literature, we know that NHE-3 is absent in rabbit MTAL and that NHE-2 is present in rabbit CTAL and macula densa cells (see introduction). In several untransfected epithelial cell lines (MDCK, Caco-2 and HT-29), endogenous NHE-1 activity was demonstrated in both the basolateral and the apical cell membrane. Noel et al. have demonstrated that, whereas NHE-3 is exclusively restricted to the apical side of epithelial cells, endogenous or ectopically expressed NHE-1 has the capacity to be expressed in both apical and basolateral membranes of polarized cells in culture (Noel et al., 1996). So data from literature (see also 4.1.2) suggest that the apical Na^+/H^+ exchanger may be isoform NHE-1 or NHE-2, but probably not NHE-3. Two observations support this hypothesis. First, we observed that both basolateral and (reverse) apical Na^+/H^+ exchange activity was completely blocked by EIPA 10 µM. Only NHE-1 and NHE-2 are completely blocked by this concentration of EIPA (IC_{50} of 0.02 and 1 µM, respectively), whereas NHE-3 and NHE-4 activity are only partially blocked (IC_{50} is 8 and 10 µM respectively) (Peti-Peterdi et al., 2000; Fliegel, 1996). Second, we observed that after sudden re-addition of Na^+ to the apical solution, no recovery to a neutral pH value occurred. Therefore, both apical and basolateral Na^+/H^+ exchanger must have been inhibited, most likely by the increasing intracellular NaCl concentration (and thus cellular swelling). Kapus et al. (Kapus et al., 1994) demonstrated that NHE-1 and NHE-2, but not NHE-3 were inhibited by hypo-osmolarity (cell swelling).

4.4.2 Bafylomycin-A_1

No data on the presence or absence of a bafilomycin-A_1 sensitive H^+-ATPase in rabbit MTAL cells have been published to our knowledge. However, since the presence of an H^+-ATPase in the apical cell membrane is correlated with HCO_3^- absorption and since no HCO_3^- is reabsorbed in rabbit TAL cells, the absence of any effect of bafilomycin A_1 on pH_i in our primary cell cultures was expected.

4.4.3 Na-P_i cotransporter

The presence of a membrane transporter that alkalinizes the cytosol only if both Na^+ and phosphate are added to the apical perfusion solution, is compatible with a Na-P_i cotransporter in the apical cell membrane of the present primary cell cultures. Since the Na-P_i cotransporter was restricted to the apical cell membrane, indirect immunofluorescence for both "epithelial" subtypes of Na-P_i cotransporters, i.e. Na-P_i 1 (rabbit type I) and Na-P_i 6 (rabbit type II), was performed. We demonstrated that Na-P_i cotransporter, type I, but not type II is expressed.

The effect of Na-P_i cotransport on pH_i was recently studied. It was demonstrated that the influx of phosphate alkalinizes the cytosol of Xenopus oocytes expressing Na-P_i 3 (human type II) or Na-P_i 5 (flounder type II) (Moschèn et al., 2001). Previous studies on the pH-dependence of Na-P_i cotransport showed that Na-P_i type II preferentially transports divalent phosphate (HPO_4^{2-}), whereas Na-P_i type III (the house-keeping" Na-P_i cotransporter) preferentially transports monovalent phosphate: its transport rate is increased by extracellular acidification. Na-P_i type I when studied in oocytes seemed to have no preference for either monovalent or divalent phosphate (Moschèn et al., 2001; Murer & Biber, 1996; Kavanaugh & Kabat, 1996). However, since $HPO_4^{2-}/H_2PO_4^-$ has a pK_a value of 6.8, the concentration of HPO_4^{2-} in the perfusion solution (pH 7.4) will be four times higher than $H_2PO_4^-$ concentration. Therefore, also the type I co-transporter is expected to alkalinize the cells by mainly transporting HPO_4^{2-}.

The finding of Na-P_i cotransport activity in the apical membrane of rabbit MTAL cells was unexpected. In *in vitro* perfused isolated rabbit TAL segments, there was no net transport of phosphate across the thick ascending limb (Rocha et al., 1977). Na-P_i 1 (= rabbit type I) was shown to be present in the brush border of rabbit proximal tubules but absent in rabbit TAL, as well by mRNA detection (Custer et al., 1993) as by immunohistochemistry (Biber et al., 1993).

Whereas Na-P_i type II is responsible for phosphate reabsorption in the proximal tubule, the function and regulation of Na-P_i, type I, is still unclear.

Cytosolic inorganic phosphate plays a central role in cellular energy metabolism and in hormone-regulated glucose homeostasis. Li et al. (Li et al., 1996) demonstrated that in rat kidneys rNa-P_i 1 (rat type I) was upregulated by increasing plasma glucose-levels, whereas Na-P_i 2 and Ram-1 (the "house-keeping" Na-P_i cotransporter) expression were unaffected. The authors did not investigate whether this rNa-P_i 1 expression was restricted to proximal tubular cells. This glucose-dependent increase in rNa-P_i 1 mRNA expression was independent of insulin, since it was observed in diabetic rats. In primary cell cultures from rat hepatocytes, high glucose concentrations (10-30 mM) also increased rNa-P_i type I mRNA (but not Ram-1 mRNA) expression, but only if insulin 10 nM was present in the medium (Li et al., 1996). Since we have used a DME/F12 "high glucose" medium containing 25 mM D-glucose, this might have induced the expression of Na-P_i 1 in these primary cell cultures of MTAL cells.

It has never been investigated whether MTAL cells are capable of expressing Na-P_i 1 *in vivo*, but in diabetic rats on low-phosphate diet, an adaptive increase in renal P_i reabsorption takes place without an increase in proximal Na-P_i cotransport activity. This might be explained by an increase in P_i reabsorption in later segments of the nephron (Abraham et al., 1992).

4.4.4 Pharmacological evaluation of the Ba^{2+} sensitive NH_4^+ transport pathway(s) in the apical cell membrane

4.4.4.1 Relative importance of the Ba^{2+} versus bumetanide sensitive pathway

The polarized pattern of changes in pH_i that we observed during ammonium pulse experiments is very typical for TAL cells (Good, 1994). It is an essential characteristic of this cell type for its role in ammonium transport (see chapter 3). In these primary cell cultures NH_4^+ entered the cells by replacing K^+ on the $Na^+/K^+/2Cl^-$ co-transporter since 100 µM of bumetanide reduced the initial acidification rate during ammonium-pulse experiments and it reduced the acid-loading of the cells under physiological conditions, i.e. in the symmetrical presence of NH_4Cl. The second major pathway for transcellular NH_4^+ reabsorption in TAL cells consists of a Ba^{2+} sensitive pathway (Greger & Schlatter, 1983). In these primary cell cultures, as in mouse MTAL (Kikeri et al., 1989), this Ba^{2+} sensitive component was more important than $Na^+/NH_4^+/2Cl^-$ mediated NH_4^+ uptake: Ba^{2+} almost completely abolished acid-loading in the steady-state experiments and in its presence, the apical cell membrane became primarily permeable to NH_3. Therefore, these primary cell cultures provided a unique opportunity to investigate the nature of this Ba^{2+}-sensitive pathway. Considerable species differences in the

relative importance of the apical Ba^{2+} sensitive pathway have been described (mouse>rabbit>rat) (Kikeri et al., 1992).

4.4.4.2 Apical K^+ channels as mediators of Ba^{2+} sensitive NH_4^+ influx

In rat and mouse TAL, two types of apical K^+ channels have been described: a low conductance and an intermediate conductance inwardly rectifying K^+ channel (Bleich et al., 1990; Wang, 1994; Lu & Wang, 2000). In rabbit, only the low conductance K^+ channel has been described (Wang et al., 1990). The low conductance K^+ channel from rat, mouse and rabbit has the same biophysical properties and is blocked by extracellular Ba^{2+}, but is insensitive to TEA. It is closely related to the rat cortical collecting duct small conductance K^+ channel, which presumably is the expression of the cloned ROMK (Wang, 1994; Lu & Wang, 2000; Palmer et al., 1997). The latter was shown to be blocked by Ba^{2+} (2 mM) and Cs^+ (2-20 mM), but not by TEA (50 mM). Also, ROMK2, which is expressed in the rat MTAL (Boim et al., 1995), was shown to conduct NH_4^+ ions (Choe et al., 2000). Thus the pharmacological profile of inhibition of NH_4^+ transport in these primary cultures indicates that the low conductance K^+ channel represents the Ba^{2+} sensitive component of apical NH_4^+ transport (Fig. 4.16). This was confirmed by the use of Tertiapin, a selective blocker of ROMK: Tertiapin 1 µM completely blocks ROMK1 and GIRK 1/4, but a closely related channel, IRK1, is insensitive to Tertiapin (Jin & Lu, 1998). The initial alkalinization upon exposure to ammonium in the presence of Tertiapin demonstrates that by blocking ROMK, the apical cell membrane has lost its characteristic high NH_4^+ permeability. But in the presence of Tertiapin, the initial alkalinization is rapidly followed by an acidification. The acidification rate is significantly decreased by Tertiapin in comparison to control ammonium-pulse experiments, but since in the presence of Ba^{2+} no such secondary acidification is observed, the Tertiapin sensitive pathway can only partially account for the Ba^{2+} sensitive pathway of NH_4^+ entry. Interestingly, the effects of bumetanide and Tertiapin were additive: when both blockers were present, no secondary acidification was observed. Therefore, it is tempting to assume that Ba^{2+} not only blocks ROMK, but also the $Na^+/K^+(NH_4^+)/2Cl^-$ co-transporter. However, Ba^{2+} does not seem to interfere directly with $Na^+/K^+/2Cl^-$ mediated NH_4^+ uptake (Heitzmann et al., 2000; Amlal et al., 1996). Ba^{2+} might decrease $Na^+/NH_4^+/2Cl^-$ co-transport activity indirectly by depolarizing the cell and thereby increasing intracellular Cl^- concentration. However, we have shown that the Ba^{2+} effect is not diminished by blockade of the $Na^+/K^+/2Cl^-$ co-transporter. Therefore, another Ba^{2+} sensitive component must be present in the apical membrane of these primary cell cultures.

Property	Rat TAL (ref. 1,7,8)	Mouse TAL (ref. 2)	Rabbit TAL (ref. 3,7)	ROMK (ref. 4,6,9,10)	Rat CCD (ref. 5)
conductance (pS)	30 (IR)	26,1 (IR)	22 (IR)	25 (IR)	35 (IR)
open probability	0.8	0.85	0.89	0.96	0.96
Voltage-dependent	no (-40 to +80 mV)	no (-60 to 0 mV)	no	no	no
pH-sensitivity	?	yes (?) (ref. 6)	no (6,9 - 7,4)	yes (6,6 -7,6)	yes (6,9 -7,4)
ATP-sensitivity	yes (2 mM)	?	yes (2 mM)	yes (1 mM)	yes (1 mM)
NH_4^+-conductance	?	?	?	yes	yes (ref. 11)
Ba^{2+}	yes (1 mM)	yes (1 mM)	yes (0,5 mM)	yes (1 mM)	yes (1 mM)
Cs^+	?	?	?	yes (2-20 mM)	?
TEA	no (10 mM)	no (10 mM)	?	no (10 mM)	no (5 mM)
Quinidine	no (1 mM)	?	?	no (0,1 mM)	?
Verapamil	?	?	?	?	?

	Rat TAL	Mouse TAL	Rabbit TAL
conductance (pS)	72 (IR)	74 (IR)	not present (ref. 3)
open probability (Po)	0.45	0.6	present (?) (ref. 7)
Voltage-dependent	yes	yes	
pH-sensitivity	yes	yes (6,5 -7,4)	
ATP-sensitivity	?	yes (1 mM)	
NH_4^+-conductance	no		
Ba^{2+}	yes (1 mM)	yes (1 mM)	
Cs^+	?	?	
TEA	yes (10 mM)	yes (10 mM)	
Quinidine	yes (1 µM)	?	
Verapamil	?	?	

References

1. Wang (1994) Am J Physiol 267:F599-F605
2. Lu et al. (2000) Kidney Blood Press res 23:75-82
3. Wang et al. (1990) Am J Physiol 258:F244-F253
4. Löffler et al. (1997) Eur J Physiol 434:151-158
5. Wang et al. (1990) Am J Physiol 259:F494-F502
6. Ho et al. (1993) Nature 362:31-38
7. Bleich et al. (1990) Eur J Physiol 415:449-460
8. Bleich et al. (1995) Eur J Physiol 429:345-354
9. McNicholas et al. (1995) Am J Physiol 275:F972-F981
10. Doi et al. (1995) FEBS Letters 375:193-196
11. Palmer et al. (1997) Am J Physiol 273:F404-410

Figure 4.16 *Overview on physical properties and sensitivity to different pharmacological blocking agents of the low and intermediate conductance K^+-channel in rat, rabbit and mouse TAL and of the cloned ROMK.*

4.4.4.3 The Ba^{2+}- and verapamil sensitive K^+/NH_4^+ exchanger

Based on their experiments on suspensions from rat TAL tubules, Amlal et al. (Amlal et al., 1994) suggested that a $K^+/H^+(NH_4^+)$ exchanger that was sensitive to Ba^{2+} and verapamil could account for the Ba^{2+} sensitive component. In the symmetrical presence of ammonium, verapamil 100 µM (a concentration that completely blocks the K^+/NH_4^+ anti-porter (Amlal et al., 1994)) indeed reduced acid loading in our cultured MTAL cells. Therefore, although verapamil is an aspecific blocker (apart from Ca^{2+} channels, verapamil can also block some K^+ channels (Bleich et al., 1990)), these results could support the hypothesis that a K^+/NH_4^+ anti-porter might mediate Ba^{2+} sensitive NH_4^+ entry into MTAL cells. However, since the effect of verapamil is much smaller than the Ba^{2+} effect, a verapamil sensitive K^+/NH_4^+ antiporter can not fully account for the Ba^{2+} sensitive component in these rabbit MTAL cells, as was concluded for suspensions of rat TAL tubules (Amlal et al., 1994). Furthermore, Amlal et al. (Amlal et al., 1994) also described an amiloride (1 µM) sensitive NH_4^+ conductance, which we could not confirm in our experiments.

4.4.4.4 pH sensitivity of ROMK channels

Our conclusion that the low conductance K^+ channel still conducts NH_4^+ at pH_i values of 6.8 may seem to be in contrast with the high pH sensitivity of ROMK when expressed in oocytes (McNicholas et al., 1998). However, in their model of isolated perfused mouse MTAL tubules, Kikeri et al. (Kikeri et al., 1992) have demonstrated that the Ba^{2+} sensitive NH_4^+ entry was indeed inhibited by lowering pH_i, but only by 40% at pH_i 6.8. It is possible that incompletely phosphorylated ROMK channels may respond differently to regulatory stimuli such as pH (MacGregor et al., 1998). Leipziger et al. (Leipziger et al., 2000) observed that activation of ROMK2 by protein kinase A involves a shift of the pK_a value to more acidic values, thus relieving H^+-mediated inhibition of ROMK channels. Also, concerning pH sensitivity of the low conductance K^+ channel in TAL cells, we have at our disposal patch-clamp information from rabbit TAL cells, but not from rat or mouse: in rabbit TAL, the low conductance K^+ channel was shown to be pH insensitive in the range between 6.9 and 7.4, although it must be noted that this conclusion was based on three different observations only (Wang et al., 1990).

4.4.4.5 Arguments against a role for K^+ channels

As mentioned in the introduction, experimental results have been published that provided some evidence against NH_4^+ influx via apical K^+ channels. Bleich et al. (Bleich et al., 1995) concluded that in rat TAL cells, the apical K^+ channel is not a likely candidate to mediate apical NH_4^+ transport. However, they were investigating the intermediate conductance K^+ channel that is not only sensitive to Ba^{2+}, but also to extracellular TEA. Amlal et al. (Amlal et al., 1994) still observed a Ba^{2+} sensitive NH_4^+ influx when "all K^+ channels were blocked with 100 µM quinidine". However, the low conductance K^+ channel is almost insensitive to this concentration of quinidine (Wang, 1994; Doi et al., 1995). Finally, Laamarti et al. (Laamarti & Lapointe, 1997) observed in rabbit macula densa cells that the Ba^{2+} sensitive NH_4^+ influx was not affected by increasing intracellular Ca^{2+} concentrations. However, the low conductance K^+ channel in rabbit TAL is not sensitive to increasing Ca^{2+} concentrations from 0 to 500 µM (Wang et al., 1990) (Fig. 4.14).

4.4.4.6 A new class of ammonium transporters

Two members of a family of putative ammonium transporters, RhBG and RhCG, have been recently cloned in the kidney. These proteins share homologies

with specific NH_3/NH_4^+ transporters (Mep/Amt) in primitive organisms and plants. In rat kidney, RhCG was shown to be present in distal convoluted tubules, connecting ducts, and collecting ducts, but not in proximal tubules and TAL's (Eladari et al., 2002). In mouse kidney, RhBG and RhCG were shown to be present in the same nephron segments as in rat kidney, with RhBG being expressed in the basolateral, and RhCG in the apical region of the epithelial cells (Verlander et al., 2003). Although no functional data on these transport proteins are available so far, the distribution of these proteins in rat and mouse kidney make them unlikely candidates to account for the Ba^{2+} sensitive pathway in these primary cultured MTAL cells.

4.5 Conclusions

In these primary cell cultures from rabbit MTAL, a Na^+/H^+ exchanger is present, both in the apical and the basolateral cell membrane. They both contribute to pH_i homeostasis. No functional bafilomycin-A_1 sensitive H^+-ATPase was found in these cells.

In the apical cell membrane, Na-P_i cotransporter type I is expressed and is responsible for Na^+ and HPO_4^{2-} dependent, amiloride-resistant alkalinizations. From immunohistochemsitry experiments on whole rabbit kidneys, we know that Na-P_i type I is not expressed *in vivo*. This observation underscores the importance of the composition of the cell culture medium for the expression of proteins. This also indicates that cells in culture might function differently from the *in vivo* situation.

The major pathway for apical NH_4^+ transport in these primary cell cultures is the Ba^{2+} sensitive pathway. A Tertiapin sensitive pathway, most likely a ROMK related K^+ channel, can at least partially account for this Ba^{2+} sensitive pathway.

Chapter 5

Changes in intracellular pH during metabolic inhibition

5.1 Introduction

5.1.1. Metabolic inhibition as a model of renal ischemia

Renal ischemia results from an insufficient blood supply to the kidney. Oxygen uptake by the tissue itself leads to a virtually absolute anoxia within seconds. Such anoxia inhibits mitochondrial oxidative phosphorylation completely, and the resultant decrease of ATP and increase of ADP and AMP stimulates glycolysis. As a consequence of lactate acid accumulation and proton release after hydrolysis of nucleoside phosphates, pH decreases by as much as two units. Thus, two cardinal features of ischemia are an absolute anoxia and up to a 100-fold increase of hydrogen ion concentration. Hypoxia differs from ischemia in that perfusion persists during hypoxia. Hypoxia may result from respiratory failure, tissue hypoperfusion, or a combination of the two. In contrast to ischemia, protons and other metabolites wash out, and blood-borne substances, including oxygen, constantly enter hypoxic tissue. Ischemia and hypoxia represent the extremes of a continuum, since, as hypoperfusion becomes sufficiently severe, conditions of ischemia are achieved (Herman B, Gores GJ, 1990).

MI will mimic ischemia in that virtual anoxia and absence of blood borne substrates is achieved, but mimics hypoxia in that metabolites are washed out and that O_2 remains present in the medium (which may result in the formation of ROS). In fact, with MI, the consequences of a rapid ATP-depletion are studied, and this is the primary event, both in hypoxia and ischemia. (Burke & Schrier, 1997). As discussed in chapter 1, the absence of xanthine oxidase (an important source of ROS in rat kidney cells) in the rabbit TAL may limit the amount of ROS formed during MI.

In general, an increase in the free intracellular Ca^{2+} concentration ($[Ca^{2+}]_i$), alterations in intra- and extracellular pH, cell swelling due to the disturbance of normal Na^+ and K^+ concentrations in the cytosol, production of free radicals and changes in phospholipid metabolism (such as production of arachidonic acid) may be involved in the process (see chapter 1). It seems that their relative importance in contributing to ischemic cell damage may vary with cell type and with experimental protocol. There is obviously no single cause responsible for ischemic cell injury. Two issues that have received considerable attention are the roles of intra- and extracellular pH and the increase in $[Ca^{2+}]_i$ (Shanley & Johnson, 1991).

When focusing on renal cell ischemia in particular, only a very limited number of studies can be found where pH_i and $[Ca^{2+}]_i$ were actually measured, the vast majority of which were performed on proximal tubular cells (see chapter 1). Unfortunately, these studies provide only one measurement at the end of ischemia

or during the reperfusion period. However, the high complexity of cellular ischemia necessitates to gain insight into the change of these parameters during the course of IRI and into their interdependence. As already mentioned, the number of studies of this type is very limited. When focusing on the distal tubular cells, more particularly the MTAL, no data of this type are currently available.

5.1.1 ATP, $[Ca^{2+}]_i$ and pH_i measurements in distal tubular cells during ischemia-reperfusion injury

In view of its key role in the pathophysiology of ARF (see chapter 1), it is surprising to find only one publication in which the effects of ATP depletion on the MTAL cell have been investigated. In this paper, $[Ca^{2+}]_i$ was measured in primary cultured rabbit MTAL cells that were subjected to 60 minutes of ischemia. A slow increase of the calcium concentration towards an apparent plateau phase (469 nM), with a rapid decline to pre-ischemic levels upon reperfusion was observed (Rose et al., 1994b). To our current knowledge, no other data on the cellular pathophysiology of ischemia in the MTAL cell are available.

The effect of MI on $[Ca^{2+}]_i$ in MDCK cells (an immortalized cell line derived from distal tubular cells) was investigated on two occasions. McCoy et al. (McCoy et al., 1988) observed an increase in $[Ca^{2+}]_i$ from 112 to 649 nM during 15 minutes of MI at 37° C. In our laboratory, $[Ca^{2+}]_i$ was measured in MDCK cells during 1 hour of MI at room temperature: $[Ca^{2+}]_i$ increased from 68 to 283 nM during the first 30 minutes of MI. However, during the next 40 minutes of MI, $[Ca^{2+}]_i$ gradually decreased to 138 nM, which was attributed to calcium sequestration into mitochondria (Smets et al., 2004).

In 1996, Lash et al. (Lash et al., 1996) explored for the first time the cellular energetics of distal (cortical) tubular cells to MI. In our laboratory, ATP measurements were performed on A6 and MDCK cells (Despa, 2000; Smets, 2001)(see discussion).

Apart from the pH_i measurements during MI in A6 and MDCK cells in the L.U.C. laboratory, no pH_i measurements on distal tubular cells in general or more specifically MTAL cells were found. The potential importance of this type of studies is illustrated by the recent observation that *in vivo*, inhibition of NHE-3 seems to be protective in renal IRI (Hropot et al., 2003). In order to unravel the mechanism behind this kind of protection, studies at the cellular level in proximal and distal (more specifically MTAL cells) are mandatory. Therefore the goal of this study is to investigate the time course of changes in pH_i and $[Ca^{2+}]_i$ in parallel during MI in distal tubular cells

5.2 Solutions and chemicals

The **standard** perfusion solution was HB-BSS as described in chapter 3. The solution for **metabolic inhibition** (MI) contained (in mM): 2.5 NaCN, 10 DOG, 128 NaCl, 5 KCl, 1 $CaCl_2$, 1.2 $MgSO_4$, 2 $NaH_2PO_4.H_2O$, 1 L-alanine, 5 glycine, 20 HEPES, final pH brought to 7.4 TRIS and osmolality to 320 mosm/kg H_2O with mannitol. For **reperfusion** the standard HB-BSS was used. **Na^+-free** solution was the same as described in chapter 4. **Na^+-free** solutions for **metabolic inhibition** contained KCN in stead of NaCN.

All chemicals were from Sigma Chemical Company, St Louis, MO, USA. Blockers were dissolved in ethanol or DMSO, the final concentration of these solvents never exceeded 1 pro mille.

5.3 Results

5.3.1 ATP measurements

First, the changes in ATP content of the primary cell cultures in response to MI were measured. All data are expressed relative to the ATP content of control primary cell cultures (see materials and methods 2.7). The controls were time-matched, so the relative ATP content after 60 minutes of MI and 60 minutes of recovery was compared to the ATP content of cells that were incubated for 2 hours in HB-BSS. Every single ATP measurement represents the ATP content of one confluent primary cell culture. As shown in Figure 5.1, the ATP content declined very rapidly after initiation of MI: it dropped by more than 50% after only 60 seconds (45.7 ± 4.9% (n=3) of the ATP content was left). After 10 minutes of MI only 1.7 ± 0.1% (n=3) of initial ATP content was left and this declined further to 0.4 ± 0.1% (n=3) after 15 minutes. ATP levels remained below 1% of the original value during the whole period of MI.

Subsequently different combinations of CN^-, DOG, pyruvate and glucose were used to determine the main source of ATP production in these primary cell cultures (Fig. 5.2). When only the mitochondrial respiratory chain was blocked with CN^- but anaerobic glycolysis was possible due to the presence of glucose in the perfusion solution, ATP content declined to 81.1 ± 5.6% (n=3) of the starting value after 60 minutes. When only anaerobic glycolytic ATP production was stopped by the addition of DOG in the presence of pyruvate to fuel aerobic ATP production by mitochondria, ATP fell after 60 minutes to 47.9 ± 4.2% (n=3) of its original value. These results indicate that the cells in primary culture have a high glycolytic capacity and that anaerobic glycolysis can maintain high intracellular ATP levels. In

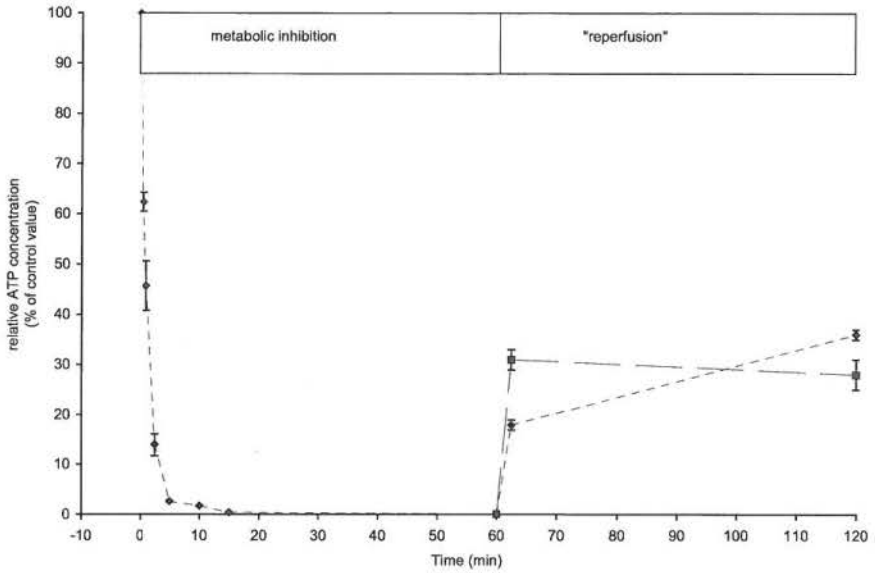

Figure 5.1 *Relative changes in ATP concentration during 1 hour of metabolic inhibition followed by 1 hour of reperfusion. Values at different time-points are expressed relative to the ATP concentration of time-matched controls. Each point represents the mean relative ATP concentration of three different primary cell cultures. (◆): reperfusion with pyruvate (10 mM) (n=3). (■): reperfusion with glucose (10 mM) (n=3).*

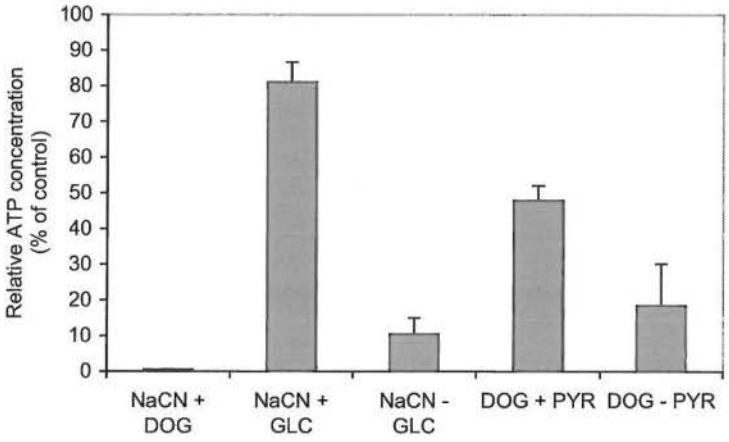

Figure 5.2 *Relative ATP concentrations after 1 hour of metabolic inhibition using different combinations NaCN, DOG, pyruvate (PYR) and glucose (GLC) (n=3). For numeric values, see text.*

conditions where ATP production by anaerobic glycolysis is inhibited, mitochondrial ATP production can maintain ATP concentration at half of its normal value. In addition a series of experiments was performed in which CN^- was added to the perfusion solution in the absence of external glucose. After incubation during 60 minutes, ATP levels had dropped to 10.5 ± 4.5% (n=3) of their pre-ischemic value, indicating that intracellular glycogen stores are able to fuel anaerobic glycolysis. In another series of experiments, glycolysis was blocked with DOG in the absence of external pyruvate. Under these conditions ATP levels dropped to 18.5 ±11.6% (*n*=3) of control values, indicating that other sources than glucose can provide substrates for mitochondrial ATP production.

For studying the reversibility of 60 minutes of MI with CN^- and DOG, three protocols were used. In all protocols CN^- and DOG were washed out, and glucose or pyruvate or both were added to the perfusion solution. ATP levels were measured after 1 hour of "reperfusion" (Fig. 5.1). In the presence of glucose, ATP levels recovered to 28 ± 3% (*n*=3) of pre-ischemic values. In the presence of pyruvate, ATP content recovered to 36 ± 1% (*n*=3) of control values and with the combination of glucose and pyruvate ATP content reached 36 ± 4% (*n*=3) of the pre-ischemic value. Since it was unexpected that glucose and pyruvate were almost equally suitable for recovering ATP content, ATP concentrations were also measured 150 seconds after the start of "reperfusion". With pyruvate, ATP levels had recovered to 18 ± 1% (*n*=3) of initial levels, but with glucose, recovery had already reached its maximal level, since cellular ATP content had reached 31 ± 2% (*n*=3) of control values by this time. Since glucose was shown to be at least as effective as pyruvate for recovery of ATP content after MI, in all subsequent experimental protocols glucose was used in the "reperfusion" solution.

5.3.2 Cellular staining with EtHD-1 and calcein

For determination of (ir)reversibility of MI (CN^- and DOG together), a LIVE/DEAD viability kit was used (see materials and methods 2.8.1). Cells with compromised membranes exhibit red-fluorescence from the live-cell–impermeant nucleic acid stain EtHD-1. Cells with intact cell membranes are able to use non-specific cytosolic esterases to convert non-fluorescent calcein-AM into bright green-fluorescent calcein. Both fluorescent dyes were added to the perfusion solution at the end of the ischemia/reperfusion period and the number of necrotic cells per microscopic field was counted. This technique was chosen because it provides spatial information that can be combined with other microfluorescence signals (e.g. BCECF). First, the duration of MI necessary to cause necrotic cell death was examined. As shown in Figure 5.3, after 60 minutes of MI followed by 60

minutes of "reperfusion", the number of necrotic cells was not increased as compared to time-matched controls. Only after 120 minutes of ischemia plus 60 minutes of "reperfusion", the number of necrotic cells in the confluent monolayers began to rise (significantly different from controls, $p < 0.05$). Surprisingly, the number of necrotic cells did not increase further after 3 hours of ischemia. These data indicate that cell necrosis occurs only after ischemic periods of more than 1 hour and therefore studying 60 minutes of MI focuses on reversible cell injury. However, since it is possible that cells become necrotic only after prolonged periods of "reperfusion", we also evaluated primary cell cultures that were subjected to 1 hour of MI after 2 and 3 hours of "reperfusion". As shown in Figure 5.4, no increase in number of necrotic cells could be detected even after these prolonged reperfusion periods. Therefore, studying 60 minutes of MI in these primary cell cultures is compatible with studying "reversible ischemic damage".

5.3.3 $[Ca^{2+}]_i$ measurements

At the start of Fura-2 experiments, a control experiment for autofluorescence was performed. The 380 nm signal obtained from unloaded cultured MTAL cells decreased abruptly at the start of MI, whereas the 340 nm signal increased slightly. Upon "reperfusion", both signals decreased minimally. As a result, the F_{340}/F_{380} ratio sharply increased (from 0.3 to 0.5) on the start of ischemia, and remained stable afterwards.

Since the autofluorescence at these wavelengths is attributed to coenzymes and flavins (Schneckenburger et al., 1996), and since these findings were opposite to previous observations on MDCK cells from our laboratory (Despa, 2000), the fluorescent characteristics of the collagen coated filter support (without cells) were investigated: when CN^- and DOG were added to the perfusion solution, a sharp decrease in the 380 nm signal was observed (340 nm slightly increased) thereby increasing the F_{340}/F_{380} ratio from 0.25 to 0.6. So the changes in autofluorescence were the result of the fluorescence characteristics of the filter support.

Primary cell cultures loaded with the Ca^{2+} sensitive dye Fura-2 were subjected to 60 minutes of MI followed by 60 minutes of reperfusion with glucose. Figure 5.5 summarizes the results of 5 separate experiments. Data are expressed as Fura-2 ratio, since attempts to calibrate fluorescence ratios were not successful in all experiments. The small increase in Fura-2 ratio at the start of MI was probably the result of a change in fluorescence characteristics of the filter support. After 8 minutes of MI, Fura-2 ratio started to rise gradually. At this moment, ATP concentration had decreased to approximately 2% of its control value. Fura-2 ratio

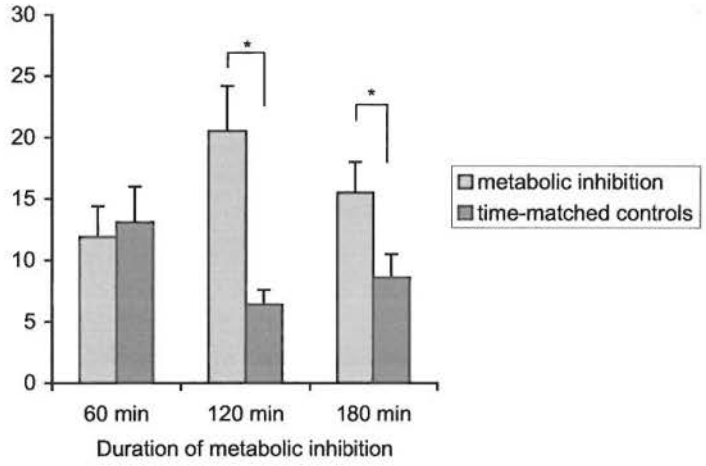

Figure 5.3 *Number of necrotic cells per field after 60, 120 and 180 minutes of metabolic inhibition (NaCN 2.5 mM and DOG 10 mM) (with 60 minutes of "reperfusion"). The number of necrotic cells is significantly increased after 2 and 3 hours of ischemia/"reperfusion" as compared to the time-matched controls (y-axis: number of necrotic cells per microscopic field) (*: $p < 0.05$).*

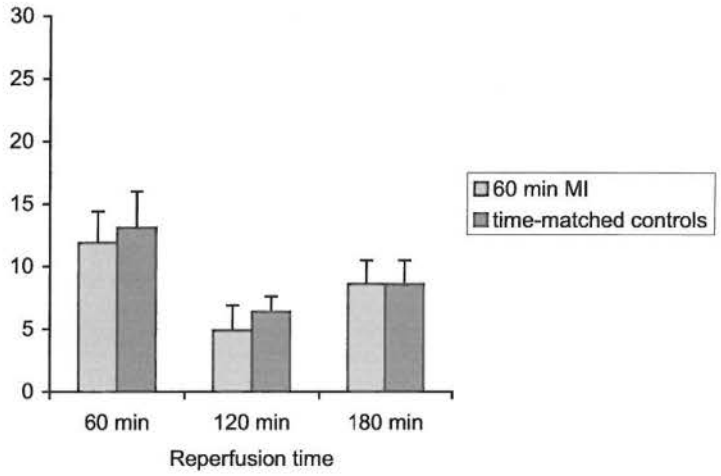

Figure 5.4 *Number of necrotic cells per field after 60 minutes of metabolic inhibition (MI) with 60, 120 and 180 minutes of "reperfusion". The number of necrotic cells does not increase with increasing "reperfusion"-time as compared to the time-matched controls (y-axis: number of necrotic cells per microscopic field).*

reached a plateau during the last 5 minutes of MI. Upon "reperfusion" Fura-2 ratio declined very rapidly to its pre-ischemic value, which was reached within 4 minutes after the start of "reperfusion".

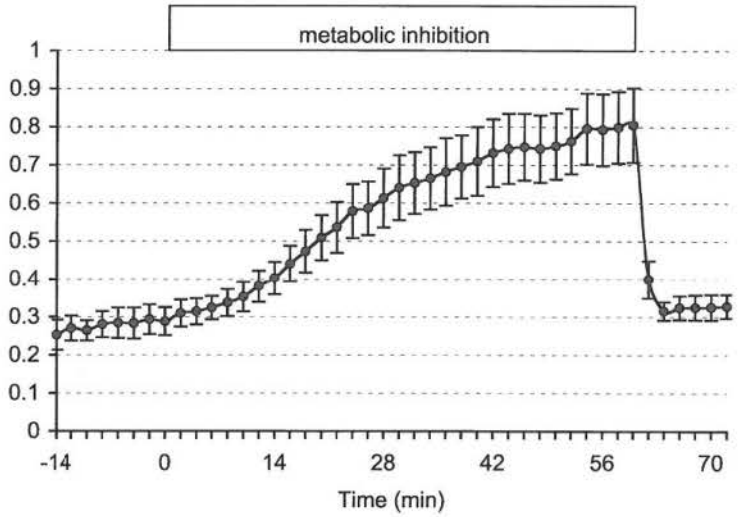

Figure 5.5 *Changes in Fura-2 ratio (y-axis) during 60 minutes of metabolic inhibition with NaCN (2.5 mM) and DOG (10 mM). "Reperfusion" was performed by washing out NaCN and DOG and by the re-addition of glucose (10 mM) to the apical and basolateral perfusion solutions. Values are mean ± SE (n=5).*

5.3.4 Cell pH_i measurements

At the start of BCECF experiments, a control experiment for autofluorescence was performed. The ratio of the 495 nm and 440 nm signal obtained from unloaded cultured MTAL cells was stable throughout the MI and "reperfusion" period. In a first series of experiments, pH_i was measured using the same protocol of MI as for ATP measurements and Ca^{2+} measurements (Fig. 5.6). During the first 4 minutes of ATP depletion, the cytosol started to acidify. However, from 4 to 10 minutes after initiation of MI, the cells alkalinized to a value above resting pH_i. This alkalinization was followed by a slow acidification to reach the lowest pH_i value of 6.92 ± 0.08 (n=4) after 50 minutes of ATP depletion, after which it stabilized. Upon "reperfusion", pH_i remained at this acidic value for 4 minutes, followed by a small and transient further acidification, after which pH_i started a slow recovery to reach pre-ischemic values after 20 minutes.

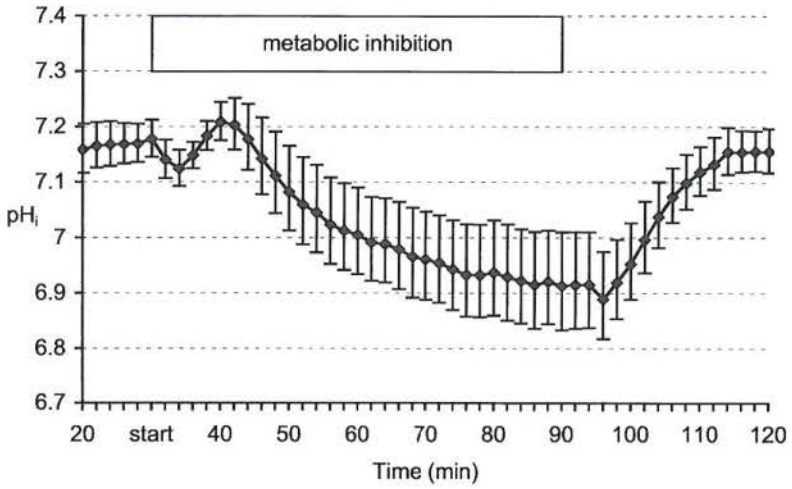

Figure 5.6 *Changes in pH_i during 60 minutes of metabolic inhibition with NaCN and DOG. "Reperfusion" was performed by washing out NaCN and DOG and by the re-addition of glucose to the apical and basolateral perfusion solutions. Values are mean ± SE (n=4).*

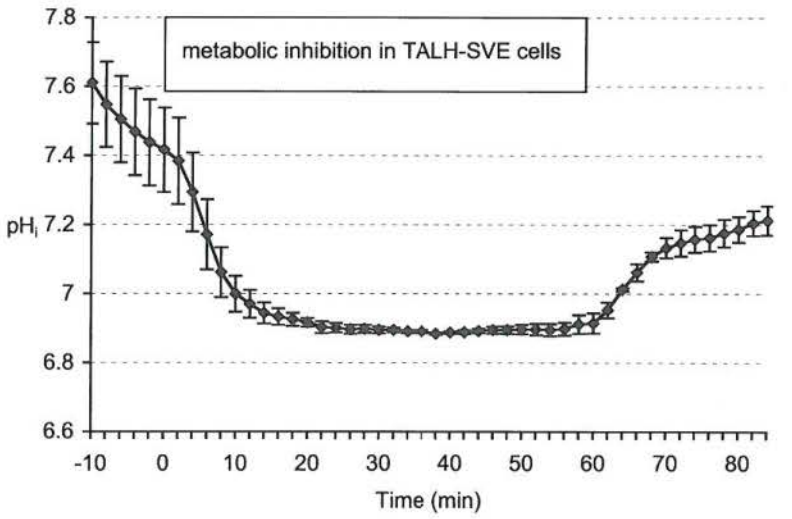

Figure 5.7 *Changes in pH_i in TALH-SVE cells during 60 minutes of metabolic inhibition with NaCN and DOG. "Reperfusion" was performed by washing out NaCN and DOG and by the re-addition of glucose to the apical and basolateral perfusion solutions. Values are mean ± SE (n=3).*

Because the transient alkalinization during the first phase of MI was unexpected, we used the same protocol with confluent TALH-SVE cells, to exclude the possibility of artifacts inherent to the experimental set-up. As shown in Figure 5.7, changes in pH_i in TALH-SVE cells consisted of a slow acidification during MI followed by a slow and complete pH_i recovery upon "reperfusion". Therefore, the results obtained with the primary cell cultures were related to the specific phenotype of these cells.

Since one explanation for the alkalinization might be the activation of NHE activity, we performed a series of MI experiments in the presence of EIPA 10 µM. We previously demonstrated that this concentration of EIPA effectively blocks all NHE activity in these cells. The results from 5 different experiments are summarized in Figure 5.8. Also in the bilateral presence of EIPA, a transient alkalinization during the first 20 minutes of MI was observed. In its absolute value, this alkalinization, (expressed as $\Delta[H^+]_i$) was even larger, although p was not significant. The subsequent acidification also was not different from the acidification in the absence of EIPA (p=0.73), although it had not reached a stable value at the end of the ischemia period. EIPA was not present in the "reperfusion" solutions.

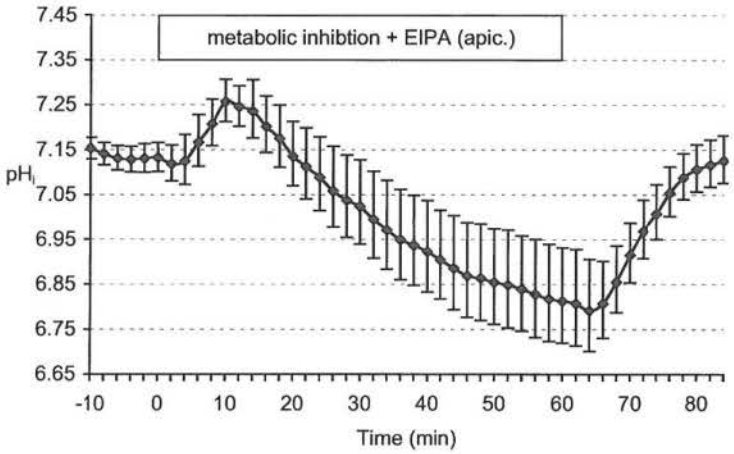

Figure 5.8 *Changes in pH_i during 60 minutes of metabolic inhibition with NaCN (2.5 mM) and DOG (10 mM). EIPA (10 µM) was added to the apical and basolateral ischemia solution. Values are mean ± SE (n=4).*

In a next series of experiments, the effects of CN^- and DOG on pH_i were investigated separately. Inhibition of the mitochondrial respiratory chain by CN^- initially caused the cells to acidify, rapidly followed by a transient alkalinization, after which the cytosol slowly acidified from pH_i 7.23 ± 0.04 to pH_i 7.19 ± 0.03

(n=4). Although by the end of the 60 minutes ischemia period, pH_i had only reached its pre-ischemic value, the cells further alkalinized upon wash-out of CN^- to pH_i 7.26 ± 0.03 (n=4) (Fig. 5.9). In Figure 5.10, the data of four experiments in which glycolysis was blocked with DOG are summarized. Under these circumstances, at the end of the 60 minutes ischemia period, 19% of the intracellular ATP content was left. Immediately after the addition of DOG, a transient alkalinization of the cytosol took place, followed by an acidification to pH_i 6.84 ± 0.02 (n=4) at 60 minutes, without reaching a stable value. The total change in $[H^+]_i$ during the alkaline transient was not different from the alkaline transient during CN^- induced energy depletion.

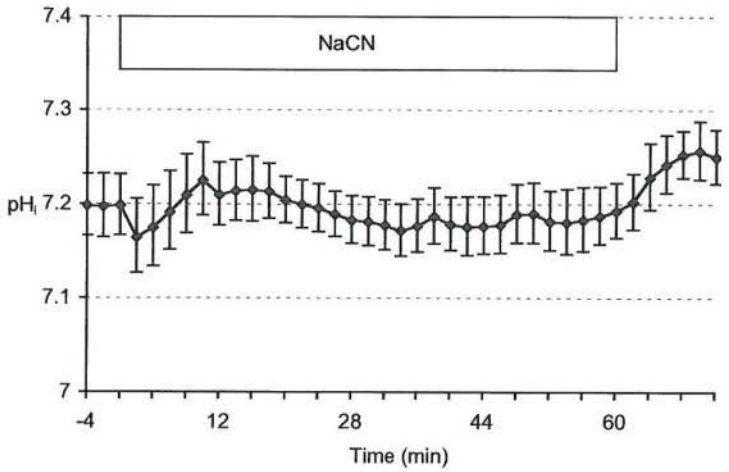

Figure 5.9 *Changes in pH_i during inhibition of the mitochondrial respiratory chain with NaCN (2.5 mM). Anaerobic glytolytic ATP-production was still possible because glucose (10 mM) was present in all perfusion solutions. This maintains the ATP-concentration at 81% of the control value after 60 minutes. Values are mean ± SE (n=4).*

Finally, MI experiments were performed in the absence of P_i in the apical perfusion solution. Now the change in pH_i consisted of a simple acidification after initiation of MI, and a slow recovery upon reperfusion (Fig. 5.11). Since this indicated that HPO_4^{2-} influx was responsible for the alkaline transient, a series of experiments was performed in the absence of Na^+ in the apical solutions. Reverse activity of the apical Na^+/H^+ exchanger was prevented by the addition of EIPA 10 µM to all apical solutions. Resting pH_i in these conditions was 6.95 ± 0.06 (n=4). At the start of MI (KCN was used to replace NaCN), pH_i started to fall, to stabilize after 40 minutes at pH_i 6.45 ± 0.03 (n=4). This acidification was significantly larger than the acidification observed with all previous protocols (p<0.05). Again a

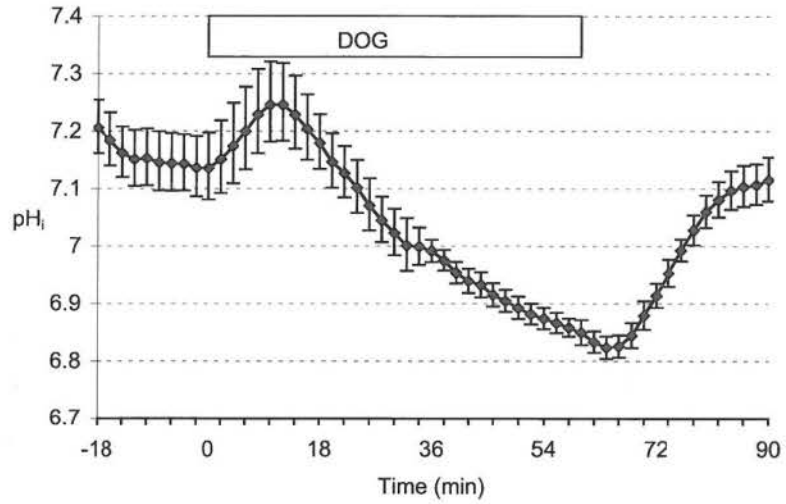

Figure 5.10 *Changes in pH_i during inhibition of anaerobic glytolytic ATP-production with DOG (10 mM) in the absence of glucose. Under these conditions, mitochondrial ATP-production can maintain the ATP-concentration at 19% of the control value after 60 minutes. Values are mean ± SE (n=4).*

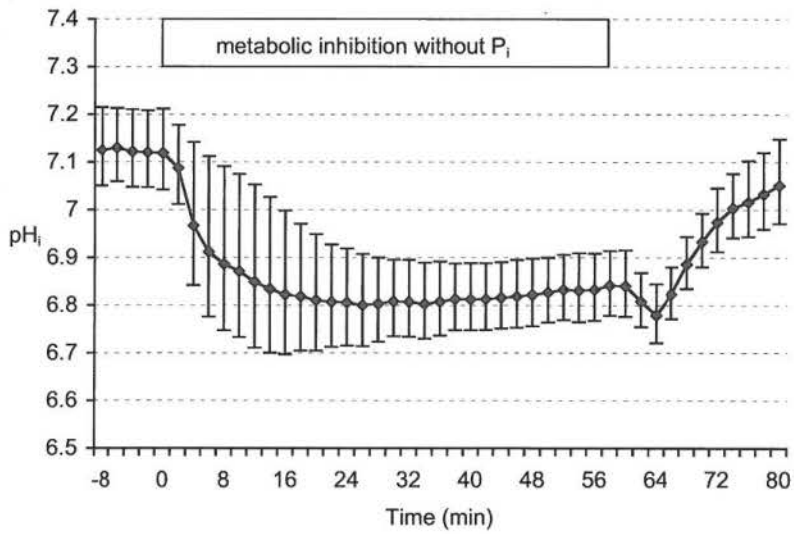

Figure 5.11 *Changes in pH_i during 60 minutes of metabolic inhibition with NaCN (2.5 mM) and DOG (10 mM). P_i was omitted from the apical ischemia solution. Values are mean ± SE (n=4).*

complete return of pH_i towards resting value was observed upon "reperfusion", despite the absence of Na^+ in the apical "reperfusion" solution (Fig. 5.12).

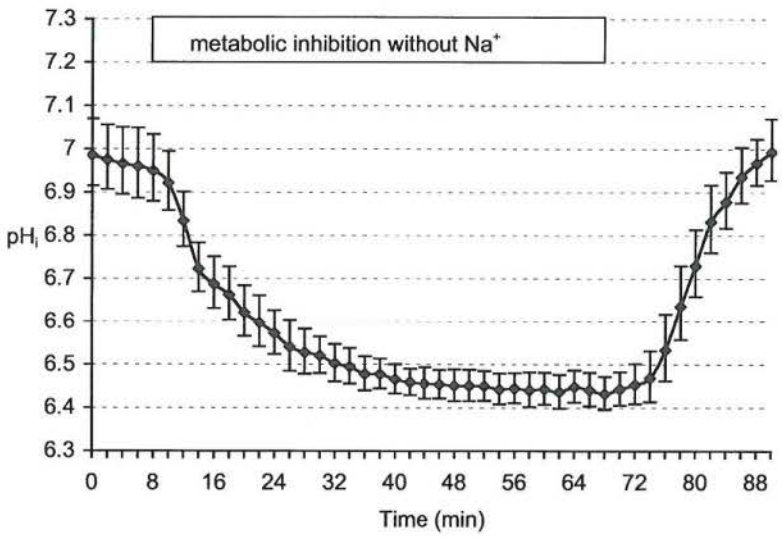

Figure 5.12 *Changes in pH_i during 60 minutes of metabolic inhibition with KCN (2.5 mM) and DOG (10 mM). Na^+ was replaced by $NMDG^+$ in all apical superfusion solutions and EIPA (10 µM) was added to all apical solutions to prevent reverse operation of the apical Na^+/H^+-exchanger. Values are mean ± SEM (n=4).*

5.3.5 Combination of BCECF-measurements and EtHD-1 staining

To search for correlations between the pattern of changes in pH_i (observed during 120 minutes of MI and 60 minutes of reperfusion) and the progression to cell necrosis, nuclei of necrotic cells were stained with eEtHD-1 at the end of the experiment. The BCECF signal of "regions of interest" that corresponded to the cytoplasm of the necrotic cells on one hand, or living cells on the other, was retrospectively analyzed. This technique ("multiparameter digitized microscopy") was first used in cultured hepatocytes. It allows studying and relating specific steps in the evolution of (ir)reversible injury to each other as they occur, rather than trying to infer cause and effect relationships from very large groups of heterogeneously dying cells (Herman et al., 1990; Gores et al., 1989).

In our experimental set-up, the use of this technique did not result in reproducible observations for several reasons. First, the selected area with the "region of interest" function of the V for Windows™ software is always a square surface and therefore only a very rough approximation of the cytoplasmic area of a

single cell. Second, cells that stained positive for EtHD-1 at the end of the experiment often were poorly loaded with BCECF at the start of the experiment. Since BCECF-AM has been used as a viability dye itself (Kolber et al., 1988), this may indicate that the cells that became necrotic during MI, were the ones in "bad shape" at the onset of experiment. Finally, the opposite observation was made as well: cells that were selected because they were homogeneously loaded with BCECF at the start of the experiment, never became permeable for EtHD-1 at the end of the ischemia and "reperfusion" period.

Another goal for investigating renal IRI with digital microfluorescence, was based on the observation that *in vivo* ATN has a patchy appearance, affecting mainly groups of cells (see Chapter 1). Also in monolayers of cultured MTAL cells, necrosis rather seemed to affect small groups of cells, single necrotic cells being the exception (Fig. 5.13).

In Figure 5.14, the changes in $[ATP]_i$, Fura-2 ratio and pH_i during 60 minutes of MI and "reperfusion" in P_i-containing solutions are summarized.

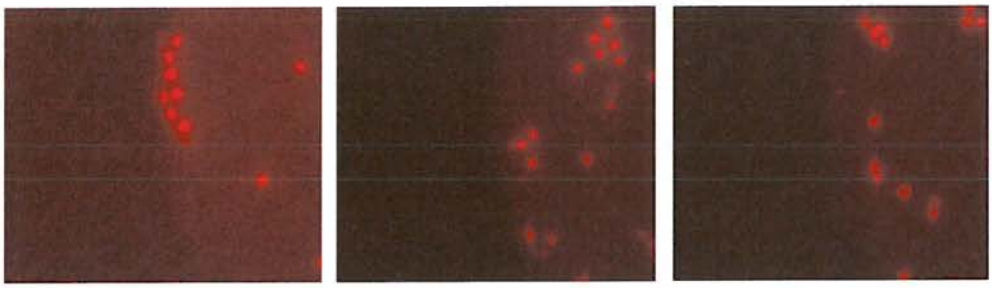

Figure 5.13 *Three representative images of Ethidium-homodimer staining of the nuclei of necrotic cells after 2 hours of metabolic inhibition and 1 hour of "reperfusion". Necrosis seems to affect preferentially small groups of cells.*

5.4 Discussion

5.4.1 Changes in ATP

After the start of MI, the relative intracellular ATP content in these primary cell cultures decreased very rapidly (it dropped to less than 50% after only 60 seconds and to less than 2% after 10 minutes of MI). For comparison, in MDCK cells (an immortalized cell line with several properties of distal tubular cells) ATP content decreased to 30% after 5 minutes of MI with NaCN and DOG (Despa, 2000; McCoy et al., 1988). In freshly isolated distal (cortical) tubular cells that were subjected to MI with iodoacetate and KCN, ATP concentration decreased to 20% after 30 minutes (Lash et al., 1996).

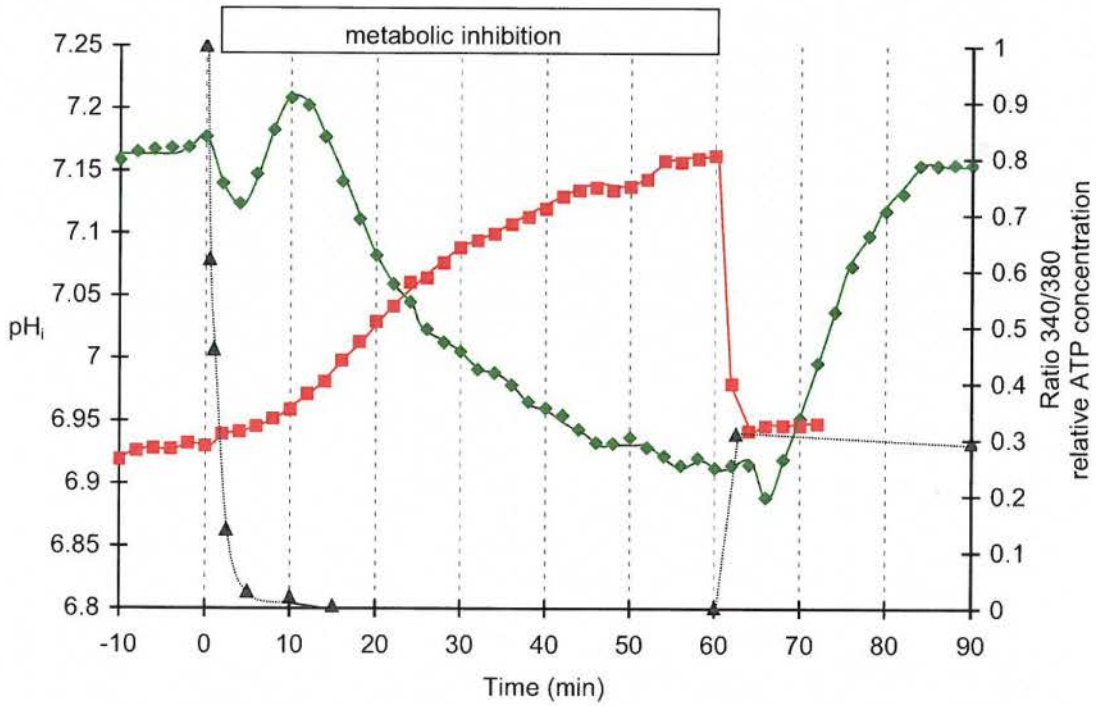

Figure 5.14 *Summary of changes in ATP-concentration (▲), Fura-2 ratio (■) and pH$_i$ (◆) during 60 minutes of metabolic inhibition with NaCN (2.5 mM) and DOG (10 mM). Data are the same as presented in Figure 5.1, 5.5 and 5.6, respectively. For clarity, SE-bars were omitted from the graph.*

The most likely explanation for this difference is the presence of a very high energy turnover in the primary cultured cells. Na^+,K^+-ATPase activity has been reported to be quite high in CTAL and MTAL, so that the turnover rate of the ATP pool is very fast (ATP half-life is about 4-5 s) (Morel & Doucet, 1992).

MTAL and CTAL cells contain high activities of glycolytic enzymes (Morel & Doucet, 1992) (see chapter 1). Additionally, it has been demonstrated that cells in culture have an increased glycolytic activity as a characteristic of proliferation (Tang et al., 1989). Therefore it is not surprising that (anaerobic) glycolysis is the predominant pathway for ATP production in these cultured MTAL cells. When glycolysis was blocked with DOG and no pyruvate was added to fuel mitochondrial ATP production, the cells were still capable of producing some ATP (19% of control after one hour incubation). The substrates for this mitochondrial ATP production might be the glucogenic amino acids alanine and/or glycine (both present in the perfusion solution) that can be converted to pyruvate. However, Weinberg et al. have shown that glycine is cytoprotective independent of preservation of tubule cell ATP levels (Weinberg et al., 1989). Another possible source of acetyl-CoA is the β-oxidation of endogenous fatty acids.

As discussed in chapter 2, the glucose-derivative DOG, is phosphorylated to DOG-6-P by the intracellular glycolytic hexokinase. By undergoing extensive phosphorylation DOG depletes existing ATP stores (Lieberthal et al., 1998). In conditions where ATP can be generated by oxidative phosphorylation, this may lead to intracellular phosphate depletion, and thereby limit the ATP production capacity. Thus, in the experiments where DOG and pyruvate were added to the cells, the capacity of mitochondria to produce ATP by oxidative phosphorylation, may be underestimated.

Recovery of ATP content after MI was only partial. This has been described previously after CN^- and DOG treatment, for example in MDCK cells (Despa, 2000; McCoy et al., 1988). Doctor et al. have attributed this partial ATP recovery to incomplete reversibility of the inhibition of glycolysis and mitochondrial respiration (Doctor et al., 1994). Although CN^- binds irreversibly to the binuclear center of cytochrome *c* oxidase (Panda & Robinson, 1995), O_2 can partially reverse CN^- inhibition *in vitro* (Delhumeau et al., 1994). Conversely, although DOG is a competitive (and thus reversible) inhibitor of glycolysis, its blocking effect remains at a high and constant level *in vivo* even after the circulating DOG has decreased to a relatively low plasma concentration (Wick et al., 1957). Another cause for the partial ATP recovery might be a decreased ATP production capacity of the cells: isolated proximal tubular cells subjected to 60 minutes of hypoxia developed a severely compromised energetic function through the development of the mitochondrial permeability transition (Weinberg et al., 1997). Finally, in freshly

isolated distal tubules it was shown that after 2 hours of MI, total adenine nucleotide content had decreased by 74%, which could not be accounted for by accumulation of degradation products (Lash et al., 1996).

Although we demonstrated that both pyruvate and glucose are capable of (partially) reversing MI, in all subsequent experiments glucose was preferred over pyruvate because the sudden addition of pyruvate might seriously disturb intracellular NAD^+/NADH ratio due to the high activity of lactate dehydrogenase (see chapter 2).

5.4.2 LIVE/DEAD viability testing

Since Lieberthal et al. (Lieberthal et al., 1998) have demonstrated that severe ATP depletion in cultured renal cells uniformly leads to cell necrosis, no markers for apoptosis were used in this study and cell necrosis was visualized with EtHD-1. The number of necrotic cell started to rise after 2 hours of MI. This is in agreement with the notion that primary cultured cells are more sensitive to ischemia than immortalized cell lines (Ardaillou et al., 2000). Surprisingly, the number of necrotic cells did not further increase after 3 hours of MI. The most likely explanation for this observation is that necrotic cells after some time detach from the filter support and are washed away. This is a general feature of necrosis and this phenomenon was previously reported to occur in cultured proximal tubular cells (Lieberthal et al., 1998). This might also explain why the number of necrotic cells in the time-matched controls has a tendency to decrease after 2 hours.

5.4.3 $[Ca^{2+}]_i$

The immediate, small increase of Fura-2 ratio upon addition of CN^- and DOG is a result of the change in autofluorescence from the filter support. In 1994, Rose et al. have also measured Fura-2 signals during a 60 minute period of substrate-free anoxia in primary cell cultures from rabbit MTAL which were grown on coverslips. The pattern of changes in Fura-2 ratio was very similar to our observations, comprising a slow rise towards an apparent plateau, followed by an immediate normalization upon reperfusion. In freshly isolated proximal tubules, they demonstrated that the anoxia-induced rise in $[Ca^{2+}]_i$ was dependent on both Ca^{2+} influx as well as on release from intracellular Ca^{2+} stores (Rose et al., 1994a). The plateau phase of the Fura-2 signal might be due either to a true stabilization of $[Ca^{2+}]_i$ or to a saturation of the Fura-2 signal. The rapid decrease of Fura-2 ratio upon "reperfusion" parallels the ATP measurements, which showed a very rapid (although incomplete) recovery of cellular energy content. This may indicate that

Ca^{2+}-ATPases play a predominant role in normalizing $[Ca^{2+}]_i$. The present results are different from the MDCK experiments that were performed previously in the L.U.C. laboratory.

5.4.4 Possible causes of intracellular alkalinization during MI

In most cells exposed to ischemia and hypoxia, pH_i decreases (Burke & Schrier, 1997). Although no pH_i measurements have been performed on MTAL cells, data from the L.U.C. laboratory on MDCK and A6 cell lines indicated that also in these distal tubular cells, a gradual acidosis develops during MI (Despa, 2000; Smets, 2001).

Therefore, the finding of a transient alkalinization during the initial phase of ATP depletion was unexpected. However, some reports on (transient) alkalinizations during ATP depletion have been published previously. During ischemia in muscle and myocardial cells, phosphocreatine (PCr) breakdown usually results in a transient alkalinization at the onset of ischemia (Kemp et al., 2001; Allen et al., 1985; Eisner et al., 1989; Fry et al., 1987). PCr is a high energy phosphate donor and plays an important role not only in muscle contraction, but also in buffering intracellular energy storage. Rat MTAL cells possess a large amount of PCr (approaching that of the brain) (Takeda et al., 1994). However, in contrast to myocardial cells where ATP content starts to decline only after PCr concentration has dropped dramatically (Fry et al., 1987), in rat MTAL cells PCr and ATP concentration decrease in parallel (Bastin et al., 1987). Since PCr breakdown will only alkalinize the cells as long as ATP levels remain elevated, and since ATP concentration declines very rapidly in these primary cultures (even before the onset of the alkalinization, Fig. 5.14) it can be concluded that the alkalinization observed is not the result of PCr breakdown.

In 1999, Jorgensen et al. observed alkalinizations following an initial acidification during chemical anoxia (azide in the presence of glucose) in primary cell cultures from mouse neocortical neurons. In the presence of EIPA 50 µM only a simple acidification was observed. Therefore, the authors concluded that activation of the NHE was responsible for the alkalinization (Jorgensen et al., 1999). Since in the present experiments a transient alkalinization was observed in the presence of EIPA 10 µM, activation of the NHE can not account for the alkalinization.

To our current knowledge, we are the first investigators to describe an increase in Na-P_i type I activity as a cause of alkalinization at the onset of ATP depletion. However, in 2001, Xiao et al. (Xiao et al., 2001) have reported an increase in Na-P_i cotransport activity in rat proximal tubular cells subjected to IRI.

They observed that after 30 minutes of ischemia, in freshly isolated brush border membrane vesicles Na-P_i cotransport activity had significantly increased by 31%, whereas Na^+/glucose cotransport activity was decreased by 45%. The amounts of both Na-P_i type I and Na-Pi type II cotransporter protein were decreased after ischemia. Since Na-P_i type II is the predominant Na-P_i cotransporter in proximal cell brush borders, the authors attributed the increase in Na-P_i cotransport activity to Na-P_i type II (Xiao et al., 2001). Taking into account the present data, it is conceivable that an increase in Na-P_i type I cotransport activity was responsible for their observations.

5.4.5 Hypotheses on Na-P_i 1 activation during ischemia

A disadvantage of the use of DOG to block glycolysis, is that a substantial fraction of the total P_i is trapped as DOG-6-P (Allen et al., 1985). Therefore, an increase in Na-P_i type I cotransport activity could be related to the use of DOG. Although this hypothesis is unlikely because the alkaline transient also occurs in the presence of CN^- alone, we however can not exclude the possibility that the alkaline transient during CN^- alone has a different cause, since we did not perform the CN^- alone experiment in the absence of P_i.

In 1985 Molitoris et al. demonstrated that an increase in brush border membrane Na-P_i cotransport activity could be mediated by a decrease in cholesterol content and an accompanying increase in membrane fluidity of the BBM (Molitoris et al., 1985). This might increase the transmembrane mobility of P_i transport units. In 1990 Friedlander et al. investigated this further in primary cell cultures of rabbit proximal tubular cells. They were able to demonstrate that fluidization of apical membranes (with the local anesthetic drug benzyl alcohol) decreased the Na^+-dependent uptake of methyl α-D-glucopyranoside, but increased the Na^+-dependent P_i uptake by 31% (Friedlander et al., 1990). Montagna et al. (Montagna et al., 1998) demonstrated in the rat RAO model, that after 50 minutes of ischemia, lipid peroxidation of proximal BBM had significantly increased, which may have caused an increased membrane fluidity. Molitoris et al. (Molitoris & Kinne, 1987) have described that the reduction in Na^+-dependent D-glucose transport (which is measurable after 15 minutes of renal artery clamping) correlated with ischemia-induced changes in membrane fluidity. Taking into account these data, the increased Na-P_i cotransport activity that was observed during ischemia could be the consequence of ischemia-induced modifications of membrane properties (Xiao et al., 2001).

As discussed in chapter 4, the physiological role of Na-P_i type I cotransporters is not clear (several reports have ruled out a prominent role for Na-

P_i type I proteins in regulating body P_i homeostasis) (Werner et al., 1998). The physiological role of Na-P_i type I cotransport may be related with glycolysis and cellular energy metabolism: both in rat kidneys and in cultured hepatocytes, high glucose concentrations selectively upregulated Na-P_i type I expression (Li et al., 1996). In rat brain BNP-1 (a Na-P_i co-transporter belonging to the type I Na-P_i co-transporter family) may be involved in brain energy metabolism (Ni et al., 1995). These data suggest that Na-P_i type I serves to supply the great demand of P_i in the liver, kidney and brain as a result of their high level of glucose metabolism (Werner et al., 1998). Since ADP, AMP as well as P_i are activators (or rather de-inhibitors of ATP) for phosphofructokinase (PFK), which is (at least in muscle) the major flux-controlling enzyme of glycolysis (Voet & Voet, 1990), it is conceivable that a decrease in intracellular ATP content or an increase in ADP/ATP ratio might be the factor triggering Na-P_i type I activation.

The question arising from our experimental observations in combination with the presented data from the literature, is whether an increase in Na-P_i type I cotransport activity is beneficial for cell survival. It has been described that incubation of OK cells (model of the proximal nephron) in phosphate-free medium for 2 hours decreased intracellular ATP levels from 2.7 to 1.2 µg/mg protein, indicating the importance of adequate phosphate-supply for cellular energy homeostasis (Green et al., 1993). In freshly isolated rat proximal tubules, phosphate-free perfusion during 40 minutes elicited cellular damage. They further demonstrated an important cytoprotective role when maintaining adequate phosphate (PO_4) stores during hypoxia (Almeida et al., 1992). Also in neurons, P_i dose-dependently increases cell survival in the acute phase following oxidative insults (Glinn et al., 1998). These data suggest that an increased P_i uptake by ischemic cells might indeed be cytoprotective.

5.4.6 Possible causes of intracellular acidification during MI

As in hepatocytes subjected to MI (Gores et al., 1989), protons liberated by ATP hydrolysis may be largely responsible for the initial acidification, which parallels the fall in ATP concentration. However, in experiments where P_i was present in the apical superfusion solution, pH_i started to decrease again after a transient alkalinization, at a moment where ATP concentration had already dropped to 1% (Fig. 5.14). A contribution by lactic acid to intracellular acidosis can be excluded in the experiments where DOG was used. Moreover, these primary cultured cells acidified when glycolysis was blocked with DOG, but only a very moderate acidification was observed when cell ATP production relied entirely on anaerobic glycolysis (CN^- only experiments). Therefore, the acidification during MI

is most likely the result of a passive distribution of H^+ ions over the plasma membrane (with a membrane potential of –71 mV, pH_i would be around 6.15 (Guggino et al., 1988)). As long as the plasma membrane potential is not dissipated, passive distribution of protons can contribute to cytosolic acidification. This passive distribution might be counteracted by NHE activity (which we showed to be the major acid-extruder in these primary cultures). However, NHE activity did not counteract the acidification since EIPA did not cause a more profound acidification. This is in accordance to data from the literature. When LLC-PK_1 cells were exposed to MI, NHE activity was strongly suppressed (Burns et al., 1991). Also in hepatocytes, NHE activity was virtually abolished during MI and this was not due to intracellular Na^+ accumulation but the NHE seemed to be inhibited directly (Schoenecker & Weinman, 1994). When proximal tubular cells in culture are acutely deprived of phosphate, the NHE is substantially inhibited, probably because in physiological conditions, there is a tonic state of phosphorylation of the exchanger, although it is also possible that ATP binds directly to the exchanger (Green et al., 1993; Burns et al., 1991).

Intracellular phosphate compounds play an important role in titrating acid loads: the buffering capacity of phosphate-depleted OK cells decreased from 27 to 19 mM/pH unit. However, no change in resting pH_i value was observed in these cells when exposed to phosphate-depletion (Green et al., 1993). Also in our experiments, acidification during ischemia was not increased in the absence of phosphate apically. Only in the absence of Na^+ in the apical solution, acidification during ischemia was significantly increased. It may be that both the inhibition of apical NHE-activity and Na-P_i 1 transport activity are responsible for this observation, although this remains highly speculative.

It is striking that pH_i recovered much more slowly than $[Ca^{2+}]_i$ and ATP concentration. This may be because Ca^{2+} is immediately pumped from the cytosol by Ca^{2+} ATPases, whereas recovery of pH_i might be dependent on the recovery of other ions such as Na^+. This is in accordance with the observation that bafilomycin A_1 sensitive H^+-ATPase are not important for the pH regulation in these primary cell cultures. Furthermore, the observation that pH_i recovery did not seem to be inhibited during experiments in which no Na^+ was present in the apical solutions (Fig. 5.12), indicates that the apical NHE is not essential for pH_i recovery after MI.

5.5 Conclusions

MI produced a rapid and profound ATP depletion in primary cell cultures from rabbit MTAL. This ATP depletion was partially reversible after 1 hour of MI. An increase in the number of necrotic cells was detected after 2 hours of MI with 1

hour of "reperfusion". The changes in pH_i that were observed during MI were unexpected because a transient alkalinization took place during the first phase of MI. It was demonstrated that this was not the result of PCr breakdown or of an increase in NHE activity, but that it was the result of an increase in Na-P_i 1 cotransport activity. This increased activity may have been the result of changes in plasma membrane fluidity or may have been a response of the cell to the ATP depletion by providing extra P_i. The acidification that followed the transient alkalinization was most likely the result of the passive distribution of H^+-ions over the plasma membrane. No correlations could be made between changes in pH_i and cell death/survival. The question arising from this study is whether the increase in Na-P_i type I co-transport activity is cytoprotective.

Chapter 6

Summary and general discussion

In **chapter 1**, the importance of studying the Medullary Thick Ascending Limb segment (MTAL) of the nephron in renal ischemia-reperfusion injury is discussed. The outer medulla, which contains both straight proximal tubules and MTAL segments, is a region of the kidney that lives on the edge of hypoxia: high reabsorptive activity is combined with a limited blood supply in order to maintain concentration gradients within the medullary interstitium. It is therefore not surprising that during ischemia, the tubules in the outer medulla are the first to show signs of cellular damage. Although in human Acute Tubular Necrosis, both proximal and MTAL segments contain necrotic cells, the popularity of one specific model system (the Renal Artery Occlusion of the rat kidney) has derived most efforts to unravel the cellular pathophysiology to the proximal tubular cells. Recent findings however suggest an important role for the MTAL cell in the pathophysiology of renal ischemia-reperfusion injury. Both the production of cytokines, which play a role in inflammation, and the upregulation of genes which may be important for regeneration, are predominantly observed in the MTAL (Safirtsein et al., 1991; Gobé et al., 1999; Megyesi et al., 2002; Degreef et al., 2003). Despite these data, the number of experiments on distal tubular cells in general, or MTAL cells, is very limited.

Both freshly isolated tubular cells as well as primary cultured cells are suitable for investigations on cellular pathophysiological processes. Both *in vitro* model systems were shown to retain many characteristics of the *in vivo* situation, and importantly, to retain the same differential susceptibility pattern to ischemic and toxic damage as their *in vivo* counterparts. For these reasons, primary cell cultures from MTAL segments from rabbit kidneys were chosen as the most suitable model system for our study. Since existing methods for isolating MTAL cells result in a mixture of cell types, a new method for obtaining 100% pure starting material had to be developed.

In **chapter 3**, a simple method for obtaining functionally and morphologically intact primary cultures of cells from the medullary thick ascending limb from rabbit kidneys is described. After digesting dissected fragments of the inner stripe of the outer medulla with collagenase, a suspension of tubule fragments was obtained, the vast majority of which were MTAL segments. These were identified individually by their morphological appearance and large amounts were collected with a micropipette connected to a micromanipulator. In this way a maximal homogeneity of the starting material was ensured. Monolayers of cells were grown from these MTAL segments after seeding onto collagen coated permeable filter supports. After confluence was reached, for one week the cultures

exhibited an apical side positive transepithelial potential difference. Electron microscopic examination showed a monolayer of polarized cells with characteristics of distal tubular cells. The primary cell cultures expressed Tamm-Horsfall protein at their apical surface. cAMP-Production was stimulated by 1 µM of vasopressin, calcitonin and isoproterenol. Intracellular calcium signaling was observed after stimulation with 1 µM of adenosine, ATP and bradykinin. Additional proof of their differentiation and polarization was the net NH_4^+ influx that occurred at very high rates at the apical cell membrane and was much slower at the basolateral cell membrane, as judged by measurements of intracellular pH. This unusual pattern of NH_3/NH_4^+ permeability is an essential characteristic of the MTAL cell, since NH_4^+-reabsorption by the MTAL segment is a crucial step in mammalian acid-base homeostasis.

In **chapter 4** the determinants of intracellular pH in physiological conditions are investigated. The intracellular pH in these primary cell cultures was measured fluorimetrically by using the pH-sensitive probe BCECF. The absence of HCO_3^- reabsorption in the rabbit MTAL segment allowed us to work with HEPES-buffered, HCO_3^--free solutions without interfering with physiologically relevant transepithelial transport processes.

Experiments on Na^+-dependent alkalinizations of acidified cells, revealed the presence of Na^+/H^+-exchange activity, both in the basolateral and in the apical cell membrane. Both exchangers could be completely blocked with EIPA (10 µM). Taking into account data from the literature, the basolateral Na^+/H^+-exchanger probably is the NHE-1 isoform and the apical Na^+/H^+-exchanger could be, either NHE-1, NHE-2 or both. No evidence for a functional H^+-ATPase was found in these cells.

The experiments on Na^+-dependent alkalinizations however also revealed the presence of a Na-P_i cotransporter in the apical cell membrane. This was unexpected since no phosphate reabsorption takes place in the rabbit MTAL segment perfused *in vitro*, and since neither Na-P_i type I or Na-P_i type II is expressed in the rabbit MTAL *in vivo*. With indirect immunofluorescence, the Na-P_i cotransporter expressed in these primary cell cultures could be identified as Na-P_i type I. Whereas Na-P_i type II is responsible for the majority of phosphate reabsorption in the proximal tubule, the function of Na-P_i type I still is unclear. In proximal tubular cells and in hepatocytes, Na-P_i type I was shown to be upregulated by high glucose concentrations. Since a "high-glucose" medium was used for these primary cell cultures, the composition of the medium may have influenced the phenotype of these cultured MTAL cells.

Also in **chapter 4**, the transport pathways responsible for the high NH_4^+ permeability of the apical cell membrane were investigated. Intracellular pH was used as an indirect measure of NH_4^+/NH_3 transport into these cells. For studying the NH_4^+ transport pathways in physiologically relevant conditions, experiments were performed in the symmetrical presence of NH_4Cl (4 mM), which acidified the cells to pH_i 6.89. When in this condition blockers of apical NH_4^+ transport were added to the apical superfusion solution, the cells alkalinized due to a decreased acid (NH_4^+)-loading. The following values were observed with various drugs acting at different sites: bumetanide (0.1 mM): + 0.05 pH units, verapamil (0.1 mM) + 0.04 pH units, Ba^{2+} (2 mM) and Cs^+ (20 mM): + 0.19 pH units, Tertiapin (1µM): + 0.09 pH units, whereas TEA (10 mM) had no effect on pH_i. Depolarizing the cells by increasing K^+-concentration in the apical solution to 20 mM (in bumetanide-containing solutions) also alkalinized the cells by 0.16 pH units. So, depolarizing the apical cell membrane by either blocking the apical K^+-conductance with Ba^{2+} or by increasing the luminal K^+-concentration, inhibited the majority of NH_4^+-reabsorption in steady-state conditions. Therefore, we had to exclude the possibility that NH_4^+ entered the cells through nonspecific cation channels. This was implemented by performing classical "ammonium-pulse" experiments. Sudden exposure of the apical cell membrane to NH_4Cl acidified the cells in controls as well as in the presence of 20 mM K^+ (in bumetanide-containing solutions). In contrast, when Ba^{2+} (2 mM), Cs^+ (20 mM) or Tertiapin (1 µM) were present at the luminal side of the epithelium, the addition of NH_4Cl alkalinized the cells. These results indicated that NH_4^+ must have permeated an apical K^+ conductance, rather than an aspecific channel in the apical cell membrane.

The pharmacological profile of this apical K^+ conductance pointed towards the involvement of the small conductance K^+ channel (sensitive to both Ba^{2+} and Cs^+, but not TEA), which is closely related to the cloned ROMK channel (which can be specifically blocked with Tertiapin). To prove that this channel was expressed in these primary cell cultures, indirect immunofluorescence with a specific antibody was performed and the presence of the ROMK protein could be detected.

Our results therefore suggest that the Ba^{2+} sensitive component of NH_4^+ reabsorption is predominant over $Na^+/K^+(NH_4^+)/2Cl^-$ mediated reabsorption and that this Ba^{2+} sensitive component could (at least partially) consist of the permeation of NH_4^+ through the apical small conductance K^+ channel. These findings are in agreement with the observations in one of the first publications on this subject in Nature (Kikeri et al., 1989). However, they are in contrast to the currently accepted concept that NH_4^+ reabsorption in the MTAL occurs mainly via the $Na^+/K^+(NH_4^+)/2Cl^-$ cotransporter (50-65%) and that the Ba^{2+} sensitive component consists of a K^+/NH_4^+ antiporter (Attmane-Elakeb et al., 2001).

Although more studies are needed to clarify this issue, especially concerning the regulation of NH_4^+ reabsorption by the MTAL, it may be interesting at this point to discuss two observations made in the clinical setting. First, if the $Na^+/K^+(NH_4^+)/2Cl^-$ cotransporter is the major pathway for NH_4^+ reabsorption, one might intuitively expect that the administration of loop diuretics would cause a metabolic acidosis (NH_3 would reach the kidney cortex where it would equilibrate with the blood. It would consequently be detoxified by the liver to form urea and therefore contribute to acidification of the blood). However, administration of furosemide causes an increase in urinary net acid excretion, and chronic administration leads to metabolic alkalosis. This was explained by an increase in HCO_3^- reabsorption by the TAL cells via a decrease in intracellular Na^+ concentration and consequently an increase in apical NHE activity (DuBose & Good, 1988).

Second, Bartter's syndrome type I and type II are congenital disorders caused by mutations in the genes for the $Na^+/K^+(NH_4^+)/2Cl^-$ cotransporter and the ROMK channel, respectively. Both subtypes of this syndrome are characterized by salt wasting, hypokalemia and metabolic alkalosis (Hamilton & Butt, 2000).

These clinical observations illustrate the complexity of acid-base handling by the kidney. They also suggest that neither the $Na^+/K^+(NH_4^+)/2Cl^-$ cotransporter nor the ROMK channel are absolutely essential for adequate NH_4^+ secretion by the kidney. One possible explanation for this observation is that one can take over the function of the other.

NH_4^+ reabsorption by the MTAL segments may also be involved in the pathophysiology of renal ischemia. In rabbit kidneys, ammonia levels were shown to rise from 275 to 3000 µg/100 g wet tissue weight during ischemia. Since these concentrations were considered to be toxic, different groups have performed experiments in which ammonia formation was prevented by previous HCO_3^- loading of the animals. This not only provided functional protection, but also prevented the "blue line", i.e. the peritubular vascular congestion in the outer medulla (Fitzpatrick et al., 1982). However, the mechanisms responsible for this protection have never been thoroughly investigated.

In **chapter 5**, the cellular pathophysiology of renal ischemia-reperfusion injury in the MTAL cells was investigated. As in myocardial cells, changes in pH_i and $[Ca^{2+}]_i$ play an important role in renal cell ischemia. However, their relative importance in contributing to (or protecting from) cell necrosis remains ill defined. Ischemia was mimicked by metabolic inhibition, which was achieved with NaCN (2.5 mM) and 2-deoxyglucose (10 mM). "Reperfusion" consisted of removal of the inhibitors together with the addition of glucose (20 mM) to the solutions. Metabolic

inhibition during 60 minutes caused a profound but reversible decrease in $[ATP]_i$. The Fura-2 ratio, which reflects $[Ca^{2+}]_i$, started to rise gradually after $[ATP]_i$ had decreased to less than 5% of its control value. The Fura-2 ratio normalized very rapidly upon "reperfusion".

Intracellular pH first decreased after initiation of metabolic inhibition, followed by a transient alkalinization. When $[ATP]_i$ reached its lowest value (< 1% of control), the cells slowly acidified to reach a stable pH_i of 6.92 after 50 minutes of metabolic inhibition. During "reperfusion", pH_i slowly recovered to its pre-ischemic value after 20 minutes. In the presence of ethyl-isopropyl-amiloride (10 µM) (a selective inhibitor of the Na^+/H^+ exchanger), the pattern of changes in pH_i was unchanged and acidification was not increased, indicating that the Na^+/H^+ exchangers were inactive during ATP depletion. It is a common finding in whole-cell studies is that the activity of a transporter or channel decreases when ATP is depleted. Such ATP responses may be protective or degenerative. For example, a considerable energetic cost is incurred by pumping sodium to maintain proton extrusion. Perhaps critical energy reserves are conserved by sacrificing fast proton extrusion during ATP depletion (Hilgemann, 1997).

When P_i or Na^+ were omitted from the apical solutions during metabolic inhibition, the transient alkalinization was no longer observed and the cytosol slowly acidified. Since we previously demonstrated that only the Na-P_i type I cotransporter is expressed in these primary cell cultures, the transient alkalinization had to result from an increased Na-P_i type I cotransport activity. This finding was unexpected since, as mentioned in the previous paragraph, the activity of transporters or channels generally decreases when ATP is depleted. Two exceptions are ATP-inhibited K^+-channels and glucose uptake (Hilgemann, 1997). According to our findings, phosphate uptake by Na-P_i type I cotransport is a third exception.

Although the physiological role of the Na-P_i type I cotransporter is unknown, it has been suggested to be related with supply of P_i for glycolysis and cellular energy metabolism. In this context, we may speculate that the increased Na-P_i type I activity after initiation of metabolic inhibition, could be the result of a decreased ATP/ADP ratio. The answer to the question whether this increased Na-P_i cotransport activity is cytoprotective, remains even more speculative. However, concerning the role of the serum P_i concentration in ischemia-reperfusion injury, we can refer to two studies performed some 20 years ago. First, Zager performed renal artery occlusion experiments in rats that had been "phosphate-loaded". Increasing the serum phosphate concentration from 7.0 to 9.5 mM strongly decreased GFR after ischemic injury. The underlying mechanism is unclear, although he demonstrated that no calcium-phosphate salts were deposited (Zager,

1982). Second, because phosphate restriction is beneficial in chronic nephropathy, its effect was investigated in acute ischemic renal injury in rats. Paradoxically, the investigators found that hypophosphatemia was deleterious in this situation. They observed that hypophosphatemia was accompanied by hypercalcemia and higher calcium loading of the ischemic renal tissue and of the mitochondria (Lumlertgul et al., 1986).

One of the goals of this work was to compare the results obtained in this new model of distal tubular cells to results obtained on immortalized cell lines. The unique results obtained by using this new model of TAL cells indicate the importance of studying distal tubular cells and the observation that TALH-SVE cells behave differently may indicate that for ischemia studies, de-differentiated, immortalized cell-lines are less suitable.

Nederlandstalige samenvatting en algemene bespreking

In **hoofdstuk 1** wordt het belang besproken van het medullaire dikke stijgende deel van de lis van Henle (MTAL) in de pathofysiologie van renale ischemie. De buitenste zone van de niermedulla bevindt zich steeds op de rand van de hypoxie. Dit is het gevolg van de hoge reabsorptie-activiteit van de niercellen in combinatie met een bloedtoevoer die beperkt is om de concentratiegradiënten van het interstitium niet weg te spoelen. Het is in deze zone dat de MTAL en ook het rechte deel van de proximale tubulus (S3) zich bevindt. Het is daarom ook niet verwonderlijk dat net deze nefron-segmenten de meest kwetsbare zijn bij renale ischemie. In biopsies van patiënten met "Acute Tubulus Necrose" bevatten zowel de proximale (o.a. S3) als de distale tubuli (o.a. MTAL) necrotische cellen. Het is echter door de populariteit van één specifiek experimenteel model (met name de totale occlusie van de nier-arterie in ratten) dat de overgrote meerderheid van het onderzoek omtrent de cellulaire pathofysiologie van renale ischemie op de proximale tubuluscellen werd toegespitst. Ook recente bevindingen benadrukken echter de potentieel belangrijke rol van de MTAL cellen. Zo wordt zowel de productie van cytokines, die een rol spelen in de ontstekingsreactie, als de verhoogde expressie van genen die belangrijk zijn in het regeneratieproces, voornamelijk waargenomen in de cellen van de MTAL. (Safirtsein et al., 1991; Gobé et al., 1999; Megyesi et al., 2002; Degreef et al., 2003). Ondanks deze aanwijzingen is het aantal onderzoeken dat uitgevoerd werd op cellen van de MTAL zeer beperkt.

Voor het onderzoek naar de cellulaire veranderingen tijdens renale ischemie kunnen zowel vers geïsoleerde cellen als primaire culturen van tubuluscellen aangewend worden. Het is aangetoond dat beide *in vitro* modelsystemen veel eigenschappen uit de *in vivo* situatie behouden. Belangrijker nog misschien is het feit dat ze hetzelfde differentiële patroon (S3 *versus* MTAL) blijven vertonen wat betreft hun gevoeligheid aan ischemische en toxische schade. Omwille van beide redenen werd er in de huidige studie voor gekozen om primaire culturen van de MTAL cellen uit nieren van het konijn te gebruiken als meest geschikt modelsysteem. Er werden in het verleden reeds enkele methoden beschreven om primaire culturen van MTAL cellen te bekomen. Deze leveren echter allemaal tot op zekere hoogte een mengeling van celtypes op. Daarom bestond de eerste doelstelling van dit wetenschappelijk werk uit het ontwikkelen van een nieuwe methode om 100% zuivere primaire celculturen van de MTAL te bekomen.

In **hoofdstuk 3** wordt een eenvoudige methode voorgesteld om zuivere en functioneel intacte primaire celculturen van MTAL segmenten uit nieren van het

konijn te bekomen. Na het enzymatisch verteren door collagenase van het binnenste gedeelte van de buitenste medulla, wordt een suspensie van tubulus-fragmenten bekomen, waarvan de overgrote meerderheid bestaat uit MTAL segmenten. Deze werden één voor één volgens hun morfologie geïdentificeerd en werden vervolgens verzameld in een micro-pipet verbonden met een micromanipulator. Op deze wijze werd een maximale zuiverheid van het startmateriaal verzekerd. Nadat deze MTAL segmenten op een met collageen-bedekte filter werden aangebracht, vormde zich hieruit één laag epitheliale cellen. Van zodra confluentie bereikt werd, kon er over deze primaire celculturen een transepitheliaal potentiaalverschil (apicaal positief) gemeten worden. Onder de elektronen-microscoop werd één laag van gepolariseerde cellen met kenmerken van distale tubulaire cellen geobserveerd. Deze primaire celculturen brachten aan hun apicale zijde het Tamm-Horsfall proteïne tot expressie. De produktie van cAMP werd gestimuleerd door vasopressine, calcitonine en isoproterenol. Intracellulaire calcium-signalen werden opgemeten na stimulatie met adenosine, ATP en bradykinine. Een bijkomend bewijs van de uitgesproken polarisatie van deze cellen werd geleverd door de hoge permeabiliteit van de apicale celmembraan voor NH_4^+. Dit in tegenstelling tot de basolaterale celmembraan die voornamelijk permeabel bleek voor NH_3. Dit ongewone patroon van NH_4^+/NH_3 permeabiliteit is een essentieel kenmerk van de MTAL cellen *in vivo* aangezien NH_4^+ reabsorptie door de MTAL een cruciale rol speelt in de zuur-base huishouding door de nieren bij zoogdieren.

In **hoofdstuk 4** worden de factoren onderzocht die een rol spelen bij de pH_i homeostase onder fysiologische omstandigheden. De pH_i in deze primaire celculturen werd gemeten via microfluorescentie van de pH-gevoelige molecule BCECF. De afwezigheid van HCO_3^--reabsorptie in de MTAL van het konijn maakt het mogelijk om met HCO_3^--vrije, HEPES-gebufferde oplossingen te werken zonder daardoor fysiologisch relevante transepitheliale transportmechanismen te verhinderen.

Door het onderzoeken van Na^+-afhankelijke alkalisaties van verzuurde cellen, werd de aanwezigheid van Na^+/H^+-uitwisselaars aangetoond, zowel in de apicale als in de basolaterale celmembraan. Beide uitwisselaars werden volledig geblokkeerd door EIPA (10 µM). Aan de hand van beschikbare gegevens uit de literatuur, kan verondersteld worden dat de basolaterale Na^+/H^+-uitwisselaar bestaat uit de NHE-1 isovorm, daar waar de apicale Na^+/H^+-uitwisselaar kan bestaan uit zowel NHE-1 als NHE-2 (of beide). Er werden geen aanwijzingen gevonden voor de aanwezigheid van een functionele protonpomp (H^+-ATPase) in deze cellen.

De experimenten waarin de Na^+-afhankelijke alkalisaties werden onderzocht toonden echter ook de aanwezigheid van een natrium-fosfaat ($Na\text{-}P_i$)-cotransporter aan in de apicale celmembraan van deze primaire celculturen. Dit was geheel onverwacht aangezien er in de *in vitro* geperfuseerde MTAL van het konijn geen fosfaat reabsorptie plaatsvindt. Bovendien wordt noch $Na\text{-}P_i$ type I, noch $Na\text{-}P_i$ type II *in vivo* tot expressie gebracht in de MTAL van het konijn. Met behulp van indirecte immunofluorescentie werd de $Na\text{-}P_i$-cotransporter die in deze primaire celculturen tot expressie komt, geïdentificeerd als $Na\text{-}P_i$ type I. Daar waar de $Na\text{-}P_i$-cotransporter type II instaat voor het grootste deel van de fosfaatreabsorptie in de proximale tubulus, is de functie van $Na\text{-}P_i$ type I nog grotendeels onduidelijk. Het is aangetoond dat hoge concentraties van glucose de expressie van de $Na\text{-}P_i$-cotransporter type I doen stijgen in proximale tubulus cellen en in levercellen. Aangezien er voor deze primaire celculturen een cultuurmedium werd gebruikt met een hoge concentratie van glucose (25 mM), is het denkbaar dat de specifieke samenstelling van het cultuurmedium het fenotype van deze in cultuur gebrachte cellen heeft beïnvloed.

Eveneens in **hoofdstuk 4** wordt besproken welke *trans*-membranaire transporteiwitten instaan voor de hoge ammonium (NH_4^+)-permeabiliteit van de apicale celmembraan, die zo typisch is voor de MTAL. Het transport van NH_3/NH_4^+ in deze cellen werd onrechtstreeks gemeten, door het bestuderen van de plotse pH_i veranderingen die het gevolg zijn van NH_3/NH_4^+-transport. Om het ammoniumtransport te onderzoeken in "fysiologische" omstandigheden werden de experimenten uitgevoerd in de symmetrische aanwezigheid van NH_4Cl (4 mM), waardoor de cellen verzuurden tot een pH_i van 6.89. Wanneer onder deze omstandigheden een blokker van een apicaal NH_4^+-transporteiwit werd toegevoegd aan de apicale perfusie-oplossing, alkaliseerden de cellen door een afname van de zuur (NH_4^+)-belasting. De volgende waarden werden opgemeten bij het gebruik van verschillende blokkers: bumetanide (0.1 mM): + 0.05 pH eenheden, verapamil (0.1 mM) + 0.04 pH eenheden, Ba^{2+} (2 mM) and Cs^+ (20 mM): + 0.19 pH eenheden, Tertiapine (1µM): + 0.09 pH eenheden. TEA (10 mM) veroorzaakte geen verandering van de pH_i. Tenslotte veroorzaakte ook een depolarisatie van de apicale celmembraan (door de K^+-concentratie van de apicale perfusie-oplossing te doen stijgen tot 20 mM in bumetanide-houdende oplossingen) een alkalisatie met 0.16 pH eenheden. Uit deze resultaten komt naar voor dat het depolariseren van de apicale celmembraan door enerzijds het blokkeren van de apicale K^+-conductantie (met Ba^{2+}) of anderzijds, door een toename van de luminale K^+-concentratie, het grootste deel van de NH_4^+-reabsorptie in evenwichtstoestand blokkeerde. Om deze reden diende de mogelijkheid dat NH_4^+ de cellen binnendrong via aspecifieke (kation)-kanalen, te worden uitgesloten. Hiertoe

werden de klassieke "ammonium-puls" experimenten uitgevoerd. Een plotse blootstelling van de apicale celmembraan aan NH_4Cl veroorzaakte een verzuring van de cellen, zowel in controle-omstandigheden als in de aanwezigheid van bumetanide en een verhoogde K^+-concentratie (20 mM) in de apicale perfusie-oplossing. In tegenstelling hiermee alkaliseerden de cellen wanneer Ba^{2+} (2 mM), Cs^+ (20 mM) of Tertiapine (1 µM) aanwezig waren aan de apicale zijde van het epitheel. Deze resultaten bewijzen dat NH_4^+ de cellen binnendringt via een apicale K^+-conductantie, en niet via een aspecifiek kanaal in de apicale celmembraan.

Het farmacologisch profiel van deze apicale K^+-conductantie wees op de betrokkenheid van het lage conductantie K^+-kanaal (gevoelig aan Ba^{2+} en Cs^+, maar niet aan TEA) dat nauw verwant is aan het gecloneerde ROMK kanaal (dat specifiek kan geblokkeerd worden met Tertiapine). Om aan te tonen dat dit kanaal tot expressie werd gebracht in deze primaire celculturen werd er met een specifieke antistof een indirecte immunofluorescente kleuring uitgevoerd. Daarmee werd de aanwezigheid van het ROMK proteïne in deze primaire celculturen vastgesteld.

Samengevat suggereren deze resultaten dat de Ba^{2+}-gevoelige component van NH_4^+-reabsorptie kwantitatief belangrijker is dan de $Na^+/K^+(NH_4^+)/2Cl^-$-gemediëerde reabsorptie en dat deze Ba^{2+}-gevoelige component (althans gedeeltelijk) bestaat uit de permeatie van NH_4^+ doorheen het apicale lage conductantie K^+-kanaal. Deze bevindingen komen overeen met de observaties in één van de eerste publicaties over dit onderwerp in Nature (Kikeri et al., 1989). Ze staan echter in contrast tot het huidige concept dat NH_4^+-reabsorptie door de MTAL vooral gebeurt via de $Na^+/K^+(NH_4^+)/2Cl^-$-cotransporter (50-65%) en dat de Ba^{2+}-gevoelige component bestaat uit een (verapamil-gevoelige) K^+/H^+-uitwisselaar (Attmane-Elakeb et al., 2001).

Hoewel er méér studies vereist zijn om dit vraagstuk op te helderen, in het in het bijzonder wat betreft de regulatie van de NH_4^+-reabsorptie door de MTAL, is het misschien interessant om hier twee bevindingen uit de klinische setting te bespreken. Ten eerste, indien de $Na^+/K^+(NH_4^+)/2Cl^-$-cotransporter de belangrijkste component is van de NH_4^+-reabsorptie, zou men, intuïtief, verwachten dat de toediening van lisdiuretica een metabole acidose zou uitlokken (ammonium zou namelijk de niercortex bereiken en terug in het bloed terecht komen, waarna het door de lever zou omgezet worden tot ureum en zo zou bijdragen tot verzuring van het bloed). Echter, toediening van furosemide veroorzaakt een stijging van de netto renale zuur-excretie, en chronische toediening leidt tot metabole alkalose. Dit kan verklaard worden door een toename van de de HCO_3^--reabsorptie door de MTAL ten gevolge van een verminderde intracellulaire Na^+-concentratie en een daardoor toegenomen apicale NHE-activiteit (DuBose & Good, 1988).

Ten tweede, het syndroom van Bartter type I and type II zijn aangeboren aandoeningen veroorzaakt door mutaties in de genen voor de $Na^+/K^+(NH_4^+)/2Cl^-$-cotransporter en het ROMK-kanaal, respectievelijk. Zowel type I als type II van dit syndroom worden gekenmerkt door het verlies van zout, hypokaliëmie en metabole alkalose (Hamilton & Butt, 2000).

Deze klinische observaties illustreren de complexiteit van de zuur-base regeling door de nieren. Ze suggereren echter ook dat noch de $Na^+/K^+(NH_4^+)/2Cl^-$-cotransporter noch het ROMK-kanaal essentieel zijn voor een voldoende NH_4^+-secretie door de nieren.

NH_4^+-reabsorptie door de MTAL zou verder ook een rol kunnen spelen in de pathofysiologie van renale ischemie. In de nieren van het konijn werd aangetoond dat de ammoniakconcentratie steeg tijdens ischemie van 275 tot 3000 µg/100 g nat gewicht. Aangezien deze concentraties als toxisch beschouwd worden, hebben verschillende onderzoeksgroepen experimenten uitgevoerd waarin de ammoniakvorming werd tegengegaan door de proefdieren op voorhand "op te laden" met bicarbonaat. Dit beschermde niet enkel de nierfunctie, maar verhinderde ook de vorming van de zogenaamde "blauwe lijn", die het gevolg is van de peritubulaire vasculaire congestie in de buitenste medulla (Fitzpatrick et al., 1982). De mechanismen die verantwoordelijk zijn voor deze bescherming van de nierfunctie zijn echter sindsdien nooit verder onderzocht.

In **hoofdstuk 5** werd de cellulaire pathofysiologie van renale ischemie-reperfusie schade in cellen van de MTAL onderzocht. Zoals in myocardiale cellen, spelen veranderingen in pH_i en $[Ca^{2+}]_i$ een belangrijke rol in renale ischemie. Hun relatieve belang in het bijdragen tot (of het beschermen tegen) celnecrose blijft echter tot op heden onduidelijk. In de hier voorgestelde studie werd ischemie nagebootst door metabole inhibitie, die werd verkregen met NaCN (2.5 mM) en 2-deoxyglucose (10 mM). "Reperfusie" bestond uit het verwijderen van deze blokkers tesamen met de toediening van glucose (20 mM) aan de perfusie-oplossingen. Metabole inhibitie gedurende 60 minuten veroorzaakte een uitgesproken doch omkeerbare daling van de $[ATP]_i$. De Fura-2 ratio, die een maat is voor de $[Ca^{2+}]_i$, liep geleidelijk op nadat de $[ATP]_i$ gedaald was tot minder dan 5% van de uitgangswaarde. De Fura-2 ratio normaliseerde snel bij "reperfusie".

Onmiddellijk na de start van de metabole inhibitie daalde de pH_i, gevolgd door een transiënte alkalisatie. Van zodra $[ATP]_i$ zijn laagste peil had bereikt (< 1% van de uitgangswaarde), verzuurden de cellen opnieuw om te stabiliseren op pH_i 6.92 na 50 minuten metabole inhibitie. Tijdens de "reperfusie" herstelde de pH_i traag om na 20 minuten terug de pre-ischemische waarde te bereiken. In aanwezigheid van ethyl-isopropyl-amiloride (10 µM) (een selectieve blokker van de

Na^+/H^+-uitwisselaar), was het patroon van de verandering van pH_i ongewijzigd en de mate van verzuring was niet toegenomen, wat erop wijst dat de Na^+/H^+-uitwisselaars niet actief zijn tijdens ATP-depletie. Een vermindering van de activiteit van een transport eiwit of een kanaal is inderdaad niet uitzonderlijk tijdens ATP-depletie. Dit kan zowel een beschermend als een nadelig effect hebben. Zo wordt er bijvoorbeeld een aanzienlijke hoeveelheid energie verbruikt bij het naar buiten pompen van Na^+ (via de Na^+/K^+-pomp) om de H^+-extrusie (via de Na^+/H^+-uitwisselaar) op peil te houden. Misschien worden er kritische energie-reserves opgespaard door het opofferen van snelle H^+-extrusie tijdens ATP depletie (Hilgemann, 1997).

Indien P_i of Na^+ werd weggelaten uit de apicale perfusie-oplossingen tijdens metabole inhibitie, werd de transiënte alkalisatie niet meer waargenomen en verzuurde het cytosol geleidelijk. Omdat er voordien werd aangetoond dat enkel de Na-P_i type I-cotransporter tot expressie komt in deze primaire celculturen, dient de transiënte alkalisatie toegeschreven te worden aan een verhoogde activiteit van de Na-P_i type I-cotransporter. Dit is een onverwachte bevinding aangezien, zoals in de vorige paragraaf vermeld, de activiteit van ionen-kanalen en transport-proteïnes gewoonlijk afneemt tijdens ATP-depletie. Twee bekende uitzonderingen op deze algemene regel zijn ATP-geïnhibeerde K^+-kanalen en de opname van glucose (Hilgemann, 1997). Volgens de hier voorgestelde bevindingen is de opname van P_i door de Na-P_i type I-cotransporter een derde uitzondering.

Hoewel de rol van de Na-P_i type I-cotransporter in de celfysiologie nog grotendeels onbekend is, wordt er gesuggereerd dat ze een rol speelt in de P_i-bevoorrading van de glycolyse en het energie metabolisme van de cellen. Vanuit dit oogpunt kan verondersteld worden dat de toegenomen activiteit van de Na-P_i type I cotransporter bij aanvang van metabole inhibitie, het gevolg kan geweest zijn van een afgenomen ATP/ADP verhouding.

Het antwoord op de vraag of deze toegenomen Na-P_i-cotransport activiteit een beschermende functie heeft voor de cel, is nog meer speculatief. Toch kunnen we wat betreft de rol van de fosfaat-concentratie in ischemie en reperfusie schade verwijzen naar 2 studies die zo'n 20 jaar geleden werden gepubliceerd. Zager (Zager, 1982) voerde renale arterie occlusie experimenten uit in ratten die voordien werden "opgeladen" met fosfaat. Hij observeerde dat het stijgen van de fosfaat plasma-concentratie van 7 tot 9.5 mM de glomerulaire filtratie snelheid sterk deed afnemen na ischemische schade. Het mechanisme dat hiervoor verantwoordelijk was werd niet opgehelderd, hoewel wel werd aangetoond dat er géén calcium-fosfaat zouten werden afgezet. In een andere studie werd het effect van hypofosfatemie onderzocht in acute ischemische schade omdat fosfaatrestrictie een gunstig effect bleek te hebben bij chronische nefropathieën. In tegenstelling

hiermee stelden de onderzoekers vast dat hypofosfatemie schadelijk was bij acuut ischemisch lijden. Ze constateerden dat hypofosfatemie gepaard ging met hypercalciëmie en een een hogere Ca^{2+}-opstapeling in het ischemisch nierweefsel en de mitochondriën (Lumlertgul et al., 1986).

Eén van de bedoelingen van dit werk was het vergelijken van de resultaten verkregen met dit nieuwe model van distale tubulus cellen met de resultaten van continue cellijnen. De unieke resultaten die verkregen werden door het gebruik van dit nieuwe model van de MTAL bevestigen het belang van het bestuderen van de distale tubulus tijdens nier-ischemie. De observatie dat de TALH-SVE cellen zich verschillend gedragen van de primaire celculturen vormt een aanwijzing dat voor de studie van niercel-ischemie het gebruik van geïmmortaliseerde cellijnen minder geschikt zou kunnen zijn.

References

1. Abraham Mi, Woods RE, Breedlove DK, Kempson SA (1992) Renal adaptation to low-phosphate diet in diabetic rats. Am J Physiol 262:F731-F736

2. Alcorn D, Emslie KR, Ross BD, Ryan GB, Tange JD (1981) Selective distal nephron damage during isolated kidney perfusion. Kidney Int 19:638-647

3. Allen DG, Morris PG, Orchard CH, Pirolo JS (1985) A nuclear magnetic resonance study of metabolism in the ferret heart during hypoxia and inhibition of glycolysis. J Physiol 361:185-204

4. Allen ML, Nakao A, Sonnenburg WK, Burnatowska-Hledin M, Spielman WS, Smith WL (1988) Immunodissection of cortical and medullary thick ascending limb cells from rabbit kidney. Am J Physiol 255: F704-F710

5. Allen F, Tisher CG (1976) Morphology of the ascending thick limb of Henle. Kidney Int 9:8-22

6. Almeida AR, Wetzels JF, Bunnachak D, Burke TJ, Chaimovitz C, Hammond WS, Schrier RW (1992) Acute phosphate depletion and in vitro proximal tubule injury: protection by glycine and acidosis. Kidney Int 41(6):1494-1500

7. Alpern RJ (2000) Renal acidification mechanisms. In: Brenner BM (ed) Brenner and Rectors's The Kidney. W.B. Saunders Company, Philadelphia London Toronto Montreal Sydney Tokyo, pp 455-519

8. Alvarez A, Martul E, Veiga F, Forteza J (1994) Functional, histologic, and ultrastructural study of the protective effects of verapamil in experimental ischemic acute renal failure in the rabbit. Ren Fail 16(2):193-207

9. Amlal H, Paillard M, Bichara M (1994) NH_4^+ transport pathways in cells of medullary thick ascending limb of rat kidney. J Biol Chem 269(35):21962-21971

10. Amlal H, Legoff C, Vernimmen C, Paillard M, Bichara M (1996) Na^+-$K^+(NH_4^+)$-$2Cl^-$ cotransport in medullary thick ascending limb: control by PKA, PKC, and 20-HETE. Am J Physiol 271:C455-C463

11. An J, Varadarajan SG, Camara A, Cgen Q, Novalija E, Gross GJ, Stowe DF (2001) Blocking Na(+)/H(+) exchange reduces [Na(+)](i) and [Ca(2+)](i) load after ischemia and improves function in intact hearts. Am J Physiol 281(6):H2398-2409

12. Ardaillou, Ronco, Rondeau, Friedlander (2000) Biology of renal cells in culture. In: Brenner BM (ed) Brenner and Rectors's The Kidney. W.B. Saunders Company, Philadelphia London Toronto Montreal Sydney Tokyo, pp 93-191

13. Aronson PS, Boron WF, Boulpaep EL (2003) Physiology of membranes. In: Boron WF, Boulpaep EL (eds) Medical Physiology. Saunders, Philadelphia London New York St. Louis Sydney Toronto, pp50-86

14. Asako H, Kubes P, Wallace J, Wolf RE, Granger DN (1992) Modulation of leukocyte adhesion in rat mesenteric venules by aspirin and salicylate. Gastroenterology 103:146-152

15. Attmane-Elakeb A, Amlal H, Bichara M (2001) Ammonium carriers in the medullary thick ascending limb. Am J Physiol 280:F1-F9

16. Aw TY, Wilson E, Hagen TM, Jones DP (1987) Determinants of mitochondrial O_2 dependence in kidney. Am J Physiol 253:F440-447

17. Bailly C (1998) Transducing pathways involved in the control of NaCl reabsorption in the thick ascending limb of Henle's loop. Kidney Int 53 Suppl 65: S29-S35

18. Bak MI, Ingwall JS (2003) Contribution of Na(+)/H(+) exchange to Na(+) overload in the ischemic hypertrophied hyperthyroid rat heart. Cardiovasc res 57(4):1004-1014

19. Bastin J, Cambon N, Thompson M, Lowry OH, Burch HB (1987) Change in energy reserves in different segments of the nephron during brief ischemia. Kideny Int 31:1239-1247

20. Beck FX, Ohno A, Dorge A, Thurau K (1995) Ischemia-induced changes in cell element composition and osmolyte contents of outer medulla. Kidney Int 48-449-457

21. Beeri R, Symon Z, Brezis M, Ben-Sasson SA, Baehr PH, Rosen S, Zager RA (1995) Rapid DNA fragmentation from hypoxia along the thick ascending limb of rat kidneys. Kidney Int 47(6):1806-1810

22. Bell ML, Lazarus HM, Herman AH, Egdahl RH, Rutenburg AM (1971) pH dependent changes in cell membrane stability. Proc Soc Exp Biol Med 136:298-300

23. Biber J, Custer M, Werner A, Kaissling B, Murer H (1993) Localization of Na-P_i 1, a Na-P_i cotransporter, in rabbit kidney proximal tubules. I. Localization by immunohistochemistry. Pflügers Arch 424:210-215

24. Bleich M, Schlatter E, Greger R (1990) The luminal K^+ channel of the thick ascending limb of Henle's loop. Pflügers Arch 415:449-460

25. Bleich M, Köttgen M, Schlatter E, Greger R (1995) Effect of NH_4^+/NH_3 on cytosolic pH and the K^+ channels of freshly isolated cells from the thick ascending limb of Henle's loop. Pflügers Arch 429:345-354

26. Boim MA, Ho K, Shuck ME, Bienkowski MJ, Block JH, Slightom JL, Yang Y, Brenner BM, Hebert SC (1995) ROMK inwardly rectifying ATP-sensitive K^+ channel II. Cloning and distribution of alternative forms. Am J Physiol 268:F1132-1140

27. Bond JM, Chacon E, Herman B, Lemasters JJ (1993) Intracellular pH and Ca^{2+} homeostasis in the pH paradox of reperfusion injury to neonatal rat cardiac myocytes. Am J Physiol 265:C129-C137

28. Bonventre JV, Weinberg JM (2003) Recent advances in the pathophysiology of ischemic acute renal failure. J Am Soc Nephrol 14:2199-2210

29. Bourgeois S, Massé S, Paillard M, Houillier P (2002) Basolateral membrane Cl^--, Na^+-, and K^+-coupled base transport mechanisms in rat MTALH. Am J Physiol 282:F655-668

30. Brady HR, Brenner BM, Clarkson MR, Lieberthal W (2000) Acute Renal Failure. In: Brenner BM (ed) Brenner and Rectors's The Kidney. W.B. Saunders Company, Philadelphia London Toronto Montreal Sydney Tokyo, pp 1201-1262

31. Bretschneider HJ, Helmchen U, Kehrer G (1988) Nierenprotektion. Klin Wochenschr 66(18):817-827.

32. Breyer MD, Jacobson HR, Davis LS, Breyer RM (1993) In situ hybridisation and localization of mRNA for the rabbit EP_3 receptor. Kidney Int 43:1372-1378

33. Brezis M, Rosen S (1995) Hypoxia of the renal medulla - its implication for disease. New Engl J Med 332(10):647-655

34. Brodsky SV, Yamamoto T, Tada T, Kim B, Chen J, Kajiya F, Goligorsky MS (2002) Endothelial dysfunction in ischemic acute renal failure: rescue by transplanted endothelial cells. Am J Physiol 282:F1140-F1149

35. Burckhardt G, Di Sole F, Helmle-Kolb C (2002) Tne Na^+/H^+ exchanger gene family. J Nephrol 5:S3-21

36. Burg M, Green N, Sohraby S, Steele R, Handler J (1982) Differentiated function in cultured epithelia from thick ascending limbs. Am J Physiol 242: C229-C233

37. Burke TJ, Schrier RW (1997) Pathophysiology of cell ischemia. In: Schrier RW, Gottschalk CW (eds) Diseases of the Kidney. Little Brown, Boston, pp 1013-1048

38. Burnatowska-Hledin MA, Spielman WS (1991) Effects of adenosine on cAMP production and cytosolic Ca2+ in cultured rabbit medullary thick limb cells. Am J Physiol 260: C143-C150

39. Burns KD, Homma T, Harris RC (1991) Regulation of Na^+-H^+ exchange by ATP depletion and calmodulin antagonism in renal epithelial cells. Am J Physiol 261:F607-F616

40. Canfield PE, Geerdes AM, Molitoris BA (1991) Effect of reversible ATP depletion on tight-junction integrity in LLC-PK1 cells. Am J Physiol 261:F1038-F1045

41. Carini R, Autelli R, Bellomo G, Dianzani MU, Albano E (1995) Sodium-mediated cell swelling is associated with irreversible damage in isolated hepatocytes exposed to hypoxia or mitochondrial toxins. Biochem Biophys Res Commun 206:180-185

42. Cha SH, Sekine T, Endou H (1998) P2 purinoreceptor localisation along rat nephron and evidence suggesting existence of subtypes P2Y1 and P2Y2. Am J Physiol 274: F1006-F1014

43. Chamberlin ME, LeFurgey A, Mandel LJ (1984) Suspension of medullary thick ascending limb tubules from the rabbit kidney. Am J Phys 247: F955-F964

44. Chan L, Shapiro JL (1989) Contributions of nuclear magnetic resonance to study of acute renal failure. Ren Fail 11(2-3):79-89

45. Chen W, Guéron M (1992) The inhibition of bovine heart hexokinase by 2-deoxy-D-glucose-6-phosphate: characterization by ^{31}P NMR and metabolic implications. Biochimie 74:867-873

46. Chini EN, Dousa TP (1996) Microdissection and microanalysis of specific nephron segments from mammalian kidney. In: Zalups RK, Lash LH (eds) Methods in renal toxicology. CRC Press, Boca Raton New York London Tokyo, pp 97-107

47. Choe H, Sackin H, Palmer LG (2000) Permeation properties of inward-rectifier potassium channels and their molecular determinants. J Gen Physiol 115:391-404

48. Conger JD (2001) Vascular alterations in Acute Renal failure: roles in initiation and maintenance. In: Molitoris BA, Finn WF (eds) Acute Renal Failure. WB Saunders Company, Philadelphia, pp 13-29

49. Counillon L, Pouysségur J (2000)a The members of the Na^+/H^+ exchanger gene family: their structure, function, expression, and regulation. In: Seldin DW, Giebisch G (eds) The Kidney: physiology and pathophysiology. Lippincot Williams & Wilkins, Philadelphia, pp 223-234

50. Counillon L, Pouysségur J (2000)b The expanding family of eucaryotic Na^+/H^+ exchangers. J Biol Chem 275(1):1-4

51. Custer M, Meier F, Schlatter E, Greger R, Garcia-Perez A, Biber J, Murer H (1993) Localization of NaPi-1, a Na-P_i cotransporter, in rabbit kidney proximal tubules. I. mRNA localization by reverse transcription/polymerase chain reaction. Pflügers Arch 424:203-209

52. Custer M, Lötscher M, Biber J, Murer H, Kaissling B (1994) Expression of Na-P_i cotransport in rat kidney: localization by RT-PCR and immunohistochemistry. Am J Physiol 266:F767-F774

53. Daemen MA, van 't Veer C, Denecker G, Heemskerk VH, Wolfs TG, Clauss M, Vandenabeele P, Buurman WA (1999) Inhibition of apoptosis induced by ischemia-reperfusion prevents inflammation. J Clin Invest 104(5):541-549

54. Dagher PC (2000) Modeling ischemia in vitro: selective depletion of adenine and guanine nucleotide pools. Am J physiol 279:C1270-C1277

55. De Greef KE, Ysebaert DK, Dauwe S, Persy V, Vercauteren SR, Mey D, De Broe ME (2001) Anti-B7-1 blocks mononuclear cell adherence in vasa recta after ischemia. Kidney Int 60:1415-1427

56. De Greef KE, Ysebaert DK, Persy V, Vercauteren SR, De Broe ME (2003) ICAM-1 expression and leukocyte accumulation in inner stripe of outer medulla in early phase of ischemic compared to $HgCl_2$-induced ARF. Kidney Int 63:1697-1707

57. Delhumeau GA, Cruz-Mendoza AM, Lojero GG (1994) Protection of cytochrome c oxidase against cyanide inhibition by pyruvate and α-ketoglutarate: effect of aeration *in vitro*. Tox Apll Pharm 126:345-351

58. De Rouffignac C, Di Stefano A, Wittner M, Roinel N, Elalouf JM (1991) Consequences of differential effects of ADH and other peptide hormones on thick ascending limb of mammalian kidney. Am J Physiol 260: R1023-R1035

59. Despa S (2000) Microfluorimetry of epithelial cells: lifetime-based sensing of Na^+ concentration and the effects of chemical hypoxia. Publication D/2000/2451/6 (p 95) in the Royal Library Albert I, Brussels

60. De Vries B, Matthijsen RA, Wolfs TG, Van Bijnen AA, Heeringa P, Buurman WA (2003) Inhibition of complement factor C5 protects against renal ischemia-reperfusion injury: inhibition of late apoptosis and inflammation. Transplantation 75(3):375-382

61. Dittert D-D, Siebert AG, Kallerhoff M, Ringert RH (1997) Extracellular HTK perfusion and intracellular acidification in ischemic dog kidneys: a ^{31}P NMR spectroscopic study. J Urol 157:1064-1069

62. Dobyan DC, Bulger RE (1982) Renal carbonic anhydrase. Am J Physiol 243 :F311-F324

63. Doctor RB, Bacallao R, Mandel LJ (1994) Method for recovering ATP content and mitochondrial function after chemical anoxia in renal cell cultures. Am J Physiol 266:C1803-C1811

64. Doi T, Fakler B, Schultz JH, Ehmke H, Brändle U, Zenner HP, Süssbrich H, Lang F, Ruppersberg JP, Busch AE (1995) Subunit-specific inhibition of inward-rectifier K^+ channels by quinidine. FEBS Letters 375:193-196

65. Dong Z, Patel Y, Saikumar P, Weinberg JM, Ventakachalam MA (1998) Development of porous defects in plasma membranes of adenosine triphosphate-depleted Madin-Darby canine kidney cells and its inhibition by glycine. Lab Invst 78(6):657-668

66. Donohoe JF, Venkatachalam MA, Bernard DB, Levinsky NG (1978) Tubular leakage and obstrucion after renal ischemia: Structural-functional correlations. Kidney Int 13:208-222

67. Drugge ED, Carroll MA, McGiff JC (1989) Cells in culture from rabbit medullary thick ascending limb of Henle's loop. Am J Physiol 256: C1070-C1081

68. DuBose Jr TD, Good DW (1988) Effects of diuretics on renal acid-base transport. Sem Nephrol 8(3):282-294

69. Eaton DC, Hamilton KL, Johnson KE (1984) Intracellular acidosis blocks the basolateral Na-K pump in rabbit urinary bladder. Am J Physiol 247:F946-F654

70. Edelstein CL, Ling H, Schrier RW (1997) The nature of renal cell injury. Kidney int 51:1341-1351

71. Edelstein CL, Yaqoob MM, Alkhunaizi AM, Gengaro PE, Nemenoff RA, Wang KK, Schrier RW (1996) Modulation of hypoxia-induced calpain activity in rat renal proximal tubules. Kidney Int 50(4):1150-1157

72. Eisner DA, Nichols CG, O'Neill SC, Smith GL, Valdeolmillos M (1989) The effect of metabolic inhibition on intracellular calcium and pH in isolated rat ventricular cells. J Physiol (411):393-418

73. Eladari D, Cheval L, Quentin F, Bertrand O, Mouro I, Cherif-Zahar B, Cartron JP, Paillard M, Doucet A, Chambrey R (2002) Expression of RhCG, a new putative NH_3/NH_4^+ transporter, along the rat nephron. J Am Soc Nephrol 13(8):1999-2008

74. Eveloff J, Haase W, Kinne R (1980) Separation of renal medullary cells: isolation of cells from the thick ascending limb of Henle's loop. J Cell Biol 87:672-681

75. Fitzpatrick JM, Monson JR, Gunter PA, Watkinson LE, Wickham JE (1982) Renal accumulation of ammonia: the cause of post-ischemic functional loss and the "blue line". Brit J Urol 54:608-612

76. Fliegel L (1996) The Na^+/H^+ exchanger, Springer-Verlag, Heidelberg, Germany

77. Flores J, DiBona D, Beck C, Leaf A (1972) The role of cell swelling in ischemic renal damage and the protective effect of hypertonic solute. J Clin Invest 51:118-126

78. Friedlander G, Le Grimellec C, Amiel C (1990) Increase in membrane fluidity modulates sodium-coupled uptakes and cyclic AMP synthesis by renal proximal tubular cells in primary culture. Biochim Biophys Acta 1022(1):1-7

79. Fry CH, Harding DP, Mounsey JP (1987) The effects of cyanide on intracellular ionic exchange in ferret and rat ventricular myocardium. Proc R Soc Lond 230:53-75

80. Garza-Quintero R, Weinberg JM, Ortega-Lopez J, Davis JA, Venkatachalam MA (1993) Conservation of structure in ATP-depleted proximal tubules: the role of calcium, polyphosphoinositides, and glycine. Am J Physiol 265:F605-623

81. Giebisch G, Wang W (2000) Renal tubule potassium channels: function, regulation and structure. Acta Physiol Scand 170:153-173

82. Giebisch G, Windhager E (2003)(a) Transport of sodium and chloride. In: Boron WF, Boulpaep EL (eds) Medical Physiology. Saunders, Philadelphia London New York St. Louis Sydney Toronto, pp774-789

83. Giebisch G, Windhager E (2003)(b) Transport of urea, glucose, phosphate, calcium, magnesium and organic solutes. In: Boron WF, Boulpaep EL (eds) Medical Physiology. Saunders, Philadelphia London New York St. Louis Sydney Toronto, pp790-813

84. sGlinn M, Ni B, Irwin RP, Kelley SW, Lin SZ, Paul SM (1998) Inorganic P_i increases neuronal survival in acute early phase following excitotoxic/oxidative insults. J Neurochem 70:1850-1858

85. Green J, Foellmer O, Kleeman CR, Basic MM (1993) Acute phosphate depletion inhibits the Na^+/H^+ antiporter in a cultured renal cell line. Am J Physiol 265:F440-F448

86. Greger R, Schlatter E (1983) Properties of the basolateral membrane of the cortical thick ascending limb of Henle's loop of rabbit kidney. Pflügers Arch 396: 325-334

87. Greger R, Schlatter E (1983) Properties of the lumen membrane of the cortical thick ascending limb of Henle's loop of rabbit kidney. Pflügers Arch 396:315-324

88. Grynkiewicz G, Poenie M, Tsien R (1985) A new generation of Ca^{2+} indicators with greatly improved fluorescence properties. J Biol Chem 260:3440-3450

89. Grunewald RW, Reisse CH, Müller GA (1998) Characteristics of urea transport of cells derived from rabbit thick ascending limb of Henle's loop. Kidney Int 54:152-159

90. Gobé G, Willgoss D, Hogg N, Schoch E, Endre Z (1999) Cell survival or death in renal tubular epithelium after ischemia-reperfusion injury. Kidney Int 56:1299-1304

91. Good DW (1994) Ammonium transport by the thick ascending limb of Henle's loop. Annu Rev Physiol 56: 623-647

92. Good DW, George T, Watts BA III (1995) Basolateral membrane Na+/H+ exchange enhances HCO_3^- absorption in rat medullary thick ascending limb: evidence for functional coupling between basolateral and apical membrane Na+/H+ exchangers. Proc Natl Acad Sci USA 92:12525-12529

93. Gores GJ, Nieminen AL, Wray BE, Herman B, Lemasters JL (1989) Intracellular pH during "chemical hypoxia" in cultured rat hepatocytes. J Clin Invest 83:386-396

94. Guggino W, Oberleithner M, Giebisch G (1988)The amphibian diluting segment. Am J Physiol 254:F615-F627

95. Gullans, Hebert (1996) Metabolic basis of ion transport. In: Brenner BM (ed) Brenner and Rector's The Kidney. W.B. Saunders Company, Philadelphia London Toronto Montreal Sydney Tokyo, pp 237-240

96. Gumina RJ, Moore J, Schelling P, Beier N, Gross GJ (2001) Na(+)/H(+) exchange inhibition prevents endothelial dysfunction after I/R injury. Am J Physiol 281(3):H1260-1266

97. Hamilton KL, Butt AG (2000) The molecular basis of renal tubular transport disorders. Comp Biochem Physiol 126:305-321

98. Hanley MJ (1980) Isolated nephron segments in a rabbit model of ischemic acute renal failure. Am J Physiol 239:F17-F23

99. Hansson R, Johansson S, Jonsson O, Petersson S, Waldenstrom J (1986) Kidney protection by pre-treatment with free radical scavengers and allopurinol: renal function at recirculation after warm ischemia in rabbits. Clin Sci 71(3):245-251

100. Heitzmann D, Warth R, Bleich M, Henger A, Nitschke R, Greger R (2000) Regulation of the $Na^+2Cl^-K^+$ cotransporter in isolated rat colon crypts. Pflügers Arch 439:378-384

101. Helbert MJF, Dauwe SHE, De Broe ME (1999) Flow cytometric immunodissection of the human nephron in vivo and in vitro. Exp Nephrol 7:360-376

102. Helbert MJF, Dauwe SHE, De Broe ME (2001) Flow cytometric immunodissection of the human distal tubule and cortical collecting duct system. Kidney Int 59:554-564

103. Hendrikx M, Rega F, Jamaer L, Valkenborgh T, Gutermann H, Mees U (2001) Na(+)/H(+)-exchange inhibition and aprotinin administration: promising tools for myocardial protection during minimally invasive CABG. Eur J Cardiothorac Surg 19(5):633-639

104. Herman B, Gores GJ, Nieminen AL, Kawanishi T, Harman A, Lemasters JJ (1990) Calcium and pH in anoxic and toxic injury. Critical Reviews in Toxicology 21(2):127-148

105. Heyman SN, Lieberthal W, Rogiers P, Bonventre JV (2002) Animal models of acute tubular necrosis. Curr Opin Crit Care 8:526-534

106. Heyman SN, Shina A, Brezis M, Rosen S (2002) Proximal tubular injury attenuates outer medullary hypoxic damage: studies in perfused rat kidneys. J Am Soc Nephrol 10(4):259-266

107. Hilgemann DW (1997) Cytoplasmic ATP-dependent regulation of ion transporters and channels: mechanisms and messengers. Annu Rev Physiol 59:193-220

108. Hoenderop JGJ, Nilius B, Bindels RJM (2003) Epithelial calcium channels: from identification to function and regulation. Pflügers Arch 446:304-308

109. Horster M (1979) Primary culture of mammalian nephron epithelia. Pflügers Arch 382: 209-215

110. Horster MF, Sone M (1990) Primary culture of isolated tubule cells of defined segmental origin. Method Enzymol 191: 409-426

111. Hoyer JR, Seiler MW (1979) Pathophysiology of Tamm-Horsfall protein. Kidney Int 16: 279-289

112. Hropot M, Juretschke H-P, Langer KH, Schwark J-R (2001) S3226, a novel NH3 inhibitor, attenuates ischemia induced acute renal failure in rats. Kidney Int 60:2283-2289

113. Iino Y, Burg MB (1981) Effect of acid-base status in vivo on bicarbonate transport by rabbit renal tubules in vitro. Jpn J Physiol 32:99-107

114. Ittert DD, Siebert AG, Kallerhoff M, Ringert RH (1997) Extracellular HTK perfusion and intracellular acidification in ischemic dog kidenys: a ^{31}P NMR spectroscopic study. J Urol 157:1064-1069

115. Jans F,Vandenabeele F, Helbert M, Lambrichts I, Ameloot M, Steels P (2000) A simple method for obtaining functionally and morphologically intact primary cultures of the medullary thick ascending limb of Henle's loop (MTAL) from rabbit kidneys. Pflügers Archiv – Eur J Physiol 440:643-651

116. Jin W, Lu Z (1998) A novel high-affinity inhibitor for inward-rectifier K^+ channels. Biochemistry 37:13291-13299

117. Jorgensen NK, Petersen SF, Amgaard I, Schousboe A, Hoffmann EK (1999) Increases in $[Ca^{2+}]_i$ and changes in intracellular pH during chemical anoxia in mouse neocortical neurons in primary culture. J Neurosc Res 56:358-370

118. Kaissling B, Kriz W (1992) Morphology of the loop of Henle, distal tubule, and collecting duct. In: Windhager EE (ed) Renal Physiology. Oxford University Press, New York, pp 109-167

119. Kapus A, Grinstein S, Wasan S, Kandasamy R, Orlowski J (1994) Functional characterization of three isoforms of the Na^+/H^+ exchanger stably expressed in Chinese Hamster Ovary cells. J Biol Chem 269(38):23544-23552

120. Karmazin M (1988) Amiloride enhances postischemic ventricular recovery: possible role of Na^+-H^+ exchange. Am J Physiol 255:H608-615

121. Katsura K-I, Ekholm A, Siesjö BK (1992) Coupling among changes in energy metabolism, acid-base homeostasis, and ion fluxes in ischemia. Can J Physiol Pharmacol 70:S170-S175

122. Kavanaugh MP, Kabat D (1996) Identification and characterization of a widely expressed phosphate/retrovirus receptor family. Kidney Int 49:959-963

123. Kelly KJ, Plotkin Z, Dagher PC (2001) Guanosine supplementation reduces apoptosis and protects renal function in the setting of ischemic injury. J Clin Invest 108:1291-1998

124. Kelly KJ, Plotkin Z, Vulgamott SL, Dagher PC (2003) P53 mediates the apoptotic response to GTP depletion after renal ischemia-reperfusion: protective role of a p53 inhibitor. J Am Soc Nephrol 14(1):128-138

125. Kemp GH, Roussel M, Bendahan D, Fur YL, Cozzone PJ (2001) Interrelations of ATP synthesis and proton handling in ischaemically exercising human forearm muscle studied by ^{31}P magnetic resonance spectroscopy. J Physiol 535(3):901-928

126. Kikeri D, Sun A, Zeidel ML, Hebert SC (1989) Cell membranes impermeable to NH_3. Nature 339:478-480

127. Kikeri D, Sun A, Zeidel ML, Hebert SC (1992) Cellular NH_4^+/K^+ transport pathways in mouse medullary thick limb of Henle. J Gen Physiol 99:435-461

128. Kitayama J, Kitazono T, Yao H, Oboshi H, Takaba H, Ago T, Fujishima M, Ibayashi S (2001) Inhibition of Na^+/H^+ exchanger reduces infarct volume of focal cerebral ischemia in rtas. Brain res 922(2):223-228

129. Knepper MA, Kim GH, Fernandez-Llama P, Ecelbarger CA (1999) Regulation of thick ascending limb transport by vasopressin. J Am Soc Nephrol 10: 628-634

130. Knight DR, Smith AH, Flynn DM, Macandrew JT, Ellery SS, Kong JX, Marala RB, Wester RT, Guzman-Perez A, Hill RJ, Magee WP, Tracey WR (2001) A novel sodium-hydrogen exchanger isoform-1 inhibitor, zoniporide, reduces ischemic myocardial injury in vitro and in vivo. J Pharm Exp Ther 297:254-259

131. Kolber MA, Quinones RR, Gress RE, Henkart PA (1988) Measurement of cytotoxicity by target cell release and retention of the fluorescent dye bis-carboxyethyl-carboxyfluorescein (BCECF). J Immunol Methods 108:255-264.

132. Koushanpour E, Kriz W (1986) An overview of the structural and functional organization of the kidney. In: Koushanpour E, Kriz W (eds) Renal Physiology. Springer-Verlag, New York, pp 41-52

133. Laamarti MA, Lapointe J-Y (1997) Determination of NH_4^+/NH_3 fluxes across apical membrane of macula densa cells: a quantitative analysis. Am J Physiol 273:F817-F824

134. Ladefoged SD, Andersen CB (1994) Calcium channel blockes in kidney transplantation. Clin Transplant 8:128-133

135. Lameire N, Vanholder R (2001) Pathophysiologic features and prevention of human and experimental acute tubular necrosis. J Am Soc Nephrol 12:S20-S32

136. Lash LH, Tokarz JJ, Pegouske DM (1995) Susceptibility of primary cultures of proximal tubular and distal tubular cells from rat kidney to chemically induced toxicity. Toxicology 103:85-103

137. Lash LH, Tokarz JJ, Chen Z, Pedrosi BM, Woods EB (1996) ATP depletion by iodoacetate and cyanide in renal distal tubular cells. J Pharm Exp Ther 276:194-205

138. Leaf A (1973) Cell swelling: a factor in ischemic tissue injury. Circulation 48:455-458

139. Lear S, Silva P, Kelley VE, Epstein FH (1990) Prostaglandin E2 inhibits oxygen consumption in rabbit medullary thick ascending limb. Am J Physiol 258:F1372-F1378

140. Leipziger J, MacGregor GG, Cooper JG, Xu J, Hebert SC, Giebisch G (2000) PKA site mutations of ROMK2 channel shift the pH dependence to more alkaline values. Am J Physiol 279:F919-926

141. Levine JS, Lieberthal W (2001) Terminal pathways to cell death. In: Molitoris BA, Finn WF (eds) Acute Renal Failure. WB Saunders Company, Philadelphia, pp 30-59

142. Levy EM, Viscoli CM, Horwitz RI (1996) The effect of acute renal failure on mortality. A cohort analysis. JAMA 275(19):1489-1494

143. Li H, Ren P, Onwochei M, Ruch RJ, Xie Z (1996) Regulation of rat Na^+/P_i cotransporter-1 gene expression: the roles of glucose and insulin. Am J Physiol 271:E1021-E1028

144. Lieberthal W, Nigam SK (1998) Acute Renal Failure. I. Relative importance of proximal vs. Distal tubular injury. Am J Physiol 275:F623-F632

145. Lieberthal W, Menza SA, Levine JS (1998) Graded ATP depletion can cause necrosis or apoptosis of cultured mouse proximal tubular cells. Am J Physiol 274(2):F315-F327

146. Lu M, Wang W (2000) Two types of K^+ channels are present in the apical membrane of the thick ascending limb of mouse kidney. Kidney Blood Press Res 23:75-82

147. Kumlertgul D, Harris DC, Burke TJ, Schrier RW (1986) Detrimental effect of hypophosphatemia on the severity and progression of ischemic acute renal failure. Mineral Electrolyte Metab 12:204-209

148. MacDonald C, Watts P, Stuart B, Kreuzburg-Duffy U, Scott DM, Kinne RKH (1991) Studies on the phenotype and karyotype of immortalised rabbit kidney epithelial cell lines. Exp Cell Res 195: 458-461

149. MacGregor GG, Xu JZ, McNicholas CM, Giebisch G, Hebert SC (1998) Partially active channels produced by PKA site mutation of the cloned renal K^+ channel, ROMK2 (kir1.2). Am J Physiol 275:F415-F422

150. Malis CD, Bonventre JV (1986) Mechanism of calcium potentiation of oxygen free radical injury to renal mitochondria. J Biol Chem 261(30):14201-14208

151. Martin (2001) Neuronal cell death in nervous system development, disease and injury. Int J Mol Med 7:455-478

152. Mason J, Welsch J, Torhorst J (1987) The contribution of vascular obstruction to the functional defect that follows renal ischemia. Kidney Int 31(1):65-71

153. Matsumoto T, Miura T, Miki T, Genda S, Shimamoto K (2002) Blockade of the Na^+-Ca^{2+} exchanger is more efficient than blockade of the Na^+-H^+ exchanger for protection of the myocardium from lethal reperfusion injury. Cardiovasc Drugs Ther 16(4):295-301

154. McCoy CE, Selvaggio AM, Alexander EA, Schwartz JH (1988) Adenosine triphosphate depletion induces a rise in cytosolic free calcium in canine renal epithelial cells. J Clin Invest 82:1326-1332

155. McNicholas CM, MacGregor GG, Islas LD, Yang Y, Hebert SC, Giebisch G (1998) pH-dependent modulation of the cloned renal K^+ channel, ROMK. Am J Physiol 275:F972-981

156. Megyesi J, Andrade L, Vieira JM, Safirstein RL, Price PM (2002) Coordination of the cell cycle is an important determinant of the syndrome of acute renal failure. Am J physiol 283:F810-F816

157. Meng H, Lonsberry BB, Pierce GN (1991) Influence of perfusate pH on the postischemic recovery of cardiac contractile function: involvement of sodium-hydrogen exchange. J Pharmacol Exp Ther 258:772-777

158. Molecular Probes Handbook (2002), Web Edition (http://www.molecularprobes.com/handbook)

159. Môller HE, Gaupp A, Dietl KH, Buchholz B, Vestring T (2000) Tissue pH in human kidney transplants during hypothermic ischemia. Magn Res Im 18:743-751

160. Molitoris BA, Alfrey AC, Harris RA, Simon FR (1985) Renal apical membrane cholesterol and fluidity in regulation of phosphate transport. Am J Physiol 249:F12-F19

161. Molitoris BA, Kinne R (1987) Ischemia induces surface membrane dysfunction. Mechanism of altered Na^+-dependent glucose transport. J Clin Invest 80(3):647-654

162. Moncada S, Erusalimsky JD (2002) Does nitric oxide modulate mitochondrial energy generation and apoptosis? Nature Rev 3(3):214-220

163. Monnens L, Starremans P, Bindels R (2000) Great strides in the understanding of renal magnesium and calcium reabsorption. Nephrol Dial Transpl 15:568-571

164. Montagna G, Hofer CG, Torres AM (1998) Impairment of cellular redox status and membrane protein activities in kidneys from rats with ischemic acute renal failure? Biochim Biophys Acta 1407(2):99-108

165. Morel F (1981) Sites of hormone action in the mammalian nephron. Am J Physiol 240: F159-F164

166. Morel F, Doucet A (1992) Functional segmentation of the nephron. In: Seldin DW, Giebisch G (eds) The Kidney: physiology and pathophsyiology. Raven Press, New York, pp 1049-1086

167. Moschèn I, Setiawan I, Bröer S, Murer H, Lang F (2001) Effect of NaPi-mediated phosphate transport on intracellular pH. Pflügers Arch 441:802-806
168. Murer H, Biber J (1996) Molecular mechanisms of renal apical Na/phosphate cotransport. Annu Rev Physiol 58:607-618

169. Murphy E, Chamberlin ME, Mandel LJ (1986) Effects of calcitonin on cytosolic Ca in a suspension of rabbit medullary thick ascending limb tubules. Am J Physiol 251: C491-C495

170. Myers BD, Chui F, Hilberman M, Michaels AS (1979) Transtubular leakage of glomerular filtrate in human acute renal failure. Am J Physiol 237(4):F319-F325

171. Nakhoul NL, Lopes AG, Chaillet JR, Boron WF (1988) Intracellular pH regulation in the S3 segment of the rabbit proximal tubule in HCO_3^--free solutions. J Gen Physiol 92:369-393

172. Ni B, Wu X, Yan G, Wang J, Paul SM (1995) Regional expression and cellular localization of the Na^+-dependent inorganic phosphate co-transporter of the rat brain. J Neurosci 15:5789-5799

173. Nissenson AR (1998) Acute Renal Failure: Definition and pathogenesis. Kindey Int 53 (Suppl 66):S7-S10

174. Nitschke R, Fröbe U, Greger R (1991) Antidiuretic hormone acts via V1 receptors on intracellular calcium in isolated perfused rabbit cortical thick ascending limb. Pflügers Arch 417: 622-632

175. Noël J, Roux D, Pouysségur J (1996) Differential localization of Na^+/H^+ exchanger isoforms (NHE1 and NHE3) in polarized epithelial cell lines. J Cell Sci 109:929-939

176. Padanilam BJ (2003) Cell death induced by acute renal injury: a perspective on the contributions of apoptosis and necrosis; Am J Physiol 284:F608-F627

177. Paillard M (1998) H^+ and HCO_3^- transporters in the medullary thick ascending limb of the kidney: molecular mechanisms, function and regulation. Kidney Int 53:S36-41

178. Palmer LG, Choe H, Frindt G (1997) Is the secretory K channel in the rat CCT ROMK? Am J Physiol 273:F404-F410

179. Panda M, Robinson NC (1995) Kinetics and mechanism for the binding of HCN to cytochrome *c* oxidase. Biochemistry (34):10009-10018

180. Peti-Peterdi J, Chambrye R, Bebok Z, Biemesderfer D, St. John P, Abrahamson DR, Warnock DG, Bell PD (2000) Macula densa Na^+/H^+ exchange activities mediated by apical NHE2 and basolateral NHE4 isoforms. Am J Physiol 278:F452-F463

181. Rab H, Star R (2001) Inflammatory response and its consequences in acute renal failure. In: Molitoris BA, Finn WF (eds) Acute Renal Failure. WB Saunders Company, Philadelphia, pp 89-100

182. Racusen LC (2001) The morphologic basis of acute renal failure. In: Molitris BA, Finn WF (eds) Acute renal failure: a companion to Brenner and rector's The kidney. WB Saunders Company, Philadelphia, pp1-12

183. Redlin M, Werner J, Habazettl H, Griethe W, Kuppe H, Pries AR (2001) Cariporide (HOE 642) attenuates leukocyte activation in ischemia and reperfusion. Anesth Analg 96(6):1472-1479

184. Reeves WB, Andreoli TE (2000) Sodium chloride transport in the loop of Henle, distal convoluted tubule, and collecting duct. In: Seldin DW, Giebisch G (eds) The Kidney. Lippincot Williams & Wilkins, Philadelphia, pp 1333-1369

185. Rocha AS, Magaldi JB, Kokko JP (1977) Calcium and phosphate transport in isolated segments of rabbit Henle's loop. J Clin Invest 59(5):975-983

186. Rose UM, Bindels RJM, Jansen JWCM, van Os H (1994a) Effects of Ca^{2+} channel blockers, low Ca^{2+} medium and glycine on cell Ca^{2+} and injury in anoxic rabbit proximal tubules. Kidney Int 46:223-229

187. Rose UM, Hartog A, Jansen JW, Van Os CH, Bindels RJ (1994b) Anoxia-induced increases in intracellular calcium concentration in primary cultures of rabbit thick ascending limb of Henle's loop. Biochim Biophys Acta 1226(3):291-299

188. Rose UM, Abrahamse SL, Jansen JWCM, Bindels RJM, van Os CH (1995) Cellular acidification occurs during anoxia in cultured, but not in freshly isolated, rabbit proximal tubular cells. Pflügers Arch 429:722-728

189. Rosen S, Heyman SN (2001) Difficulties in understanding human "acute tubular necrosis": limited data and flawed animal models. Kidney Int 60:1220-1224

190. Russ U, Balser C, Scholz W, Albus U, Lang HJ, Weichert A, Schölkens BA, Gögelein H (1996) Effects of the Na^+/H^+-exchange inhibitor HOE642 on intracellular pH, calcium and sodium in isolated rat ventricular myocytes. Pflügers Arch 433:26-34

191. Safirstein R, DiMari J, Megyesi J, Price P (1998) Mechanisms of renal repair and survival following acute injury. Semin Nephrol 18(5):519-522

192. Safirstein R, Megyesi J, Saggi SJ, Price PM, Poon M, Rollins BJ, Taubman MB (1991) Expression of cytokine-like genes JE and KC is increased during renal ischemia. Am J Physiol 261:F1095-F1101

193. Sakaida I, Nagatomi A, Okita K (1996) Protection by glycine against chemical ischemia produced by cyanide in cultured hepatocytes. J Gastroenterol 32(5):684-690

194. Salameh A, Dhein S, Beuckelmann DJ (2002) Role of the Na(+)/H(+) exchanger in [Ca(2+)](i) and [Na(+)](i) handling during intracellular acidosis. Effect of cariporide (HOE 642). Pharmacol Res 45(1):35-41

195. Schäfer C, Ladilov YV, Schäfer M, Piper HM (2000) Inhibition of NHE protects reoxygenated cardiomyocytes independently of anoxic Ca^{2+} overload and acidosis. Am J Physiol 279:H2143-H2150

196. Schafer JA, Watkins ML, Li L, Herter P, Haxelmans S, Schlatter E (1997) A simplified method for isolation of large numbers of defined nephron segments. Am J Physiol 273: F650-F657

197. Schneckenburger H, Gschwend MH, Konig K, Sailer R, Strauss WSL (1996) Fluorescence lifetime imaging and spectroscopy in photobiology and photomedicine. In: Slavik J (ed) Fluorescence microscopy and fluorescent probes. Plenum Press, New York, pp 71-78

198. Schoenecker JA, Weinman SA (1994) Maintenance of cellular acidification in cyanide-treated hepatocytes results from inhibition of Na^+/H^+ exchange. Am J Physiol 266:G892-G898

199. Scott DM, Macdonald C, Brzeski H, Kinne R (1986) Maintenance of expression of differentiated function of kidney cells following transformation by SV40 early region DNA. Exp Cell Res 166: 391-398

200. Shanley PF, Sharpio JI, Chan L, Burke TJ, Johnson GC (1988) Acidosis and hypoxic medullary injury in the isolated perfused kidney. Kidney Int 34:791-796

201. Shanley PF, Johnson GC (1991) Calcium and acidosis in renal hypoxia. Lab Inv 65(3):298-305

202. Sheridan AM, Bonventre JV (2000) Cell biology and molecular mechanisms of injury in ischemic acute renal failure. Curr Opin Nephrol Hypertens 9:427-434

203. Sheridan AM, Schwartz JH, Kroshian VM, Tercyal AM, Laraia J, Masino S, Lieberthal W (1993) Renal mouse proximal tubular cells are more susceptible than MDCK cells to chemical anoxia. Am J Physiol 265:F342-F350

204. Simon DB, Lu Y, Choate KA, Velazquez H, Al-Sabban E, Praga M, Casari G, Bettinelli A, Colussi G, Rodriguez-Soriano J, McCredie D, Milford D, Sanjad S, Lifton RP (1999) Paracellin-1, a renal tight junction protein required for paracellular Mg2+ resorption. Science, 285(5424):103-106

205. Smets I (2001) Metabolic inhibition as an in vitro model of ischemic acute renal failure. In: Cellular defence mechanisms in renal distal tubular A6 cells facing metabolic inhibition. Royal Library Albert I, Brussels, D/2001/2451/35

206. Smets I, Caplanusi A, Despa S, Molnar Z, Radu M, vandeVen M, Ameloot M, Steels P (2004) Ca^{2+} uptake in depolarised mitochondria is mediated via the reversed action of the mitochondrial Na^+/Ca^{2+} exchanger in metabolically inhibited MDCK cells. Am J Physiol 286(4):784-794

207. Snowdowne KW, Borle AB (1985) Effects of low extracellular sodium on cytosolic ionized calcium: Na^+-Ca^{2+} exchange as a major calcium influx pathway in kidney cells. J Biol Chem 260(28):14998-15007

208. Stoelting RK, Dierdorf SF (2002) Renal diseases. In: Stoelting RK, Dierdorf SF (eds) Anesthesia and Co-Existing Disease. Churchill Livingstone, Philadelphia, pp 341-372

209. Studer RK, Borle AB (1979) Effect of pH on the calcium metabolism of isolated rat kidney cells. J Membr Biol 48(4):325-341

210. Suki WN, Rouse DN, Kokko JP (1980) Calcium transport in the thick ascending limb of Henle. Heterogeneity of function in the medullary and cortical segments. J Clin Invest 66:10041009

211. Symons JD, Schaefer S (2001) Na(+)/H(+) exchange subtype 1 inhibition reduces endothelial dysfunction in vessels from stunned myocardium. Am J Physiol 281(4):H1575-1582

212. Takeda M, Jung KY, Endou H, Koide H (1994) Intranephron distribution of creatine content in rats. Biochem Mol Biol Int 32(3):435-440

213. Tang MJ, Suresh KR, Tannen RL (1989) Carbohydrate metabolism by primary cultures of rabbit proximal tubules. Am J Physiol 256(3 Pt 1):C532-C539

214. Thomas JA, Buchsbaum RN, Zimniak A, Racker E (1979) Intracellular pH measurements in Ehrlich ascites tumor cells utilising spectroscopic probes generated in situ. Biochemsitry 18:2210-2218

215. Tinel H, Kinne-Saffran E, Kinne RH (2002) Calcium-induced calcium release participates in cell volume regulation of rabbit TALH cells. Pflügers Arch 443(5-6):754-761

216. Ueda N, Kaushal GP, Shah SV (2000) Apoptotic mechanisms in acute renal failure. Am J Med 108:403-415

217. Trinh-Trang-Tan M, Bouby N, Coutaud C, Bankir L (1986) Quick isolation of rat medullary ascending limbs. Pflügers Arch 407: 228-234

218. Valentich JD, Stokols MF (1984) An established cell line from mouse kidney medullary thick ascending limb. I. Cell culture techniques, morphology, and antigenic expression. Am J Phsyiol 251: C299-C311

219. Vandewalle A, Wirthensohn G, Heidrich HG, Guder WG (1981) Distribution of hexokinase and phophoenolpyruvate carboxykinase along the rabbit nephron. Am J Physiol 240(6):F492-500

220. van Heeswijk MP, Geertsen JA, van Os CH (1984) Kinetic properties of the ATP-dependent Ca^{2+} pump and the Na^{+}/Ca^{2+} exchange system in basolateral membranes from rat kidney cortex. J Membr Biol 79(1):19-31

221. Verlander JW, Miller RT, Frank AE, Royaux IE, Kim YH, Weiner ID (2003) Localization of the ammonium transporter proteins RhBG and RhCG in mouse kidney. Am J Physiol 284(2):F323-F337

222. Verri T, Markovich D, Perego C, Norbis F, Stange G, Sorribas V, Biber J, Murer H (1995) Cloning of a rabbit renal Na-P_i cotransporter, which is regulated by dietary phosphate. Am J Physiol 268:F626-F633

223. Voet D, Voet JG (1990) Glycolysis. In: Voet D, Voet JG (eds) Biochemistry. John Wiley and Sons, New York, pp 425-460

224. von Recklinghausen IR, Kinne RK, Jans AW (1992) Ammonium chloride-induced acidification in renal TALH SVE.1 cells monitored by 31P-NMR. Biochim Biophys Acta 1136(2): 129-135

225. Vornov JJ, Thomas AG, Jo D (1996) Protective effects of extracellular acidosis and blockade of sodium/hydrogen ion exchange during recovery from metabolic inhibition in neuronal tissue culture. J Neurochem 67:2379-2389

226. Wakabayashi S, Shigekawa M, Pouysségur J (1997) Molecular physiology of vertebrate Na^{+}/H^{+} exchangers. Phys Rev 77(1):51-74

227. Wang W, White S, Geibel J, Giebisch G (1990) A potassium channel in the apical membrane of rabbit thick ascending limb of Henle's loop. 258:F244-F253

228. Wang W (1994) Two types of K^{+} channel in thick ascending limb of rat kidney. Am J Physiol 267:F599-605

229. Wang W, Jittikanont S, Falk SA, Li P, Feng L, Gengaro PE, Poole BD, Bowler RP, Day BJ, Crapo JD, Schrier RW (2003) Interaction among nitric oxide,

reactive oxygen species, and antioxidants during endotoxemia-related acute renal failure. Am J Physiol 284:F532-F537

230. Watts BA, Good DW (1994) Effects of ammonium on intracellular pH in rat medullary thick ascending limb: mechanisms of apical membrane NH_4^+ transport. J Gen Physiol 103:917-936

231. Weinberg JM (1988) Adenine nucleotide metabolism by isolated kidney tubules during oxygen deprivation. Bioch Med Metab Biol 36:319-329

232. Weinberg JM, Davis JA, Abarzua M, Kiani T (1989) Relationship between cell adenosine triphosphate and glutathione content and protection by glycine against hypoxic proximal tubule cell injury. J Lab Clin Med 113(5):612-622

233. Weinberg JM, Davis JA, Roeser NF, Venkatachalam MA (1991) Role of increased cytosolic free calcium in the pathogenesis of rabbit proximal tubule cell injury and protection by glycine or acidosis. J Clin Invest 87(2):581-590

234. Weinberg JM, Davis JA, Roeser NF, Ventakachalam MA (1994) Role of intracellular pH during cytoprotection of proximal tubule cells by glycine or acidosis; J Am Soc Nephrol 5:1314-1323

235. Weinberg JM, Roeser NF, Davis JA, Vankatachalam MA (1997) Glycine-protected , hypoxic, proximal tubules develop severely compromised energetic function. Kidney int 52:140-151

236. Weinberg JM, Venkatachalam MA, Goldberg H, Roeser NF, Davis JA (1995) Modulation by Gly, Ca, and acidosis of injury-associated unesterified fatty acid accumulation in proximal tubule cells. Am J Physiol 268:F110-121

237. Weinberg JM, Venkatachalam MA, Roeser NF, Nissim I (2000) Mitochondrial dysfunction during hypoxia/reoxygenation and its correction by anaerobic metabolism of citric cycle intermediates. PNAS 97(6):2826-2831

238. Werner A, Dehmelt L, Nalbant P (1998) Na^+-dependent phosphate cotransporters: the NaPi protein family. J Exp Biol 201:3135-3142

239. Wick AN, Drury DR, Nakada HI, Wolfe JB (1957) Localization of the primary metabolic block produced by 2-deoxyglucose. J Biol Chem 224:963-969

240. Wiegele G, Brandis M, Zimmerhackl LB (1998) Apoptosis and necrosis during ischemia in renal tubular cells (LLC-PK_1 and MDCK). Nephrol Dial Transpl 13:1158-1167

241. Wilson PD, Schrier RW (1986) Nephron segment and calcium as determinants of anoxic cell death in renal cultures. Kidney Int 29:1172-1179

242. Wittner M, Weidtke C, Schlatter E, di Stefano A, Greger R (1984) Substrate utilization in the isolated perfused cortical thick ascending limb of rabbit nephron. Pflügers Arch 402:52-62

243. Xiao Y, Desrosiers RR, Béliveau R (2001) Effect of ischemia-reperfusion on the renal brush-border membrane sodium-dependent phosphate cotransporter NaP_i-2. Can J Physiol Pharmacol 79:206-212

244. Yamamoto T, Tada T, Brodsky SV, Tanaka H, Noiri E, Kajiya F, Goligorsky MS (2002) Intravital videomicroscopy of peritubular capillaries in renal ischemia. Am J Physiol 282:F1150-F1155

245. Yin M, Zhong Z, Connor HD, Bunzendahl H, Finn WF, Rusyn I, Li X, Raleigh JA, Mason RP, Thurman RG (2002) Protective effect of glycine on renal injury induced by ischemia-reperfusion in vivo. Am J Physiol 282:F417-423

246. Yolota N, Burne-Taney M, Rabb H (2002) Opposing roles for the STAT4 and STAT6 signal transduction pathways in renal ischemia-reperfusion injury. J Am Soc Nephrol 13: 31A (Abstract)

247. Ysebaert DK, Degreef KE, Vercauteren SR, Ghielli M, Verpooten GA, Eyskens EJ, De Broe ME (2000) Identification and kinetics of leukocytes after severe ischaemia/reperfusion renal injury. Nephrol Dial Transplant 15:1562-1574

248. Zager RA (1982) Hyperphosphatemia: a factor that provokes severe experimental acute renal failure. J Lab Clin Med 100(2):230-239

249. Zeiske W, Smets I, Ameloot M, Steels P, van Driessche W (1999) Intracellular pH shifts in cultured kidney (A6) cells: effects on apical Na+ transport. Am J Physiol 277:C469-479

250. Zimmerhackl LB, Rostasy K, Wiegele G, Rasenack A, Wilhelm A, Lohner M, Brandis M, Kinne RKH (1996) Tamm-Horsfall protein as a marker of tubular maturation. Pediatr Nephrol 10: 448-452

Dankwoord

Vooreerst wil ik mijn promotor Prof. Dr. P. Steels bedanken. Het is door zijn boeiende hoorcolleges hier aan het L.U.C. dat mijn interesse voor de fysiologie is gegroeid. Na mijn verdere opleiding tot arts in Leuven gaf hij me de mogelijkheid om terug te keren naar Diepenbeek en 4 jaren te besteden aan wetenschappelijk onderzoek. Ik ben hem dankbaar voor het vertrouwen dat hij in me stelde. Hij gaf me een grote vrijheid bij het uitvoeren van dit onderzoek, en was steeds bereid (én bereikbaar) om me te helpen wanneer ik vragen had of niet goed wist welke richting uit te gaan.

Verder wil ik mijn co-promotoren, Prof. Dr. M. Ameloot en Prof. Dr. P. Wouters bedanken. Prof. Ameloot is een rots in de branding van de microfluorescentie. Maar al te vaak dreigden experimenten verloren te gaan, maar met zijn bereidwillige en deskundige hulp zijn heel wat kostbare celculturen van een roemloze ondergang gered. Prof. Wouters is het inspirerend voorbeeld voor talloze assistenten anesthesie die voor, tijdens of na hun klinisch werk ook nog aan wetenschappelijk onderzoek willen doen. Als co-assistent anesthesie heb ik hem bereid gevonden om ook mij te begeleiden. Tijdens onze talloze meetings wist hij zijn enthousiasme steeds op mij over te zetten, en zijn bemerkingen hielpen me om de oorspronkelijke doelstellingen van mijn onderzoek steeds voor ogen te houden. Verder hebben zijn bondige, maar zeer terechte opmerkingen de kwaliteit van deze thesis aanzienlijk verbeterd.

Prof. Dr. H. Martens, rector van het L.U.C., en Prof. Dr. E. Van Kerhove, decaan van de faculteit Geneeskunde, wil ik bedanken voor het creëren van een stimulerende universitaire omgeving die zowel mijn opleiding geneeskunde als mijn onderzoek mogelijk gemaakt heeft.

De leden van de jury, Prof. Dr. E. Van Kerkhove, Prof. Dr. R. Beauwens, Prof. Dr. M. Schetz, Prof. Dr. E. Schlatter, Prof. Dr. N. Lameire, Prof. Dr. W. Van Driessche en Prof. Dr. L. Verresen, wens ik te bedanken voor het nauwkeurig nalezen van het manuscipt en het formuleren van opmerkingen die zeker hebben bijgedragen tot de kwaliteit van dit werk.

Prof. Dr. E. Vandermeersch wil ik bedanken voor zijn steun. Hij heeft me aangemoedigd om aan wetenschappelijk onderzoek te doen, en heeft me ook tijdens mijn werk in de kliniek gesteund bij het schrijven van deze thesis.

Alle collega's van het labo Fysiologie wil ik bedanken voor de hulp bij grote en kleine problemen, maar in het bijzonder wil ik iedereen bedanken voor de aangename werksfeer. Aan de koffiepauzes aan de grote tafel heb ik al vaak met enige heimwee teruggedacht.

In het bijzonder wil ik de collega's van het eerste uur, Ilse en Bart, bedanken. Zij hebben mij wegwijs gemaakt in het "labo", een plaats waar ik voordien nog geen voet had gezet. Met computerproblemen kon ik steeds bij Bart terecht, voor problemen met de celculturen had Ilse meestal een oplossing.

Voor praktische hulp bij de experimenten kon ik terecht bij de vaste krachten van het labo Fysiologie: Patrick wil ik bedanken voor het vervaardigen van de perfusiekamers en micropipetten, Roland voor zijn hulp bij om het even welk "elektrisch" probleem. Jo, Agnes en Wilfried ben ik erg dankbaar voor hun hulp bij het bereiden van allerlei oplossingen en hun hulp in het celcultuurlabo. Marc Withofs en Magda Ieven wil ik bedanken voor hun deskundige hulp bij het maken en verwerken van fotografisch materiaal. Josette, Kathleen en Paula wil ik bedanken voor hun hulp bij administratieve aangelegenheden.

Van de vakgroep Biochemie wil ik Prof. Dr. L. Vanduffel en Raf Lemmens bedanken voor hun begeleiding en advies bij het gebruik van de Cytosensor.

Van de vakgroep Histologie wil ik Dr. F. Vandenabeele, Prof. Dr. I. Lambrichts en Prof. Dr. J. Creemers bedanken voor hun hulp bij het interpreteren van de elektronenmicroscopische opnames, en in het bijzonder wil ik hierbij Mark Jans bedanken voor zijn enorme hulp bij het voorbereiden en het bekijken van de talloze coupes.

Ook de fysiologen van de K.U.Leuven hebben me meermaals een helpende hand toegestoken. Prof. Dr. W. Vandriessche wil ik bedanken voor zijn advies i.v.m. de elektrofysiologische metingen. Prof. Dr. B. Nilius wens ik te bedanken voor zijn hulp bij het zoeken naar het ECaC-kanaal.

Prof. Dr. M. De Broe en Dr. M. Helbert van de Universitair Ziekenhuis Antwerpen ben ik veel dank verschuldigd voor het demonstreren van enkele immunohistochemsiche kleuringen, waaronder die voor het Tamm-Horsfall proteïne.

This work could be accomplished only with the kind help of Prof. Dr. E. Schlatter and Dr. M. Bleich and Ingrid (Westfalische Wilhelms Universität, Münster) who demonstrated the enzymatic dissection of the rabbit kidney.

Verder wil ik ook Steffen Fieuws (K.U.Leuven) bedanken voor zijn deskundige hulp bij de statistische berekeningen.

De stafleden anesthesie van het Ziekenhuis Oost-Limburg wil ik bedanken voor hun hulp en steun in de laatste rechte lijn naar mijn thesisverdediging.

Ten slotte kom ik bij de mensen die ik meegesleurd heb in dit avontuur. Mijn ouders, schoonouders, zus en broer, schoonzussen schoonbroers, wil ik bedanken voor hun steun en geduld die ze me de afglopen jaren getoond hebben. Heel in het bijzonder wil ik natuurlijk mijn ouders bedanken, zonder hen was niets van dit alles mogelijk geweest. Ze hebben me heel erg veel gegeven: een

gelukkige, onbezorgde jeugd en een heleboel kansen waaronder de mogelijkheid om geneeskunde te studeren in Diepenbeek en Leuven. Dank jullie wel hiervoor.

En laatst, maar niet in het minst, richt ik dit dankwoord aan mijn liefste echtgenote Lizelot. Er zijn zovele dingen waarvoor ik haar dankbaar ben, maar bij deze gelegenheid moet het gezegd dat ik dit immense werk niet tot een goed einde had kunnen brengen zonder haar voortdurende steun en aanmoedigingen. De enorme zelfdiscipline en werkkracht die ze elke dag toonde tijdens haar bijkomende studie tandheelkunde, hebben mijzelf steeds gemotiveerd met volharding aan dit onderzoeksproject verder te werken. Maar vooral voor haar liefdevol geduld en begrip tijdens die eindeloze reeks van vakantie- en weekenddagen die aan dit werk zijn opgeofferd, ben ik haar het meeste dank verschuldigd.

List of publications

Publications in International Journals

Jans F, Vandenabeele F, Helbert M, Lambrichts I, Ameloot M, Steels P (2000) A simple method for obtaining functionally and morphologically intact primary cell cultures of the medullary thick ascending limb of Henle's loop (MTAL) from rabbit kidneys. Pflügers Arch – Eur J of Physiol 440:643-651

Published abstracts

Jans F, Laskay G, Ameloot M, Steels P (1998) Primary cell culture of the medullary thick ascending limb (MTAL) of rabbit kidneys. Pflügers Arch – Eur J Physiol 436:R30

Laskay G, Jans F, Ameloot M, Steels P (1998) Monitoring of intracellular Mg^{2+} concentration in MDCK cells by steady-state and time-resolved microfluorimetry. Pflügers Arch – Eur J Physiol 436:R30

Jans F, Ameloot M, Steels P (1999) Study of ammonium transport in primary cultures of rabbit renal medullary thick ascending limb cells (MTAL). Pflügers Arch – Eur J Physiol 439:R240

Jans F, Ameloot M, Steels P (2001) Role of the Na^+/H^+-exchanger and the Na-P_i cotransporter-cotransporter in pH_i regulation in rabbit MTAL primary cell cultures. Pflügers Arch - Eur J Physiol 442:R135

Jans F, Ameloot M, Wouters P, Steels P (2002) Evidence for increased activity of the Na-P_i cotransporter type I during metabolic inhibition in primary cell cultures of MTAL segment from rabbit kidneys. J Am Soc Nephrol 13:137A

Scientific awards

Award from the European Renal Association (ERA) for the outstanding scientific presentation: "*Study of NH_4^+-transport in primary cultures of rabbit MTAL*", Nice, september 2000.

Bijzondere Prijs van de Belgische Vereniging voor Nefrologie (BVN-SBN) voor de posterpresentatie: "*Pharmacological evidence that NH_4^+-absorption occurs mainly through a ROMK-type channel in primary cell cultures from MTAL*", Brussel, maart 2001.